

GEOLOGY OF THE ITALIAN MOUNTAIN INTRUSIVES AND
ASSOCIATED Pb-Ag REPLACEMENT DEPOSITS
CRESTED BUTTE AND TAYLOR PARK
QUADRANGLES, GUNNISON
COUNTY, COLORADO

By

EMERY BERNARD ROY

//

Bachelor of Arts

University of Minnesota, Duluth

Duluth, Minnesota

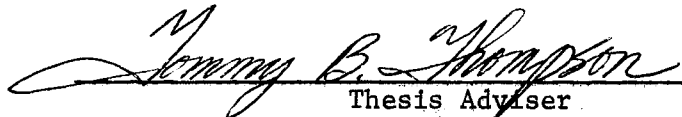
1970

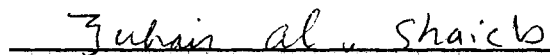
Submitted to the Faculty of the Graduate College
of the Oklahoma State University
in partial fulfillment of the requirements
for the Degree of
MASTER OF SCIENCE
July, 1973

NOV 16 1973

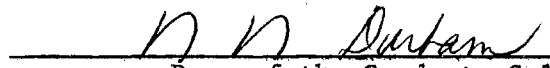
GEOLOGY OF THE ITALIAN MOUNTAIN INTRUSIVES AND
ASSOCIATED Pb-Ag REPLACEMENT DEPOSITS
CRESTED BUTTE AND TAYLOR PARK
QUADRANGLES, GUNNISON
COUNTY, COLORADO

Thesis Approved:


Thesis Adviser






Dean of the Graduate College

867468

PREFACE

Italian Mountain is located on the eastern flanks of the Elk Mountains of Gunnison County in central Colorado at longitude $106^{\circ} 45'00''$ and latitude $39^{\circ}57'30''$. The particular area mapped is approximately 4 miles in length and $2 \frac{3}{4}$ miles wide. The author conducted the field work for his Master's thesis over the Italian Mountain area during the summer of 1972 (from July 2 to August 16). The actual field work consisted of geologic mapping, the collection of rock chip samples for trace metal analysis, and the collection of hand samples for petrographic work. Mapping was done on aerial photographs obtained from the U. S. Forest Service out of Denver, Colorado. Regular nine by nine photographs, at the scale of 1:15,840, were satisfactory in displaying the geology and sample locations. Geologic mapping on the aerial photos was transferred to a topographic base map in order to give the geology a depth dimension and to facilitate the construction of topographic profiles and structural cross sections.

Laboratory work for the author's thesis was divided into two phases: (1) petrographic, and (2) trace metal analysis. The petrographic analysis consisted of describing twenty-five thin sections of the igneous rock types and polished sections of the typical mesothermal ore minerals associated with the Italian

Mountain intrusives. Some eighty-eight rock chip samples were collected over the three intrusives for trace metal (Pb, Zn, Cu, Mo) analyses.

The purposes of the author's investigation are as follows:

(1) to distinguish whether the Italian Mountain "stock" is indeed one stock or composed of several intrusive rock types intruded at different times, (2) to determine the source of the Pb, Zn, and Cu mineralization within the Paleozoic sediments surrounding the Italian Mountain intrusives, and (3) to specify metamorphic facies, within the Paleozoic sediments along the contact with the intrusives, based on mineral assemblages, and to define their approximate extent.

The author wishes to express his sincere gratitude to his thesis adviser, Dr. Tommy B. Thompson, for his guidance in the field work phase of this thesis and for the suggestions and contributions given to the author pertaining to the interpretation of trace metal values. The author also wishes to thank Dr. Zuhair Al-Shaieb for his guidance and contributions; and Dr. John Shelton, who aided with suggestions and constructive criticism in regard to the construction of structural cross sections, as well as the age relationships of the tectonic features found in the Italian Mountain area. The author would also like to express his gratitude to AMAX EXPLORATION, Inc., Denver, Colorado, for the use of some of its field equipment during the summer of 1972, and to the Agronomy Department at Oklahoma State University for its cooperation in running the author's trace metal analyses.

TABLE OF CONTENTS

| Chapter | Page |
|--|------|
| I. ABSTRACT | 1 |
| II. INTRODUCTION. | 3 |
| History. | 7 |
| Field Work and Topography. | 8 |
| Purpose of Investigation | 9 |
| Methods of Investigation | 10 |
| Previous Investigations. | 12 |
| III. STRATIGRAPHY. | 14 |
| Precambrian Basement | 15 |
| Cambrian System | 18 |
| Sawatch Quartzite | 18 |
| Ordovician System. | 19 |
| Manitou Dolomite. | 19 |
| Fremont Limestone | 19 |
| Devonian System. | 20 |
| Chaffee Formation | 20 |
| Mississippian System. | 21 |
| Leadville Limestone | 21 |
| Pennsylvanian System | 22 |
| Belden Formation. | 22 |
| Pennsylvanian to Permian System. | 23 |
| Gothic-Maroon Formations | 23 |
| IV. IGNEOUS ROCK TYPES | 24 |
| Central Monzodiorite to Granodiorite | 30 |

TABLE OF CONTENTS (Continued)

| Chapter | Page |
|--|------|
| Granodiorite Southern Intrusive. | 38 |
| Northern Quartz Monzonite Intrusive. | 43 |
| Quartz Latite to Quartz Latite Porphyry Dikes. . . | 55 |
| Quartz Latite | 55 |
| Quartz Latite Porphyry. | 58 |
| Granophyre and Aplite-Alaskite Dikelets. | 60 |
| Amphibolite of East-Central Map Area | 64 |
| Petrogenesis of Tertiary Igneous Rocks | 65 |
| V. ORE DEPOSITS. | 69 |
| Star Mine. | 72 |
| Nature of Ore Deposits. | 72 |
| Controls of Ore Deposition. | 74 |
| Genesis of Ore Deposits. | 76 |
| Stewart Mine | 77 |
| Ender Mine. | 77 |
| Spring Creek Mine. | 79 |
| New Star Mine. | 80 |
| Minor Oxide Mineralization | 84 |
| VI. STRUCTURAL GEOLOGY. | 90 |
| The Northwest Lineament. | 90 |
| The Northeast Lineament. | 93 |
| Local Structure | 93 |
| Local Structural Relationships | 95 |
| VII. CONTACT METAMORPHISM. | 100 |
| Description of Contact Metamorphic Assemblages . . | 100 |
| Stages of Contact Metamorphism | 107 |
| Types of Metasomatism. | 109 |
| ACF and A'KF Diagrams. | 111 |
| Contact Metamorphic Facies | 115 |
| VIII. TRACE METAL ANALYSIS. | 122 |
| Sampling Procedure | 123 |

TABLE OF CONTENTS (Continued)

| Chapter | Page |
|--|------|
| Trace Metal Values | 123 |
| Observations and Interpretations. | 127 |
| Correlation Coefficients | 132 |
| IX. SUMMARY AND CONCLUSIONS..... | 136 |
| REFERENCES CITED | 142 |
| APPENDIX A. MEASURED STRATIGRAPHIC SECTION | 145 |
| APPENDIX B. TABULATION OF TRACE METAL VALUES. | 151 |
| APPENDIX C. SAMPLE PREPARATION FOR ATOMIC ABSORPTION | 155 |
| APPENDIX D. PREPARATION OF STANDARD SOLUTIONS. | 158 |

LIST OF TABLES

| Table | Page |
|---|------|
| I. Generalized Stratigraphic Section of Elk Mountain | 16 |
| II. Variation in Thickness of Paleozoic Sediments of the Italian Mountain Area | 17 |
| III. Modal Analyses of Italian Mountain Igneous Rocks | 33 |
| IV. Production Statistics for Star Mine, 1927-1928 | 71 |
| V. Statistical Parameters for All Rock Types of Italian Mountain Area | 125 |
| VI. Statistical Parameters for Quartz Monzonite | 125 |
| VII. Statistical Parameters for Monzodiorite to Granodiorite . . | 125 |
| VIII. Statistical Parameters for Granodiorite of South | 125 |
| IX. Statistical Parameters for Quartz Latite Dikes | 126 |
| X. Statistical Parameters for Belden Formation | 126 |
| XI. Statistical Parameters for Leadville Limestone | 126 |
| XII. Matrices of Correlation Coefficients for the Six Rock Types of Italian Mountain | 134 |

LIST OF FIGURES

| Figure | Page |
|---|-----------|
| 1. Geologic Map of Italian Mountain Area | In Pocket |
| 2. a. View of Italian Mountain from the East | 4 |
| b. Italian Mountain Seen from Star Basin | 4 |
| 3. Location Map | 5 |
| 4. Dikelet of Quartz Monzonite Crosscutting the Central Monzodiorite to Granodiorite Intrusive | 28 |
| 5. Photomicrograph of Central Monzodiorite to Granodiorite Intrusive | 32 |
| 6. Streckeisen's Classification of Igneous Rocks | 34 |
| 7. Photomicrograph of Hornblende Veinlet in Monzodiorite of Central Intrusive | 35 |
| 8. Severely Albitized Monzodiorite | 36 |
| 9. Limonite Staining Along Southern Margin of the Central Monzodiorite Intrusive | 37 |
| 10. Cruciform Plagioclase of Southern Granodiorite | 39 |
| 11. Peripheral Phase of the Southern Granodiorite | 40 |
| 12. Resorption Quartz Crystal of the Margin of the Southern Granodiorite | 41 |
| 13. Spherulitic Arrangement of Plagioclase from Periphery of Southern Granodiorite | 42 |
| 14. Semi-diabasic Texture of the Melanogranodiorite | 45 |
| 15. Photomicrograph of the Quartz Monzonite Porphyry | 49 |
| 16. Lination of Pyroxene, Biotite and Hornblende in Quartz Monzonite of Central Italian Mountain | 52 |
| 17. Plagioclase Rimmed by More Sodid Plagioclase, Central Italian Mountain | 53 |

| Figure | Page |
|--|------|
| 18. Photomicrograph Showing Quartz Monzonite Dikelet Cross-cutting Monzodiorite | 54 |
| 19. Flow Banding in Quartz Latite Dike | 57 |
| 20. Photomicrograph of Quartz Latite Porphyry of Clara L. Mine | 60 |
| 21. Alaskite Dikelet within Northern Quartz Monzonite | 62 |
| 22. Granophyre from Northern Margin of Quartz Monzonite | 63 |
| 23. Modal Variations of the Italian Mountain Igneous Rocks | 67 |
| 24. Modes of Italian Mountain Area Igneous Rocks | 68 |
| 25. Photomicrograph of Galena Encompassing Pyrite, New Star Mine | 81 |
| 26. Triangular Pits in Galena | 81 |
| 27. Euhedral Pyrite Crystals in Dolomitic Limestone | 82 |
| 28. Chalcopyrite Replacing Pyrite within a Gangue of Dolomitic Limestone | 82 |
| 29. Sphalerite Crosscutting Chalcopyrite | 83 |
| 30. Sphalerite Veinlets Crosscutting Pyrite but not Galena | 83 |
| 31. Magnetite-Pyrite Mass in Leadville Limestone | 85 |
| 32. Same Magnetite-Pyrite Mass Above, Pyrite Seen to be Replaced by Magnetite | 86 |
| 33. Photomicrograph of Quartz Gangue from Pyrite-Magnetite Mass in Leadville Limestone | 87 |
| 34. a. Regional Geologic Map | 91 |
| b. Explanation for Regional Geologic Map | 92 |
| 35. Structural Cross Section A-A' | 97 |
| 36. Structural Cross Section B-B' | 98 |
| 37. Chemical Composition of Rocks Plotted on ACF + A'FK Diagrams | 112 |
| 38. Three Hornfels Facies of Contact Metamorphism and Their Common Mineral Assemblages | 114 |

| Figure | Page |
|---|-----------|
| 39. ACF Diagram of Hornblende-Hornfels Facies | 118 |
| 40. ACF Diagram for Pyroxene-Hornfels Facies | 118 |
| 41. Contact Metamorphic Facies Map of Italian Mountain | 121 |
| 42. Sample Location Map | In Pocket |
| 43. Mo-Trace Metal Distribution Map | In Pocket |
| 44. Cu-Trace Metal Distribution Map | In Pocket |
| 45. Pb-Trace Metal Distribution Map | In Pocket |
| 46. Zn-Trace Metal Distribution Map | In Pocket |
| 47. Plot of Mean Trace Metal Values for Rock Types | 128 |
| 48. Plot of Threshold Trace Metal Values for Rock Types | 129 |

CHAPTER I

ABSTRACT

The Italian Mountain area is located on the eastern flanks of the Elk Mountains of Gunnison County in central Colorado at longitude $106^{\circ} 45'00''$ and latitude $39^{\circ} 57'30''$. The particular area mapped is approximately four miles in length and two and three-fourths in width.

The sedimentary regime of Italian Mountain can be divided into two basic units: (1) a lower Paleozoic marine shelf-type sedimentary section, and (2) a thick section of Permo-Pennsylvanian clastic sediments, deposited in the central Colorado Basin, in the form of coalescing alluvial fans off the Sawatch and Uncompahgre Ranges.

The Tertiary (early Oligocene to early Miocene) igneous complex of Italian Mountain consists of three main igneous rock types: (1) quartz monzonite in the North Italian Mountain region, (2) monzodiorite-granodiorite in the central region, and (3) a granodiorite in the South Italian Mountain map area. It is therefore a composite intrusive complex.

Two orogenic episodes are responsible for the structural geology of Italian Mountain: (1) Sawatch uplift of Laramide time, and (2) intrusion of the Italian Mountain igneous bodies themselves. The structural features are aligned along two lineaments or trends: (1) northwest lineament, and (2) a northeast lineament.

Two distinct contact metamorphic facies are displayed by the contact zones of Italian Mountain: (1) the pyroxene-hornfels facies, and (2) the hornblende-hornfels facies. A less distinct albite-epidote-hornfels facies was noted at the outside perimeter of the hornblende-hornfels facies. Thermal metamorphic effects are expressed within the Leadville Limestone by the recrystallization of the limestone to an aggregate of coarse calcite rhombohedrons.

Trace metal analyses reveal that: (1) the mesothermal replacement deposits of Cu-Pb-Zn within the Leadville Limestone and the Cu-Mo mineralization of skarn zones were closely associated with the quartz monzonite intrusive of North Italian Mountain, and (2) the quartz latite dikes and numerous Laramide or Tertiary derived faults served as conduits along which mineralizing solutions passed.

CHAPTER II

INTRODUCTION

Italian Mountain is located on the eastern flanks of the Elk Mountains of Gunnison County in central Colorado at longitude $106^{\circ}45'$ and latitude $39^{\circ}57'30''$ (Fig.2). Italian Mountain is comprised of three separate peaks: one in the north at an elevation of 13,051 feet, a central peak at 13,378 feet, and a southern peak at 12,830 feet. The particular area mapped is approximately four miles in length and two and three-fourths miles wide. This area is bounded on the north by a line connecting the south slope of Mount Tilton and North Italian Creek; on the west by Cement Creek; on the east by South Italian Creek and Spring Creek; and on the south by an east-west line just beyond the southernmost extension of the South Italian intrusive (see Figures 1 and 3).

There are two main means of entry into the Italian Mountain area from the southwest and from the east. The southwestern route begins at Gunnison, Colorado with Highway 135 which leads north to Crested Butte (twenty-nine miles). Along Highway 135 the Highway 306 and Cement Creek cutoffs are found at eleven and twenty-two miles, respectively. Moving north along Highway 135 one encounters the town of Almont and Highway 306 which leads Northeast to Taylor Park along the Taylor River. Approximately 6 miles northeast along Highway 306 a general store is found at the Spring Creek cutoff. At a distance of twenty-two miles along the Spring Creek Road the Mosca Ranger

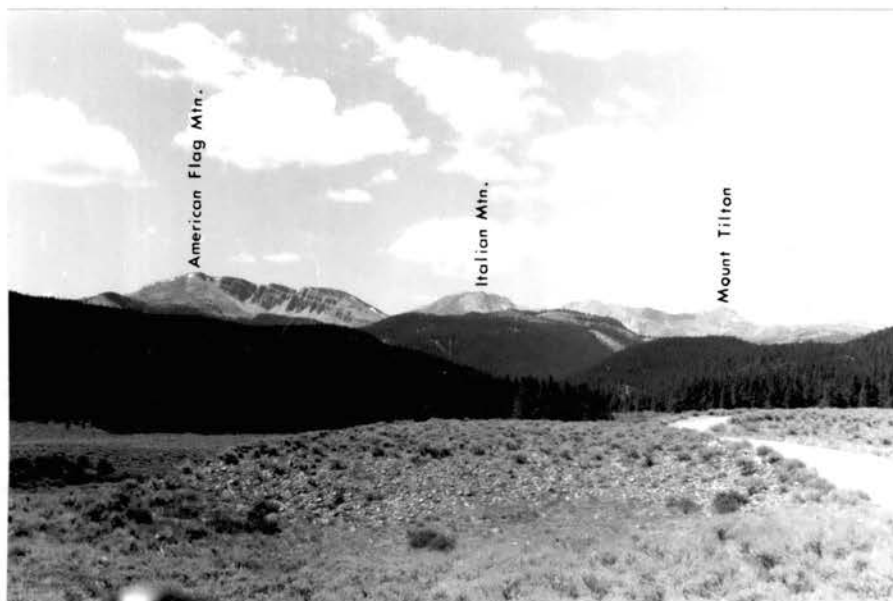
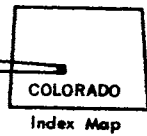
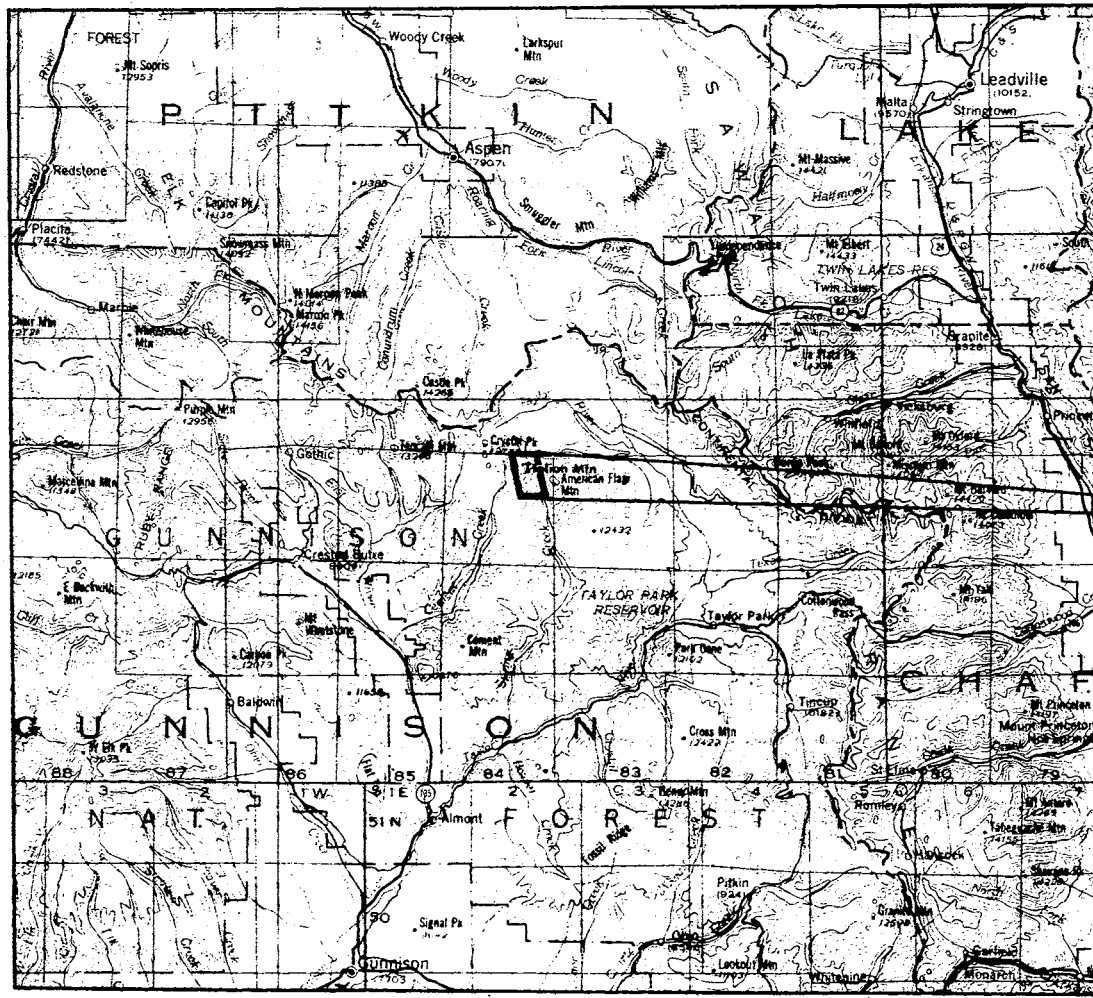


Figure 2a. View of Italian Mountain from the east along the Italian Creek Road.



Figure 2b. Italian Mountain seen from Star Basin, TQm_n-quartz monzonite, Ps-Paleozoic sediments, PE-_n Precambrian rocks.



10mi
Scale: 1 inch = 10miles

Figure 3. Location map for Italian Mountain

Station is encountered. Beyond this point the road is marshy in places and a bit rocky, and it is recommended that only four-wheel drive vehicles or pickups with short wheel bases and high clearance travel this route. The Stewart mine, located on the east flank of central Italian Mountain and the west flank of American Flag Mountain, is approximately eight miles north of the Mosca Ranger Station. The Star Mine in the Star Basin east of North Italian Mountain is reached by winding up around and over the ridge between Central Italian Mountain and American Flag Mountain.

The Cement Creek cutoff, twenty-two miles north of Gunnison along Highway 135, winds up around the west side of Italian Mountain and ends at the Ender mine. The only access to the east side of Italian Mountain from the end of the Cement Creek Road is by back-packing up and over the top of North Italian Mountain.

The eastern route into the Italian Mountain area begins at Buena Vista, Colorado, with Highway 306 which parallels the Middle Cottonwood Creek up over the Cottonwood Pass and the Continental Divide into Taylor Park. At Taylor Park Highway 306 intersects with the Taylor River Road leading northeast to Dorchester, approximately fourteen miles from Taylor Park. About two and one-half miles before Dorchester one makes a turn left onto the Italian Cement Creek road which leads to the Star Basin just east of North Italian Mountain. The Italian River road is laden with marshes, stream crossings and rock glaciers composed of Precambrian granite, all of which make travel quite slow and rough. Last summer (1972) the Gunnison National Forest Service attempted to improve the Italian Creek Road with a bulldozer and was successful in eliminating a few marsh crossings but because culverts were not installed over stream crossings deep gulleys have developed.

History

Several theories have been postulated as to why this mountain bears the name Italian Mountain (North Italian Mountain in the old literature 1894 Emmons). Many have suggested that upon approaching Italian Mountain from the east, during the late morning hours, the colors of the Italian flag (green, red, and white) can be seen gleaming forth from the peaks and slopes of the mountain. The variety of flowers which cover the slopes of Italian Mountain is very similar to that found in the Alps of northern Italy. Andy Anderson, an old-time prospector who has spent his summers at Italian Mountain for the past 18 years informed the author that several botanists have done their Ph.D. dissertations on the unusual flora of Italian Mountain. The profile presented by the northern face of Central Italian Mountain with its cathedral-shaped spires, brings to mind the majestic Cathedrals of Rome, Italy.

Italian Mountain is a noted tourist attraction of central Colorado because of the occurrence of a rare gemstone called lapis lazuli. This gemstone is a product of contact metasomatism and is found in limestone beds of the Belden Formation near the contact with the northern quartz monzonite intrusive. Lapis lazuli is found in only four places the world over: Afghanistan, Lake Baikal and Siberia (U.S.S.R.), Chile, and parts of Colorado. This gemstone is dark blue in color and consists of a mixture of lazurite $[(Na,Ca)_8(Al Si_{10}O_{34})(SO_4,S,Cl)_2]$, calcite, pyroxene, other silicates, and commonly contains small disseminated particles of pyrite.

Field Work and Topography

The normal field season for this particular part of Colorado extends from mid-June to late September. Nights are cold with temperatures dropping to the mid-thirties and to freezing especially during mid-June and late September. During the days the climate ranges from cool in mid-June to July (50's - 60's) and mild from July to the end of August (60's - 70's). The rainy season usually occurs from July through mid-August in the form of quickly developing thunderstorms in the late afternoon, coming out of the southwest or northwest.

The weather was unusual during the summer of 1972, for during the author's field season (July 2-August 16) the rain occurred mostly after 7 pm and in the early morning hours, 5-8 am. The temperature during the day, from mid-July to early August, was in the low to middle 70's.

Most of the Italian Mountain area is above the timberline, except for the Spring Creek and Cement Creek areas, thus providing for good outcrop mapping. Mapping of contacts between igneous intrusions and Paleozoic sediments was, however, hampered by the large amount of talus covering the slopes, especially along the west-central and southwestern map areas, and by rock glaciers along the train of the glacial valley occupying the central portion of North Italian Mountain.

Because Italian Mountain has suffered extensive glaciation, and because of the steep dips of sedimentary and igneous rock outcrops, the topography is quite rough in places with many steep slopes. The elevation ranges from 11,600 feet in Star Basin to over 13,200 feet at the peaks of the mountain, over a horizontal distance of one mile.

From the U-shaped valley of Cement Creek the elevation increases from 11,080 feet to over 13,200 feet at the peak of Central Italian Mountain over a horizontal distance of one mile. Moving at a good pace on foot, it takes an average of one and one quarter hours to reach the summit of North Italian Mountain from the Star Basin, and two hours to reach the same peak from the valley of Cement Creek. Every peak is accessible from some angle without the use of ropes and pitons.

Purpose of the Investigation

The author's thesis adviser Dr. Tommy B. Thompson, while doing general reconnaissance geology in the Elk Mountain-Sawatch Range area, happened upon the Italian Mountain "stock". Dr. Thompson noted that this area was well suited for a thesis project because: (1) Italian Mountain occupies a relatively small area, (2) Italian Mountain is almost entirely above timberline, making mapping easy, (3) it displays interesting contact metamorphic mineral assemblages, and (4) intrusives are in contact with Leadville Limestone which is mineralized with Pb and Ag, out away from the contact, in the Star Basin, at the head of Spring Creek (Stewart Mine), and on the southern flanks of Mount Tilton (Ender Mine - See Figure 1).

The author became very much interested in this area after doing some fairly extensive research reading. Most of the investigations dealing with the Italian Mountain area are in the form of unpublished Master's and Ph.D, thesis, which are more concerned with stratigraphy and structure rather than igneous petrography, ore deposits, and contact metamorphism. The author noted a discrepancy between these investigations as to the nature of the Italian Mountain "stock". Some call it a homogeneous granodiorite stock or a quartz

monzonite stock, and still others call it a composite quartz monzonite to granodiorite intrusive complex. Thus one of the purposes of the author's investigation was to determine whether the Italian Mountain "stock" is indeed one stock or composed of several intrusive rock types intruded at different times.

Also in the previous theses investigations the Ag-Pb ore deposits associated with the Italian Mountain intrusives were described and it was merely suggested that the mineralization was contemporaneous with the quartz monzonite intrusive phase. Therefore the author collected rock chip samples over the entire Italian Mountain intrusive or intrusives and surrounding Paleozoic sediments with the hope that geochemical trace metal analysis would reveal: (1) a definite trend or gradient from one intrusive center to the Pb-Ag mineralization or (2) high concentrations (above the normal background values for the particular rock types) of Pb, Zn, Cu, or Mo.

In previous investigations on the Italian Mountain area it has simply been noted that contact metamorphism exists and various metamorphic minerals have been described, but no attempt has been made to define metamorphic facies based upon mineral assemblages. Thus a third purpose of the author's thesis investigation is to specify metamorphic facies, within the Paleozoic sediments along the contact with the intrusives, based on mineral assemblages, and to define their approximate extent.

Methods of Investigation

The author conducted the field work for his Master's thesis during the summer of 1972 (from July 2 to August 16). The actual field work consisted of geologic mapping, the collection of rock chip

samples for trace metal analysis, and the collection of hand samples for petrographic work. Mapping was done on aerial photographs obtained from the U. S. Forest Service out of Denver, Colorado. Regular nine by nine contact prints at the scale of 1:15,840 were satisfactory in displaying the geology and sample locations. However, the nine by nine photographs, covering the Italian Mountain proper, were enlarged by a factor of 2.5 and used as a reference sheet upon which the geology and sample locations were transferred each day. Upon returning to Oklahoma State, in the fall, the geologic mapping on the aerial photos was transferred to a topographic base map in order to give the geology a depth dimension and to facilitate the construction of topographic profiles and structural cross sections. The Italian Mountain area is split between two 7.5 minute quadrangles: the Pearl Pass to the west and the Italian Creek to the east. Thus the topographic base map was constructed by splicing the two 7.5 minute quadrangles together and expanding the scale from 1:24,000 to 1:15,840 (the same scale as the aerial photographs).

Laboratory work for the author's thesis project can be divided into two phases: (1) petrographic, and (2) trace metal analysis. The petrographic analysis consisted of describing some twenty-five thin sections of the igneous rock types, and a description of five polished sections of the typical mesothermal ore deposits associated with the Italian Mountain intrusives.

Some eighty-eight rock chip samples were collected over the three intrusive rock types of Italian Mountain for trace metal analysis (Pb,Zn,Cu,Mo). One gram portions of these samples were prepared for actual trace metal analysis by first digesting them in

HF-HClO₃ + HNO₃ and finally bringing the residue into solution by boiling in 5 ml. of HCl, and diluting to a volume of 50 ml.

Standard solutions for Pb, Zn, Cu, and Mo were then prepared from 1000 ppm stock solutions. The unknown solutions were then analyzed for Pb, Zn, Cu, and Mo, by the Agronomy department at Oklahoma State University, on a Perkin-Elmer atomic absorption spectrophotometer (Model 403) equipped with a Digital Concentration Readout Accessory. The exact procedure for the preparation of samples and standard solutions may be found in Appendixes C and D.

Previous Investigations

Few professional papers have been published on the Italian Mountain area and in fact the more detailed studies are in the form of unpublished Master's and Ph.D. theses. The few professional publications are either generalized geologic maps, or stratigraphic and mineralogical studies. Given below is a listing, in chronological order, of the studies and investigations the author was able to find dealing with the Italian Mountain area.

1873-1874 - Peale, Hayden and Holmes, under the sponsorship of the Hayden Survey, gave an account in prose form of their studies conducted in the Elk Mountains. These reports are the first accounts of the geology of the Elk Mountains; pp. 58-65 refer to Italian Mountain and the surrounding area.

1894 Emmons, Cross, and Eldridge mapped the Crested Butte Quadrangle for the U.S.G.S. in Folio 9. This report includes the western half of Italian Mountain.

1927 Cross and Shannon presented an in-depth mineralogical study of contact metamorphic minerals associated with the northern quartz monzonite stock of Italian Mountain.

1944 Johnson made a stratigraphic study of the lower Paleozoic stratigraphy of the Elk Mountains which included measurements and detailed descriptions. The author uses Johnson's nomenclature for the Paleozoic strata in his thesis area.

- 1950 Garrett's Master's thesis (Colorado School of Mines), on the geology and Ag, Pb deposits of the Star Basin southeast of North Italian Mountain, Taylor Park Quadrangle, gives a good coverage of igneous petrology, petrography and the genesis of the Pb-Ag mineralization.
- 1951 Murphy deals with the geology of the upper Cement Creek area, Crested Butte Quadrangle (M.S. thesis from the University of Kentucky), and provides a good description of stratigraphy and paleoenvironments.
- 1952 Langenheim conducted a detailed stratigraphic study of the Permian-Pennsylvanian sediments in the Crested Butte Quadrangle. The author employs Langenheim's nomenclature in his thesis.
- 1956 Gaskill's thesis on the geology of the Whiterock Mountain area Crested Butte Quadrangle (M.S. thesis, University of New Mexico), gives an excellent coverage of stratigraphy and igneous petrology. Whiterock Mountain is only 2 miles to the northwest of Italian Mountain. Several geologists have suggested that the intrusives of Italian Mountain are genetically related to the Whiterock pluton.
- 1967 Slebir's thesis on the geology of the area at the head of Cement Creek, Crested Butte Quadrangle (M.S. thesis, Colorado School of Mines), is mostly a stratigraphic report.
- 1961 Prather's thesis on the geology of North Italian Mountain and the upper Spring Creek area, Taylor Park Quadrangle (M. S. thesis, University of Colorado), is a combination stratigraphic and petrologic study of the Italian Mountain area.
- 1964 Prather's thesis on the Stratigraphy and Structural Geology of the Elk Mountains, Colorado (Ph.D. thesis, University of Colorado), is an excellent account of Paleozoic to Cretaceous Stratigraphy of the Elk Mountains and the regional structural fabric of the Elk Mountains.
- 1972-1973 Cunningham's Ph. D. thesis, (Stanford University, California), is a study of the igneous petrology and ore deposits of the Italian Mountain area.

CHAPTER III

STRATIGRAPHY

Two basic units characterize the sedimentary reigne of the Italian Mountain area: (1) a lowermost Paleozoic shelf-type sedimentary section represented by the Sawatch Quartzite, Cambrian in age; Manitou Dolomite, Ordovician in age; Fremont Limestone, Ordovician in age; Chaffee Formation, Devonian in age; and the Leadville Limestone (Blue Limestone), Mississippian in age. These lower Paleozoic shelf-type deposits represent a sedimentary cycle where erosion and non-deposition were dominant over sedimentation; (2) a thick section of Permo-Pennsylvanian clastic sediments deposited in the Central Colorado basin (Eagle basin), consisting of the Belden Formation of Pennsylvanian age, the Gothic Formation of Permian age, and the Maroon Formation of Permian-Pennsylvanian age. These Pennsylvanian and Permian rocks of the Elk Mountains were deposited in a basin bounded by highlands on the northeast (Front range) and southwest sides (Uncompahgre Range). At the beginning of Pennsylvanian time, a shallow sea invaded the Central Colorado basin and deposited a low energy sequence of fissile black shale and thin beds of limestone (Belden Shale), derived from the erosion of the Leadville Limestone and Chaffee Formation (shales and sandstones). The coarse-grained sandstones and conglomerates of the Gothic Formation, which lie conformably over the Belden Formation, attest

to a period of uplift during which the Colorado trough or basin was being filled with coarse sediment from the highlands to form a geosyncline. The coarse sediments produced by continued uplift were then deposited subaerially in the form of coalescing alluvial fans off the Sawatch and Uncompahgre Ranges. Table 1 below gives a generalized stratigraphic section of the sedimentary regime of the Elk Mountains. Because of the complex structural nature of the Elk Mountains and the varied depositional environments the thicknesses of the various stratigraphic units vary from place to place, as displayed by Table II.

In order to become familiar with the Paleozoic stratigraphic units, the author measured a section in a cirque along the northeast side of American Flag Mountain (Fig. 2A). This particular area was chosen because of: its good exposures, lack of off-setting faults, ease of access, and because a comparison could be made with a similar section made in the same area by Johnson (1944) and Prather (1961). The author's measured section is found in Appendix A of this thesis.

Precambrian Basement

Precambrian granite, possibly Pikes Peak or Silver Plume, is exposed along the northern and eastern map areas where it has been faulted up by the Sawatch uplift of Laramide time. This Precambrian granite is typically coarse-grained and porphyritic with phenocrysts of pink orthoclase or microcline, (1-15 mm in length), with quartz and biotite being interstitial. To the northwest the Precambrian system grades into a quartz-biotite schist to gneiss impregnated by aplitic to pegmatitic dikes and irregular masses.

TABLE I
 GENERALIZED STRATIGRAPHIC SECTION OF THE ELK
 MOUNTAINS (MODIFIED AFTER
 PRATHER, 1964)

| Age | Formation | Thick | Description |
|-------------------------|-----------|---------|--|
| Permo- Pennsylvanian | Maroon | 0-6000' | Conglomerate and sandstone, red, arkosic; shale and siltstone, micaceous |
| Pennsylvanian | Gothic | 1500' | Conglomerate, sandstone, siltstone, and shale, brown, arkosic; marine limestone; bioherm and gypsum locally |
| | Belden | 500' | shale, fissile with interbedded black limestone |
| Mississippian | Leadville | 150' | Limestone, gray to black, upper part massive beds, lower part thin to medium bedded |
| Devonian | Chaffee | 180' | Dyer Dolomite member: dolomite and dolomitic limestone, dark gray, thin to medium-bedded. Parting member: mudstone and shale, variegated; sandstone, brown; and dolomite |
| Ordovician | Fremont | 0-85' | Dolomitic limestone, dark gray, medium to thick-bedded |
| | Manitou | 250' | Dolomite, gray, abundant stringers and nodules of black to cream colored chert |

TABLE I (Continued)

| | | | |
|-------------|---------|------|--|
| Cambrian | Sawatch | 250' | Quartzite, white to light brown, thin to medium-bedded; conglomeratic at base; sandstone, brown to greenish brown, glauconitic; sandstone, brown, shaly, calcareous. |
| Precambrian | - | - | Granite, coarse grained and porphyritic in pink potassium feldspar, gneiss to schist in places with aplite to pegmatitic dikes and patches. |

TABLE II

VARIATION IN THICKNESSES OF PALEOZOIC SEDIMENTS
OF ITALIAN MOUNTAIN AND SURROUNDING AREA
(PRATHER 1964, JOHNSON 1944,
AND GARRETT 1950)

| Location | Formation and Thickness | | | | |
|-------------------|-------------------------|---------|---------|---------|-----------|
| | Sawatch | Manitou | Fremont | Chaffee | Leadville |
| Mount Tilton | 137' | 273' | 14' | 147' | 92' |
| North Italian Mt. | 273' | 346' | 0 | 139' | 172' |
| American Flag Mt. | 249' | 242' | 86' | 178' | 306' |
| Cement Creek | 282' | 179' | 39' | 300' | 224' |
| Star Basin | 165' | 388' | 0 | 76' | 328' |

Cambrian System

Sawatch Quartzite

The Sawatch Quartzite borders the entire eastern and northern map area and lies unconformably upon the Precambrian basement. Because the Sawatch Quartzite is steeply dipping to overturned throughout the map area, it is usually found at the top of slopes leading to valleys, especially along Spring Creek. The Sawatch Quartzite is cut by several strike-slip faults along Spring Creek and it is the repetition of this formation which allows one to depict the faults themselves. Johnson (1944) divided the Sawatch Quartzite into four members: (1) lower quartzite member: consisting of medium-massive-bedded, fine-grained white quartzite with a vitreous luster, and a basal conglomerate, made up of rounded pebbles of quartz and feldspar grains, near the contact with the Precambrian basement; (2) a glauconitic quartzite member consisting of a series of brown calcareous shaly sandstones colored green in places by its high content of glauconite, and fine-grained quartzite with shale partings; (3) an upper quartzite member, with massive-bedding, consists of a fine-grained quartzite green to greenish gray in color; and (4) an upper member consisting of sandy, shaly, calcareous transition beds termed the "Peerless Shale Member". In the Italian Mountain area all the above mentioned members of the Sawatch Quartzite are present except for the Peerless Shale Member, which is absent along Spring Creek.

Ordovician System

Manitou Dolomite

The Manitou Dolomite is immediately underlain by the Sawatch Quartzite and displays a similar distribution to that of the Sawatch Quartzite (see Figure 1). The sandy dolomite beds of this formation comprise the cliffs along Spring Creek and North Italian Mountain. The Manitou Dolomite consists of a fine-grained gray to bluish-black dolomite to dolomitic limestone with a brown coarse sandy dolomite at its base. The formation is easily recognized because of the nodules and stringers of chert, (cream to metallic black in color) along bedding planes, which are especially prominent in the middle of the formation. An erosional unconformity exists between the Sawatch Quartzite below and the Manitou Dolomite above.

The Harding Sandstone of Johnson (1944) consists of a series of sandstones and shale beds representing a break in the carbonate section during Ordovician time, which suggests a recession in the seas at the time. This formation is absent in the Star Basin and on North Italian Mountain, but is fairly well defined along Spring Creek. The Harding Sandstones are thus included as part of the Manitou Dolomite on the author's geologic map.

Fremont Limestone

The Fremont Limestone is very thin or absent from North Italian Mountain and in the Star Basin but is well defined along the Spring Creek valley. Because the thickness of this formation varies so much, it was combined with the Manitou Dolomite on the geologic map. The Fremont Limestone consists of a grayish-brown to dark gray

fossiliferous limestone (corals and crinoid fragments) which weathers to a dark gray or black limestone with sharp jagged edges. At its base is found a maroon to reddish-purple shale.

Devonian System

Chaffee Formation

The Chaffee formation is exposed parallel to the other Paleozoic sediments in the Italian Mountain area and is well defined both along Spring Creek, the Star Basin, and North Italian Mountain. This formation consists of two members: (1) a lower Parting Member, and (2) an upper Dyer Dolomite. The Parting Member is composed of yellow to red colored fine-grained sandstone, sandy shale, shale, mudstone, and marl. In its lower portion the Parting Member is green in color with bedding varying from thin to thick (3-5') beds of sandstone with marly or limestone beds near the top.

The upper member of the Chaffee Formation, the Dyer dolomite, is composed of medium-bedded, fine-grained gray dolomite to dolomitic limestone with calcite vugs along bedding planes. Because the Chaffee Formation weathers to a yellowish-brown to buff color, it is set apart from the dark gray to black Leadville above and the dark gray Manitou dolomite below. The overlying Leadville Limestone is disconformable with the Chaffee Formation as evidenced by a basal sandstone and a depositional breccia at the base of the Leadville Limestone.

Mississippian System

Leadville Limestone

In the Italian Mountain area the Leadville Limestone, because of its permeability and ease of solution, has served as a host rock for the hydrothermal Ag-Zn-Pb deposits. Also because it is exposed along the contact with the northern quartz monzonite intrusive, it displays skarn development with a distinct contact metamorphic mineral assemblage.

The Leadville Limestone displays a basal quartzite member (14 feet thick), white to greenish-gray in color, and fine-grained with irregular massive-bedding. The quartzite is conglomeratic in places, especially near the new mine workings in the extreme northwest Star Basin, where it is heavily laden with disseminated pyrite. The Leadville Limestone is dark gray to bluish-black in color and its crystallinity varies from medium to fine, with massive-bedding. Out from the intrusive contact the Leadville Limestone is recrystallized and bleached white.

Toward the middle of the formation are found numerous solution cavities filled either with calcite and siderite or unconsolidated sand. Also, below this zone of solution cavities is found a zone of brecciated limestone.

The top of the Leadville Limestone is marked with sinks and solution cavities, and thus the Pennsylvanian Belden shale lies unconformably upon it.

Pennsylvanian System

Belden Shale

The Belden Formation is in contact with the Italian Mountain intrusives along the entire eastern part of the map area, and also along parts of the northern and northwestern contact zones (see Figure 1).

In the Italian Mountain area the author found the Belden Formation to consist of three basic members: (1) a basal quartzite to pebble-conglomerate (with pebbles of Leadville Limestone and black chert of the Manitou Dolomite) member; (2) a thick carbon-rich black shale member which is very fissile; and (3) a thick limestone member with interbeds of shale. The upper shaly limestone member of the Belden Formation occurs as roof pendants and included wedges within the northern quartz monzonite intrusive (see Figure 2). Within these wedges and roof pendants skarn development is the most widespread and of the greatest intensity. Elsewhere the shaly limestone member of the Belden Formation, where in contact with the intrusives, displays silicification, skarn or tactite, disseminated and vug-like masses of cubic pyrite, and lapis lazuli.

There is a gradation between the Belden Formation below and the Gothic Formation above which is characterized by a change in color from black to light brown or buff.

Pennsylvanian and Permian Systems

Gothic-Maroon Formations

Vanderwilt (1935) coined the name "Hermosa Formation" for the arkosic sandstones to conglomerates overlying the Pennsylvanian Belden Formation. Langenheim (1952) used the name "Gothic Formation" for the lower unit of the Hermosa Formation and "Maroon" Formation for the upper unit. Langenheim based his division of Vanderwilt's "Hermosa Formation" upon a sharp break in color from buff or grayish-brown in the Gothic Formation to reddish-brown or red (maroon) in the Maroon Formation. Langenheim's nomenclature, for the Pennsylvanian to Permian strata, is adhered to in this thesis.

The Gothic Formation consists of buff colored siltstone, arkosic sandstone, conglomerate (with pebbles of Leadville Limestone and black chert), massive sandy limestone, and fine-grained dark gray limestone. In the mapped area the Gothic Formation is in contact with the southern Italian Mountain granodiorite intrusive along its entire western border.

The Maroon Formation is composed of various members: (a) maroon to brick-red colored limestone-pebble conglomerate, (2) a feldspathic sandstone medium - coarse-grained, (3) a thin-bedded red siltstone, and (4) a medium-bedded calcareous reddish-purple shale. In the Italian Mountain area the Maroon Formation is only exposed in the southwest, outside the extent of the Gothic Formation (see Figure 1).

CHAPTER IV

IGNEOUS ROCK TYPES

The Tertiary igneous complex of Italian Mountain consists of three main igneous rock types: (1) quartz monzonite in the North Italian Mountain region, (2) monzodiorite to granodiorite in the central region, and (3) a granodiorite in the southern Italian Mountain map area (see Figure 1). It is thus a composite intrusive complex.

Obradovich, Mutschler, and Bryant (1969) have conducted a potassium-argon age dating study on the igneous rocks of the Elk Mountains and vicinity. They divided the post-Paleozoic intrusive plutons of the Elk Mountains, and surrounding areas, into four main groups:

(1) Felsic porphyries consisting of albite-aplite porphyry and albite-alaskite porphyry both of which are common in the Aspen mining district. These felsic porphyries take the form of sills and fault-controlled intrusives emplaced before, contemporaneously, and after high-angle faulting along the western margin of the Sawatch Range.

(2) Stocks, laccoliths, sills, and dikes, composed of granodiorite, cutting Laramide derived low-angle thrust faults in the Elk Mountains. High-angle faulting (both normal and reverse) of a younger age than the thrust faults occurred during and after the emplacement of the granodiorite plutons.

(3) Porphyritic gabbro and lamprophyre dikes and sills are found cutting group 2 granodiorite plutons in the western Elk Mountains and northern Ruby Range.

(4) Soda granite of Treasure Mountain which crosscuts dikes of group 2 and group 3. Radiometric age dates run on mica separates from fresh rock samples of the above mentioned groups indicate the following ages: (1) Late Cretaceous (67.4 ± 2.2 my - 72.2 ± 2.2 my) for group 1 plutons, (2) middle Tertiary-Oligocene (29.0 ± 1.1 my - 34.1 ± 1.4 my) for group 2 plutons, and (3) late Tertiary - late Miocene and early Pliocene- (12.3 ± 0.6 my - 12.5 ± 0.6) for group 4 plutons; no age dates were given for group 3 igneous rocks.

The group 2 Oligocene granodiorite rocks exhibit some cross-cutting relationships. Obradovich and others (1969) state that the original intrusive activity was in the form of large plutons of granodiorite such as the Mount Sopris, Snowmass, and Whiterock igneous bodies of the Elk Mountain Range (see Fig. 34). The north-east-trending Elk Range thrust fault most likely exerted structural control over the emplacement of the Snowmass and Whiterock plutons. Following the intrusion of the granodiorite plutons granodiorite porphyry dikes, sills, and laccolithic bodies were emplaced in the Elk Mountains, which in turn are crosscut by small granodiorite to quartz monzonite stocks.

A sample of light-gray granodiorite rock from the Whiterock pluton of Hayden Peak quadrangle, Pitkin County, gave a radiometric K-Ar age date of 33.9 ± 10 million years or early Oligocene. Vanderwilt, Cross and Prather have suggested that the Italian Mountain intrusives are but the surface expression of the Whiterock

granodiorite pluton at depth, and if so the Italian Mountain intrusives are of Oligocene age. On the other hand the Italian Mountain intrusives may represent later stage stocks emplaced after the large granodiorite pluton had crystallized. If this is the case the Italian Mountain intrusives are younger than early Oligocene and are quite conceivably late Oligocene to early Miocene in age.

Assuming a common parent magma for the three intrusive bodies of Italian Mountain, and based upon crosscutting relationships and the process of magmatic differentiation, the author proposes the following age relationships: (1) the monzodiorite to granodiorite central intrusive is the oldest igneous rock unit and represents the initial magma composition.

(2) With further differentiation and the concentration of volatiles a granodiorite body was forcefully intruded in the southern sector of Italian Mountain. No dike rocks were associated with this granodiorite intrusive but late stage hydrothermal solutions rich in sulphur were emitted along the margins, along various cooling fractures, and collapse faults, only to be deposited as pyrite produced by the combination of S_2 (g) with the iron in biotite and other ferromagnesian minerals, present in the host rock. These hydrothermal solutions also brought about argillic alteration, of the granodiorite host rock, where the plagioclase is altered to sericite, kaolinite, and/or montmorillonite.

(3) The final intrusive phase was that of the quartz monzonite of North Italian Mountain. This quartz monzonite body displays a definite zonation from a ferromagnesian-rich granodiorite around its perimeter, to a coarse grained quartz monzonite slightly porphyritic

in quartz and plagioclase, and with a well developed quartz monzonite porphyry at the interior, which displays phenocrysts of zoned plagioclase up to 4 cm in length and quartz phenocrysts up to 4 mm in length. At the contact between the northern quartz monzonite and the central monzodiorite - granodiorite many dikelets of quartz monzonite 1-4 inches wide, were found penetrating the darker colored monzodiorite (see Figure 4), and xenoliths of monzodiorite, some as large as five inches in diameter, were found within the quartz monzonite intrusive near the contact.

(4) Next the quartz latite to quartz latite porphyry dikes found radiating out from the perimeter of the northern intrusive body (see Figure 1) were injected into the surrounding Paleozoic sediments along fractures developed by the intrusion of the quartz monzonite and previous intrusive activity. The author believes that these quartz latite dike rocks were produced through continuing differentiation of a parent igneous melt, common to both the quartz monzonite and the dike rocks. A comparison of the average quartz, plagioclase, and potassium feldspar compositions and anorthite content of the plagioclase, common to the quartz monzonite as opposed to the quartz latite to quartz latite porphyry dike rocks, suggest that the dike rocks are a later stage differentiate of a parent magma chamber. The average plagioclase, potassium feldspar, and quartz content of the quartz monzonite is as follows: 39, 24, and 27 percent respectively, as opposed to 25, 35, and 28 percent in the quartz latite dikes. There is also a variation in the anorthite content of the plagioclase, the quartz monzonite displaying an average of An_{40} as opposed to An_{37} in the quartz latite dike rocks,

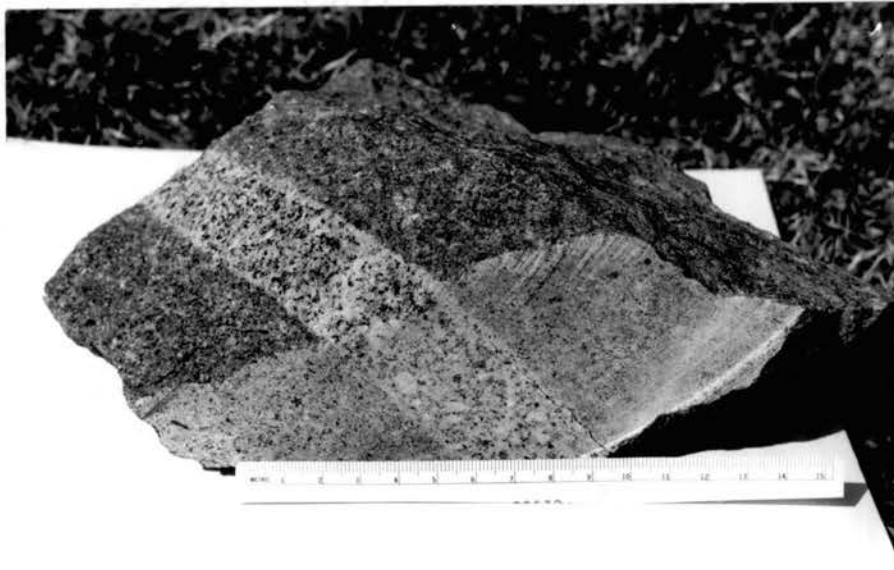


FIGURE 4. Dikelet of quartz monzonite crosscutting the central monzodiorite to granodiorite intrusive.

(see Table 3, and Figures 23 and 24, pp. 67 and 68).

Crosscutting relationships, between the quartz monzonite intrusive body and the quartz latite dike rocks, are not helpful in establishing an age relationship because nowhere was the author able to find the dikes extending into and crosscutting the quartz monzonite intrusive. This lack of apparent crosscutting relationships was due to: (a) the large amount of talus cover around the margins of the northern quartz monzonite intrusive, and (b) the nature of the emplacement of the quartz latite dikes. It is the author's belief that these dike rocks were injected at depth, along the margins of the cooling quartz monzonite intrusive, within fractures. The dike rock is exposed at the surface only along fractures or faults, within the Paleozoic sediments, allowing the ascending melt access to the surface.

(5) The last stages of magmatic melt emission before hydrothermal fluid expulsion from the parent magma chamber are represented by the series of aplite to alaskite dikelets, 3-6 inches wide, found impregnating the quartz monzonite at its extreme northwest perimeter. Also along the northern contact with the Belden Formation a granophyre zone, 1-2 feet wide, was discovered.

Much evidence suggests that these three igneous bodies were emplaced forcefully into the preexisting host rocks: (1) the Paleozoic sediments invaded by the intrusives are tilted at high angles, and in some cases are overturned. Also, the structural fabric of the surrounding sediments is indicative of forceful injection, for there exists many well developed high-angle faults both normal and reverse in nature. (2) stopping and assimilation

of the Belden Formation, especially in the central map area where veinlets of diopside and scolecite are found along fractures in the monzodiorite to granodiorite intrusive; (3) xenoliths of the Belden Formation found within the quartz monzonite of North Italian Mountain; (4) roof pendants of the Belden Formation within the quartz monzonite intrusive of North Italian Mountain, and (5) the highly fractured nature of preexisting intrusives, especially the central monzodiorite to granodiorite igneous body.

Hydrothermal alteration effects will be discussed within the context of the following individual igneous rock-type descriptions.

Central Monzodiorite to Granodiorite

This intrusive body is located in the saddle between Central Italian Mountain and South Italian Mountain (see Figure 1). A typical hand sample, void of contact metamorphic effects, is medium-grained, granular, slightly porphyritic in plagioclase with some phenocrysts 3-4 mm in length, with a color index of 23-25. A diabasic texture is displayed whereby plagioclase is encompassed by interstitial biotite and pyroxene. With a hand lens the minerals plagioclase, potassium feldspar, biotite, pyroxene, and epidote can be identified. Slight argillic alteration of the plagioclase is evident in that it powders when pressure is applied with a knife blade. Microscopic examination of a thin section (Msc-2), of this intrusive rock type, can be described as being holocrystalline, hypidiomorphic equigranular to slightly porphyritic in plagioclase with phenocrysts ranging from 3-4 mm in length. A diabasic texture, is well pronounced, with biotite and pyroxene

encompassing subhedral to euhedral plagioclase of labradorite composition (An-52). In this thesis the plagioclase composition was determined by measuring the extinction angles on crystals displaying combined Carlsbad-albite twinning. Kerr (1959) provides tables for the actual anorthite content based on the measured extinction angles. Some plagioclase displays slight alteration to albite around crystal perimeters, and many plagioclase crystals show pronounced oscillatory zoning (see Figure 5).



0 1mm

FIGURE 5. Photomicrograph of central monzodiorite to granodiorite intrusive with plagioclase (pl) displaying oscillatory zoning, and biotite (bt) with pyroxene (pyx) displaying a diabasic texture with plagioclase.

Anhedral quartz and potassium feldspar (both microcline and orthoclase) occur interstitially to plagioclase. The accessory minerals apatite, magnetite, and sphene occur as inclusions in biotite and plagioclase. In Table III, page 33, the results of modal analysis performed on a fresh representative rock sample from this intrusive, are found. Using Streckeisen's (1967) classification of igneous rocks (see Figure 6) this intrusive rock type is monzodiorite based on the plagioclase composition and content, the quartz content (which displays some variation), and the ferromagnesian mineral content.

TABLE III

MODAL ANALYSIS OF THE IGNEOUS ROCKS COMPRISING ITALIAN MOUNTAIN

| Specimen Code | Percent Plagioclase | An-Content of Plag | Percent K-Feldspar | Percent Quartz | Percent Biotite | % Pyroxene and Hornblende | Percent Accessories ¹ | Classification ² (Streckeisen) |
|---------------|---------------------|--------------------|--------------------|----------------|-----------------|---------------------------|----------------------------------|--|
| Msc-2 | 44 | An ₅₂ | 17 | 18 | 10 | 9 | 2 | Monzodiorite |
| Qmse-1 | 43 | An ₄₈ | 9 | 33 | (chloritized) | 7 | 8 | Granodiorite |
| Qmsi-4 | 43 | An ₄₉ | 12 | 26 | (chloritized) | 9 | 10 | Granodiorite |
| Qms-8 | 44 | An ₄₇ | 20 | 22 | (chloritized) | 4 | 10 | Granodiorite |
| Qmgs-1 | 44 | An ₄₆ | 12 | 32 | (chloritized) | 6 | 6 | Granodiorite |
| Qms-15b | 42 | An ₃₁ | 15 | 29 | (chloritized) | 10 | 4 | Granodiorite |
| Average | 43 | An ₄₄ | 14 | 28 | | 7 | 8 | Granodiorite |
| QmBD-1 | 35 | An ₄₉ | 19 | 30 | 10 | 6 | <1% | Quartz Monzonite |
| Qmnc-1 | 52 | An ₄₈ | 17 | 23 | 10 | 7 | 1 | Dark Colored Granodiorite With High Ferromagnesian Content |
| MQnd-0 | 28 | An ₃₂ | 31 | 28 | 3 | 8 | 2 | Quartz Monzonite |
| Qni-1 | 40 | An ₃₀ | 28 | 25.5 | 5 | - | 1.5 | Quartz Monzonite |
| Average | 39 | An ₄₀ | 24 | 27 | 7 | 5 | 1.5 | Quartz Monzonite |
| Qdc-5 | 21 | An ₃₅ | 35 | 30 | 4 | - | 10 | Quartz Latite |
| GS-1 | 20 | An ₃₅ | 34 | 30 | 12 | - | 4 | Quartz Latite Porphyry |
| Penwc-9 | 33 | An ₄₀ | 35 | 23 | 5 | - | 4 | Quartz Latite |
| Average | 25 | An ₃₇ | 35 | 28 | 7 | | 6 | Quartz Latite |

¹Accessories include chlorite, magnetite, pyrite, sphene, and apatite.²See Figure 6, Page 34.

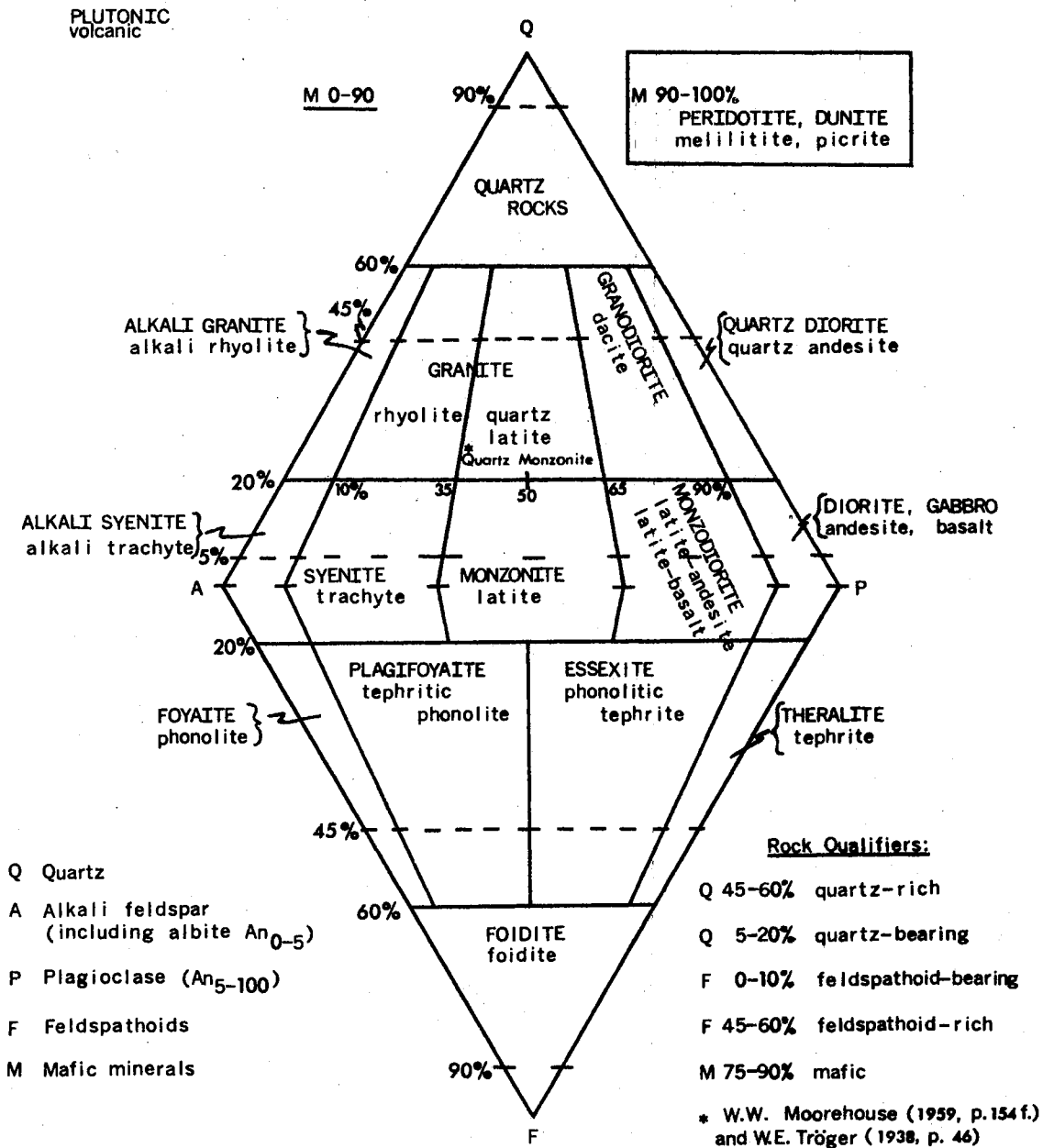
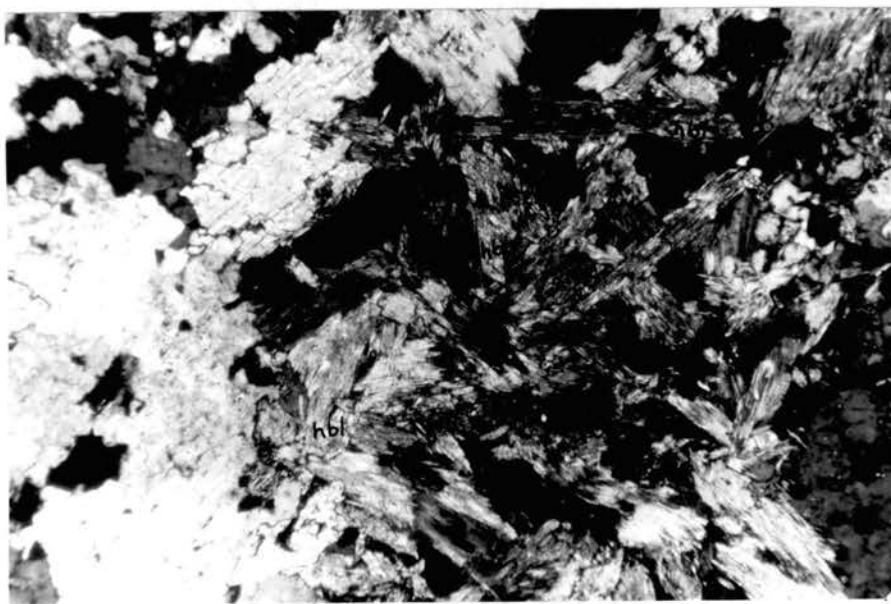


Figure 6. Classification of igneous rocks (Streckeisen-1967)

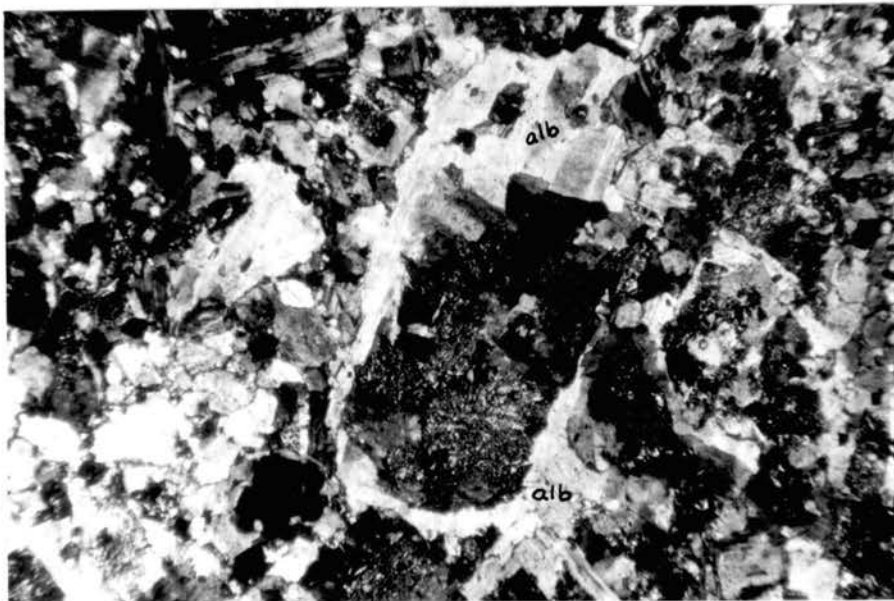
Within the interior of the stock the quartz content increases above 20 percent, and thus the rock must be classified as a granodiorite. The perimeter of this centrally located monzodiorite to granodiorite igneous intrusion displays distinct alteration mineralization due to both contact metamorphism and hydrothermal fluid emission. The effects of contact metasomatism are displayed along the northeastern and southeastern contacts with the tow-shaped wedges of Belden limey shale. Along the northeastern contact, hornblende is found along fractures within the granodiorite to monzodiorite and the plagioclase has been severely albitized and altered to epidote as illustrated, in Figures 7 and 8.



0 1mm

Figure 7. Photomicrograph of hornblende (hbl) veinlet in strongly albitized monzodiorite phase of the central intrusive, Italian Mountain.

Also within the peripheral contact area, along the southeastern part of this central stock, pod-like masses of albite, epidote, and euhedral quartz are found dispersed within the monzodiorite phase of this intrusive. This above mentioned mineral assemblage is characteristic of the albite-epidote facies of contact metamorphism. Figure 8 below, taken from the southeastern periphery again displays distinct albitization of a plagioclase and alteration of the more calcic cores to clinozoisite, a sugary textured variety of epidote, and minor sericite. Accessory magnetite and sphene are also well developed in this contact zone.



0 1mm

Figure 8. Photomicrograph of severely albitized monzodiorite of the central intrusion displaying remnant crystal outlines of plagioclase (plg) with rims of albite (alb) and cores altered to epidote (clinozoisite).

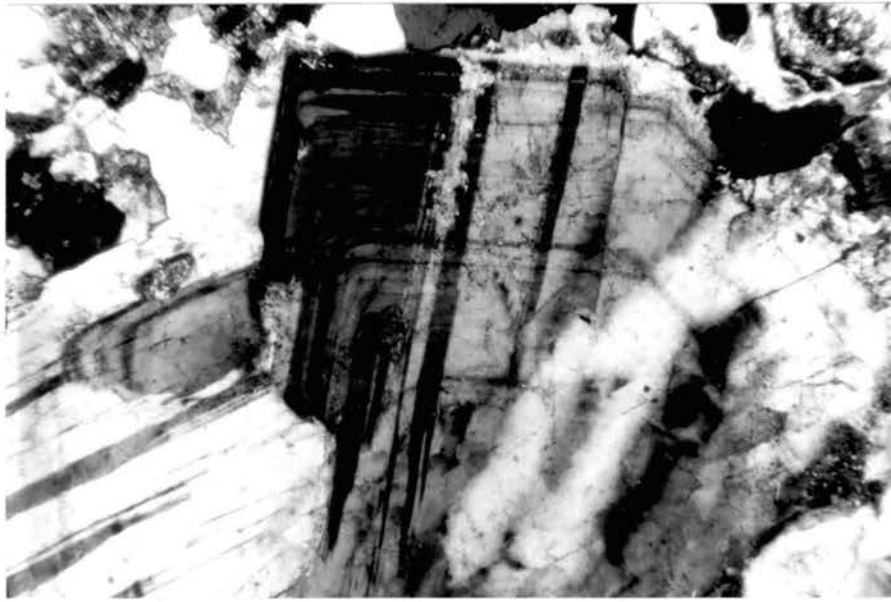
Hydrothermal alteration effects are evident within this central intrusive (Figure 9) along its northwestern contact with the northern quartz monzonite intrusive, along the southern contact with the finger-shaped wedge of Belden shale, and along a fault trending northwest-southeast, within the interior of the intrusive, where the surrounding rock is well fractured and displays well developed argillic alteration (montmorillonite and minor sericite) and pyrite mineralization. The monzodiorite to granodiorite rock is bleached to a light color, along these hydrothermally altered regions, due to the combination of the iron in the ferromagnesian minerals with sulphur to form pyrite.



Figure 9. Limonite staining along southern margin of central intrusive reflecting hydrothermal activity. Contacts between the central monzodiorite (Tm), wedge of Belden shaly limestone (Pb) and southern granodiorite stock (Tgr) are shown.

Granodiorite Southern Intrusive

A granodiorite intrusive, trending northwest to southeast, is found in the southern half of the Italian Mountain area. This intrusive body displays a variation in both texture and composition, progressing from the margins to the interior. In hand sample the marginal phase of this intrusive body is pinkish-gray in color, medium-grained, inequigranular; and is porphyritic in quartz (up to 2mm in diameter), plagioclase (3-5 mm in diameter), and chloritized biotite (1-6mm in length). Potassium feldspar is interstitial to plagioclase and biotite, and displays a pinkish-red color due to deuteric alteration and the incorporation of ferric from hydroxide. Microscopically the peripheral phase of this southern intrusive has a texture which can be described as medium-grained, interlocking, hypidiomorphic granular, and porphyritic in plagioclase, quartz and chloritized biotite. Plagioclase, in both phenocrysts (3-5 mm in diameter) and groundmass, occurs in rectangular forms some of which display oscillatory zoning (see Figure 10). The anorthite content of the plagioclase is within the andesine range (An₄₇). Argillic alteration to sericite and/or kaolinite is weakly developed and is particularly noticeable in the more calcic cores of the well zoned plagioclase crystals. Quartz occurs both as phenocrysts, ranging from 2-5mm in diameter, and interstitially to plagioclase in the groundmass. Several quartz phenocrysts display the effects of resorption and recrystallization. Figure 11 is typical example of the texture resulting from this resorption phenomena in which quartz, with inclusions of plagioclase crystals, is seen to embay six-sided cross sections of chloritized hornblende.



0 1mm

Figure 10. Photomicrograph of a sample from the peripheral phase of the southern granodiorite intrusive in which plagioclase displays oscillatory zoning and cruciform arrangement of phenocrysts.

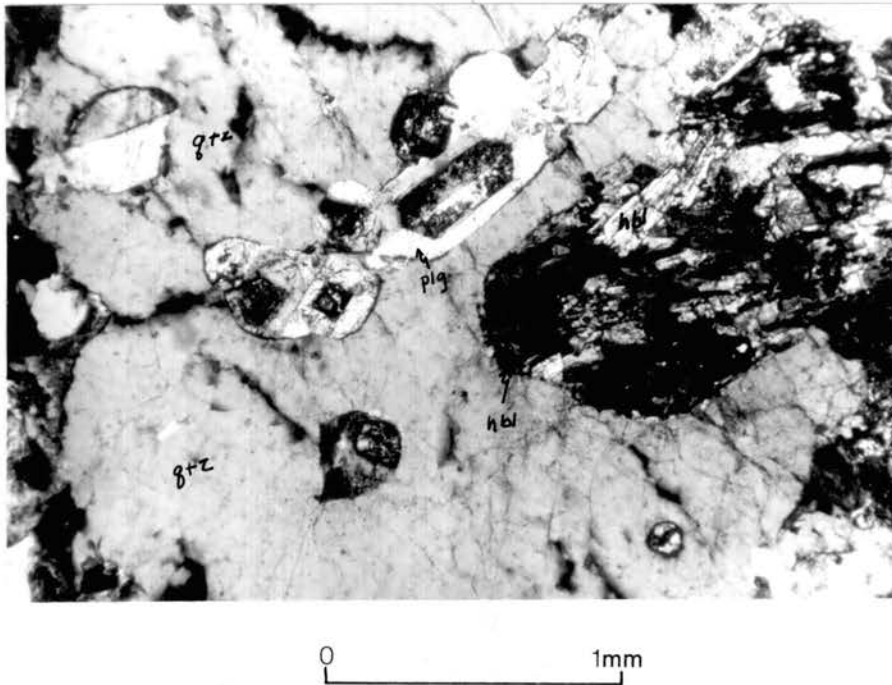


Figure 11. Photomicrograph of sample from the peripheral phase of the southern granodiorite intrusive in which resorption quartz, with inclusions of plagioclase crystals, embays six-sided cross sections of chloritized hornblende (hbl).

Biotite, whether as phenocrysts or interstitial groundmass, is chloritized and contains disseminated pyrite. The groundmass, of this peripheral phase of the southern intrusive, is composed of anhedral quartz and subhedral to anhedral potassium feldspar. Other minerals identified were: minor pyroxene and hornblende, accessory sphene and apatite, and the opaque minerals pyrite and magnetite which are found to replace biotite and hornblende.

In numerous places along its margins, especially along the northern contact with the Belden Shale and the number of faults

intersecting this southern intrusive, hydrothermal effects are transposed upon the host rocks. These hydrothermal effects are revealed in hand sample by the development of quartz phenocrysts, quartz veinlets, chloritization of biotite, and bleaching of the rock. The bleaching of the rock is due to the combination of iron, from the ferromagnesian minerals and the iron stained alkali feldspar, with sulfur in the rising hydrothermal solutions to form pyrite.

Microscopically the hydrothermal effects are displayed by: (1) formation of quartz phenocrysts of square to six sided cross section, (2) general increase in quartz content, and (3) development of strong argillic alteration represented by stringy aggregates of sericite to montmorillonite along cleavage traces in plagioclase (see Figure 12).

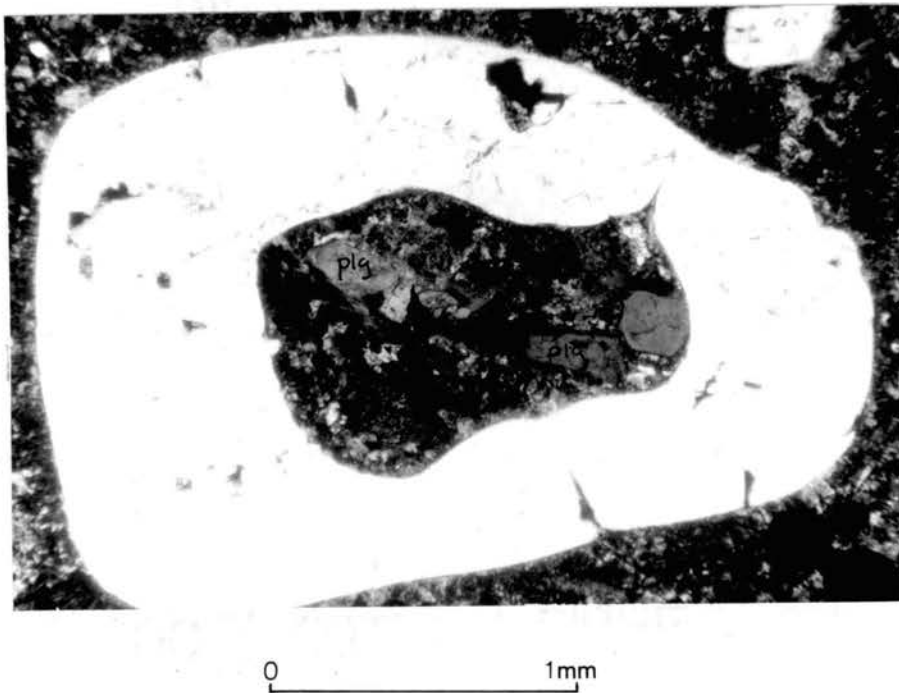
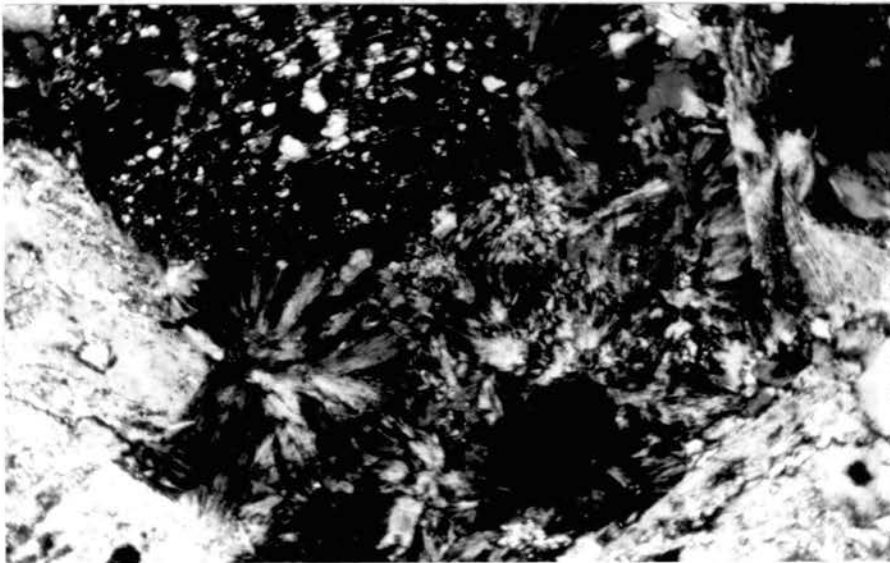


Figure 12. Photomicrograph displaying square to six-sided cross sections of quartz phenocrysts some of which display a resorption phenomena; plagioclase (plg) crystals show sericitic to montmorillonitic alteration along cleavage traces.

The groundmass, of this hydrothermally altered southern intrusive displays a peculiar spherulitic arrangement of microliths composed of plagioclase with anhedral quartz grains occurring interstitially (see Figure 13, below)



0 .25mm

Figure 13. Photomicrograph displaying the spherulitic arrangement of plagioclase microliths in the groundmass of the hydrothermally altered peripheral phase of the southern granodiorite intrusive.

The interior portion of this southern intrusive displays a variation in texture and mineral assemblages as compared with the peripheral phase. The interior displays the following characteristics: (1) has a lower color index due to the complete chloritization of biotite, and a lower percentage of ferromagesian minerals, (2) has a coarse-grained texture with plagioclase and quartz phenocrysts of equal size (up to 8 mm in diameter), (3) the potassium feldspar lacks the pinkish-red color common to the peripheral phase, and (4) there is a slight increase in the amount of potassium feldspar present.

Modal analyses of rock samples taken from both the interior and peripheral phases of this southern intrusive are recorded in Table III, page 33. Using Streckeisen's classification of igneous rocks (Figure 6, page 34), modal analyses indicate a rock of granodiorite composition. Single modal analysis of rock samples from both the interior and peripheral phases of this southern intrusive, all fall within the granodiorite range.

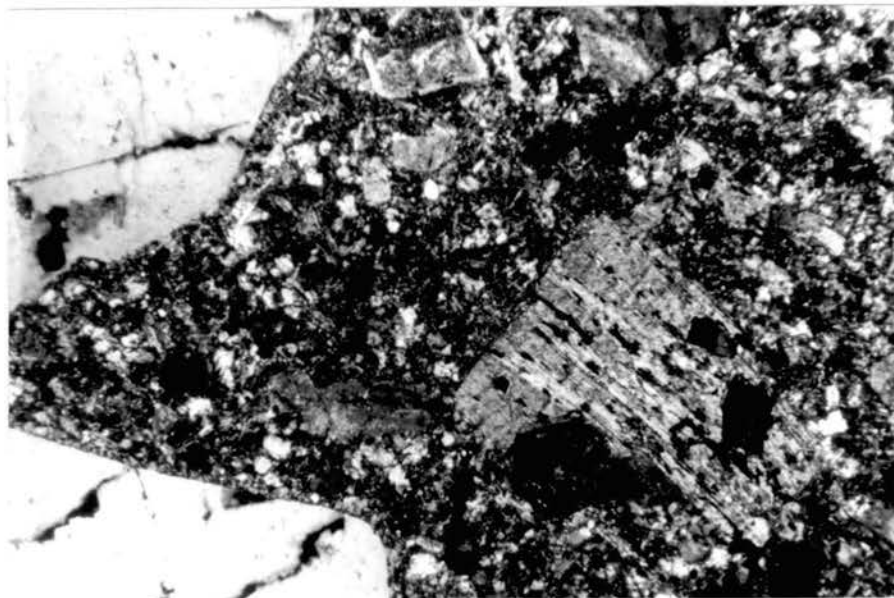
In the southern map area, where the granodiorite intrusive is in contact with the Gothic Formation, an old abandoned mine shaft was found. Mine dump samples displayed pyrite and magnetite mineralization concentrated within green shale partings. The Gothic Formation also expresses the effects of contact metamorphism by the alteration of the green shale partings to tremolite and actinolite. The granodiorite, along this contact, displays argillic alteration of plagioclase to sericite, kaolinite and/or montmorillonite, and slight silica enrichment is evident. A short distance south of this mine site a zone of pyrite mineralization, 10-20 feet wide, was found within the granodiorite along its contact with the Gothic Formation. Argillic alteration is well developed in this pyrite zone and is expressed by the alteration of plagioclase to sericite, kaolinite, and/or montmorillonite. Slickensides and chloritization of the green shale zone within the Gothic Formation was noted near the contact with the granodiorite. It therefore seems logical to speculate that this may represent a fault contact.

Northern Quartz Monzonite Intrusive

The northern most intrusive body of Italian Mountain is a composite or zoned intrusive consisting of a shell of granodiorite, with a high

ferromagnesian mineral content, 300-400 feet thick, which grades into a coarse to medium-grained quartz monzonite porphyritic in quartz and plagioclase feldspar, which in turn grades into a well developed quartz monzonite porphyry interior displaying phenocrysts of zoned plagioclase feldspar up to 2.5 inches in length and quartz phenocrysts up to 5 mm in diameter.

This shell of granodiorite, which displays a high ferromagnesian mineral content (termed melanogranodiorite by Cunningham, 1973), is well expressed along the northern and southern margins of the intrusive, but in other places it is either masked by pyrite mineralization and argillization or covered by talus. In hand sample this "melanogranodiorite" is coarse grained, dark gray to black in color (due to the relatively high concentration of biotite and magnetite), and is porphyritic in calcic plagioclase with euhedral crystals ranging from 3-9 mm in length. Little quartz is observable in hand sample and it along with potassium feldspar are interstitial to plagioclase. Microscopically this "melanogranodiorite" is coarse grained, hypidiomorphic granular, with phenocrysts of unzoned plagioclase ranging 4-9 mm in length. The plagioclase comprising the groundmass does, however, display oscillatory zoning and has an anorthite content of An_{48} , which is within the andesine range. A semi-diabasic texture is demonstrated within the groundmass by biotite partially encompassing plagioclase crystals, and pyroxene occurring interstitially to plagioclase (Figure 14).



0 1mm

Figure 14. Photomicrograph of the melanogranodiorite phase along the periphery of the northern intrusive displaying coarse grained semi-diabasic texture and high ferromagnesian content.

Quartz and alkali feldspar are entirely interstitial to plagioclase and biotite. Modal analysis performed on a rock sample taken from this melanogranodiorite shell is recorded in Table III, page 33. Based upon the quartz and plagioclase content, this igneous rock was classified as a granodiorite according to Streckeisen's classification. The prefix melano was attached to the basic classification granodiorite to account for the dark color imparted by the relatively high ferromagnesian mineral content.

This "melanogranodiorite" shell of the northwest igneous intrusive of Italian Mountain displays a variety of alteration effects along its margin depending upon the type of sediment in contact with it. In the north-central map area where Leadville Limestone is in contact with the igneous intrusive, the melanogranodiorite is enriched in anorthite, hornblende (5-10 mm in length), and pyrite. The mineral assemblage is due to contact metasomatism in which a compensating reaction took place between the melanogranodiorite and the Leadville Limestone. Calcium was supplied to the melanogranodiorite from the limestone which was in turn enriched in iron, alumina, and silica from the melanogranodiorite.

Along the northwestern and northcentral margins of the northern intrusive a more pronounced type of alteration is evident within the melanogranodiorite shell which is in contact with the shaly limestone member of the Belden Formation. The melanogranodiorite is bleached to a lighter color by the removal of ferrous iron from the biotite and addition of Al_2O_3 and Ca from the shaly limestone to form anorthite plagioclase. Minor diopside was also evident along fracture surfaces within the melanogranodiorite.

In hand sample the medium to coarse-grained quartz monzonite phase of the northern intrusive is seen to be porphyritic in plagioclase and quartz, with phenocrysts ranging from 1 to 5 mm and 0.5 to 2 mm, respectively. The overall color is light gray due to the decrease in ferromagnesian mineral content as compared to the peripheral melanogranodiorite. With a hand lens biotite, hornblende, pyroxene, quartz, plagioclase and alkali feldspar can be identified.

Microscopically this quartz monzonite phase can be described as being idiomorphic to hypidiomorphic granular, medium grained, with a seriate texture, and perphyritic in euhedral plagioclase, subhedral to anhedral quartz, and minor subhedral microcline with phenocrysts ranging from 1 to 8 mm, 0.5 to 2 mm, and 0.5 to 1.5 mm, respectively. The plagioclase is zoned in both phenocrysts and groundmass and has an average anorthite content of An₃₂. A resorption or remelting phenomena is displayed by some of the quartz phenocrysts which have inclusions of other minerals within, and embayments of groundmass. The groundmass itself is composed of alkali feldspar, both microcline and orthoclase, and quartz with biotite, diopside, and hornblende being interstitial. The accessory minerals identified were magnetite, apatite and sphene. Slight argillic alteration of this phase is manifested by the occurrence of sericite, kaolinite and/or montmorillonite along cleavage planes within the plagioclase crystals.

The results of modal analyses, performed on a representative sample from this medium to coarse grained quartz monzonite zone, are found in Table III.

Based upon the observed composition and previously noted fabric this rock may be called a porphyritic quartz monzonite according to Streckeisen's classification (See Figure 6).

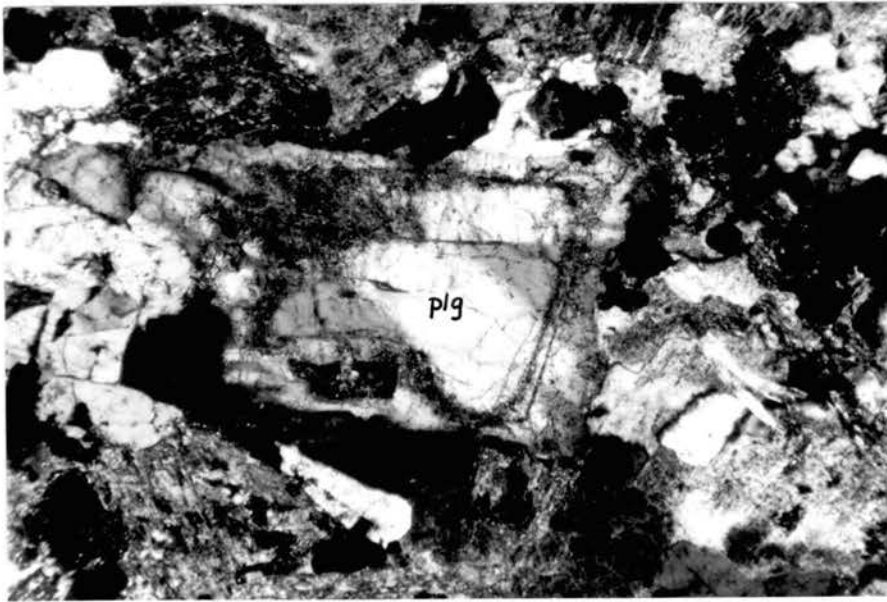
The interior phase of this zoned northern intrusive of Italian Mountain consists of a quartz monzonite porphyry. In hand sample, phenocrysts of plagioclase 1 to 3 mm in length and quartz 1-4 mm in length are easily discernable. The color of this quartz monzonite porphyry is light greenish-gray due to the low ferromagnesian mineral

content and the chloritization of biotite. The plagioclase displays zoning discernable even in hand sample, and is well argillized for it crumbles easily with pressure applied by a knife blade.

Microscopically the quartz monzonite porphyry displays a seriate texture, with an equigranular groundmass consisting of quartz and potassium feldspar (mostly microcline with minor orthoclase). Phenocrysts of euhedral to subhedral plagioclase in the form of laths and rectangles ranging in size from 1-8 mm with an anorthite content of An₃₀; anhedral to subhedral quartz displaying some resorption phenomena and ranging from 1-3 mm in size; and anhedral microcline, 1 to 5 mm in size, with replacement borders and inclusions of quartz and plagioclase, were observed in thin sections. Biotite was found to occur interstitially to plagioclase and quartz with chloritization being common. Many plagioclase crystals displayed corroded borders, and argillic alteration was evidenced by the presence of sericite and kaolinite along cleavage planes and within the more calcic cores of zoned plagioclase crystals (see Figure 15 below).

A segment of well altered igneous rock, 5-10 feet wide and 15 feet long, was found within the saddle of Belden Formation in the central map area. This small segment of igneous rock displayed silica and anorthite enrichment and slight dissemination of pyrite. To the west, an extension or offshoot of the northern intrusive was found which displays a similar alteration scheme.

The margins of this northern intrusive display dense pyrite mineralization, especially along the southeast and south-central



0 1mm

Figure 15. Photomicrograph of quartz monzonite porphyry of the interior portion of the northern intrusive which displays a porphyritic nature, lesser ferromagnesian mineral content, and argillic alteration of plagioclase.

borders. At the southeastern margins the melanogranodiorite is mineralized with disseminated pyrite, 30 feet in from the contact with the Belden Formation. This pyrite mineralization is due to sulfur seepage, in the form of ascending pneumatolytic to hydrothermal solutions, along cooling fractures into the melanogranodiorite where the S_2 (g) combined with the ferrous iron present in abundant biotite to form pyrite.

A wedge of Belden shaly limestone 25 feet wide, situated between the northern zoned intrusive and the central monzodiorite intrusive, is well mineralized in pyrite along fracture planes, and some pyrite cubes up to 3 inches in diameter were observed along with vug-like masses 5-7 inches in diameter. It is the author's belief that the intense pyrite mineralization, found within this wedge of Belden shale, was due to two stages of hydrothermal emission. The first stage of hydrothermal activity was associated with the central monzodiorite to granodiorite intrusions, which deposited finely disseminated pyrite and pyrite coatings along fracture planes. A more intense stage of pyrite mineralization was associated with the hydrothermal solutions emitted by the northern zoned intrusive, whereby the previous disseminated pyrite crystals served as nuclei upon which the pyrite cubes developed like pearls over a grain of sand.

At the peak of Central Italian Mountain a small wedge of Belden Formation (shaly limestone) is completely encompassed by quartz monzonite. Along the contact the quartz monzonite displays:

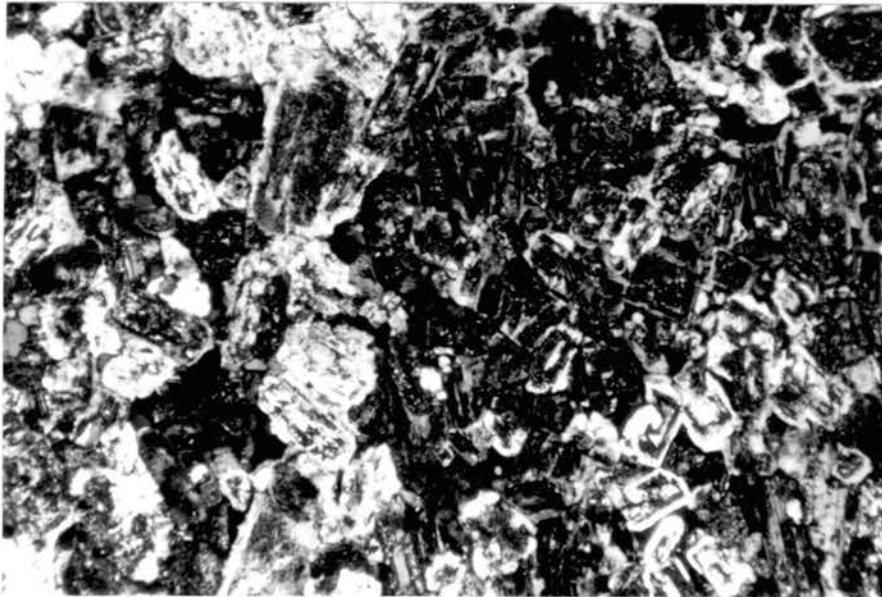
(1) a distinct lineation of biotite, hornblende, and diopside, (2) is enriched in magnetite, (3) plagioclase is argillized to kaolinite and sericite, and (4) the zoned plagioclase is rimmed by more sodic plagioclase (see Figures 15-17). The Belden shaly limestone member itself displays fine-grained diopside mineralization and pyrite mineralization along fracture planes.

Indications, as to the age relationships of the central and northern intrusive bodies of Italian Mountain, are exhibited along their contact just west of Central Mountain near the thumb-shaped wedge of Belden Formation. Here dikelets of quartz monzonite, 1 to 4 inches wide, were found penetrating the monzodiorite intrusive to the south.



0 1mm

Figure 16. Photomicrograph of quartz monzonite of Central Italian Mountain displaying lineation of biotite, diopside, and hornblende along the contact with the Belden Formation.



0 1mm

Figure 17. Same location as above photomicrograph, displays zoned plagioclase rimmed by more sodic plagioclase, which is more resistant to alteration.

Figure 18 below is a photomicrograph displaying the contact zone between the quartz monzonite dikelet and the monzodiorite of the central intrusive. The monzodiorite is much finer grained with a greater percentage of ferromagnesian minerals, and the plagioclase has been albitized.

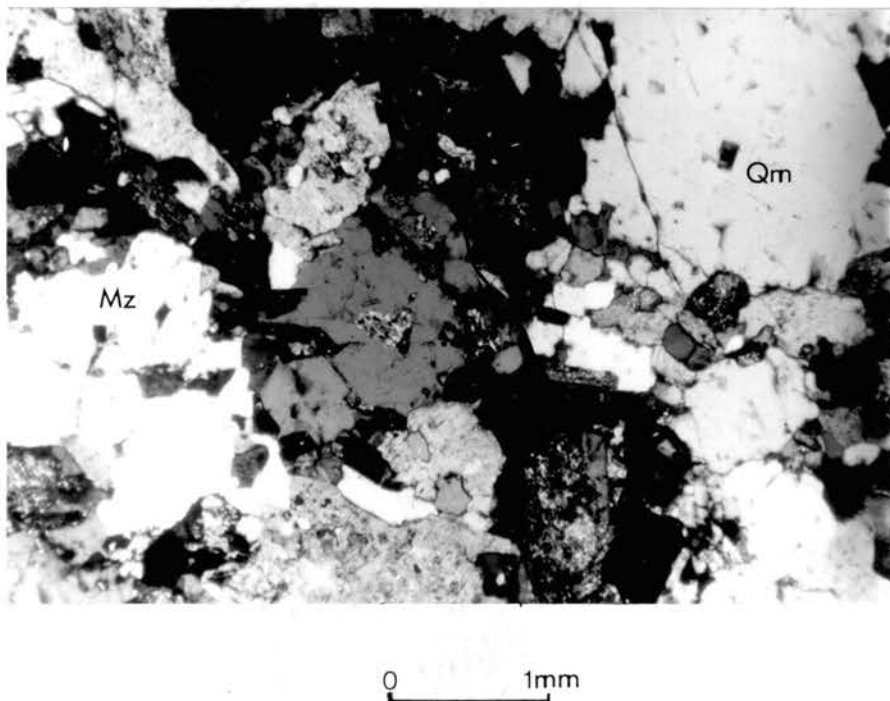


Figure 18. Photomicrograph of slide MQmD-0- shows boundary between quartz monzonite dikelet within monzodiorite (Mz). Mz is much finer grained, displays a greater ferromagnesian mineral content, and the plagioclase is albitized.

Also near the contact, xenoliths of monzodiorite were found within the quartz monzonite to granodiorite of the north.

Quartz Latite to Quartz Latite Porphyry Dikes

Branching off from the northern quartz monzonite intrusive of Italian Mountain, are numerous dikes which seemingly represent late stage offshoots of the dissipating quartz monzonite intrusive phase. Field relations are confusing in that it appears as though the quartz monzonite stock may actually crosscut these dikes, for nowhere were these dikes found to extend into the quartz monzonite proper. This lack of clarity in regard to the crosscutting relationships between the dike rocks and the quartz monzonite intrusive is due to: (1) the presence of well developed talus, along the margins of the quartz monzonite, which has effectively covered the intersections of the dikes with the stock or, (2) the nature of the dike rocks emplacement. These dike rocks could have vented at depth along fractures developed within the margins of the cooling quartz monzonite body. Access to the surface was facilitated by faults or fractures developed, within the surrounding Paleozoic sediments, by the previous explosive intrusion of the quartz monzonite stock.

Quartz Latite

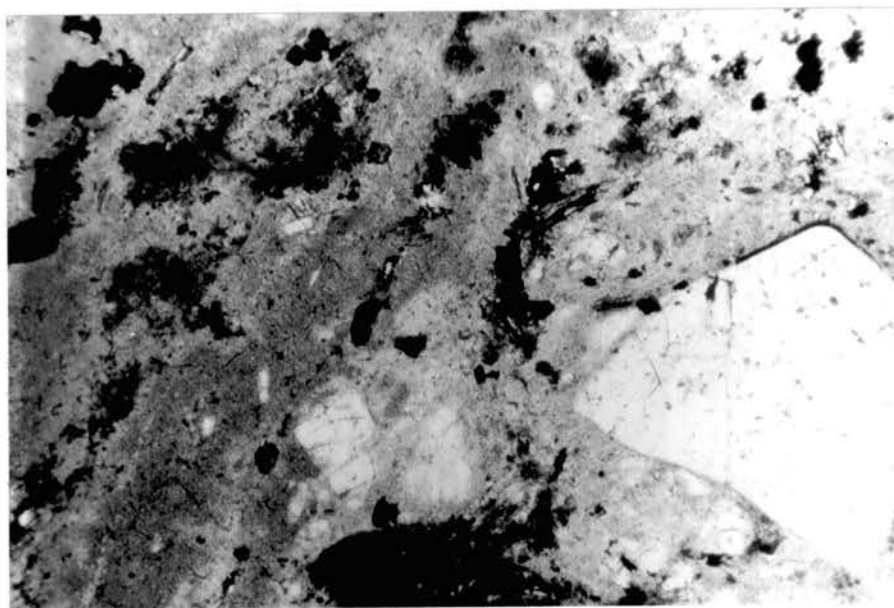
In the north-central map area, one of these dikes with an average width of 70 feet was found within the Precambrian granite porphyry. An adit cut parallel to this dike revealed pyrite mineralization in the form of small vugs 2-4 inches in diameter. The outer portion of this dike rock (10-20 feet) had suffered intense argillic alteration to kaolinite and sericite. Within this highly altered margin of the dike pink needles of some type of zeolite occur, lining

the pyrite vugs. The Precambrian granite porphyry surrounding the dike rock is dissected by numerous joint sets, parallel to the strike of the dike rock itself, along which hydrothermal solutions rich in sulfur passed, leaving behind a thin veneer of pyrite along fracture planes within the biotite rich granite porphyry. Later oxidation of the pyrite to limonite (mostly goethite) produced a large gossan zone yellowish-red to rusty-yellow in color.

In hand sample these quartz latite dikes, associated with the northern quartz monzonite intrusive, are typically porphyritic in: quartz less than 3mm in diameter, plagioclase 1-4 mm in diameter, and potassium feldspar less than 1-3 mm in diameter. The groundmass is microcrystalline with a glassy appearance which imparts a blue-gray to greenish-gray color to the rock. Biotite occurs as books and crystals of hexagonal outline, with replacement by pyrite being common. Quartz displays some square-shaped phenocrysts. Flow banding, where present, is evident on polished surfaces by the streaks of green material within the gray glassy groundmass.

Microscopically these quartz latite dikes display a definite porphyritic texture with phenocrysts of subhedral to anhedral quartz 1-6 mm in diameter, euhedral plagioclase ($An_{37}-An_{40}$) 1-4 mm in diameter, and subhedral to anhedral sanidine 1-2.5 mm in diameter. The groundmass was found to be cryptocrystalline and composed of irregular shaped aggregates of quartz and alkali feldspar. Oscillatory zoning and argillic alteration to sericite and kaolinite are displayed by plagioclase. Alkali feldspar is present as both microcline, with its characteristic checkerboard twinning,

and sanidine. Flow banding is discernable under plain light by: the streaking within the fine grained matrix, by the piling up of smaller crystals behind phenocrysts, and by the subparallel alignment of biotite flakes (see Figure 19). Other minerals identified microscopically were : biotite, the secondary minerals-chlorite, epidote, sericite and kaolinite, and the accessory minerals - magnetite and apatite.



0 1mm

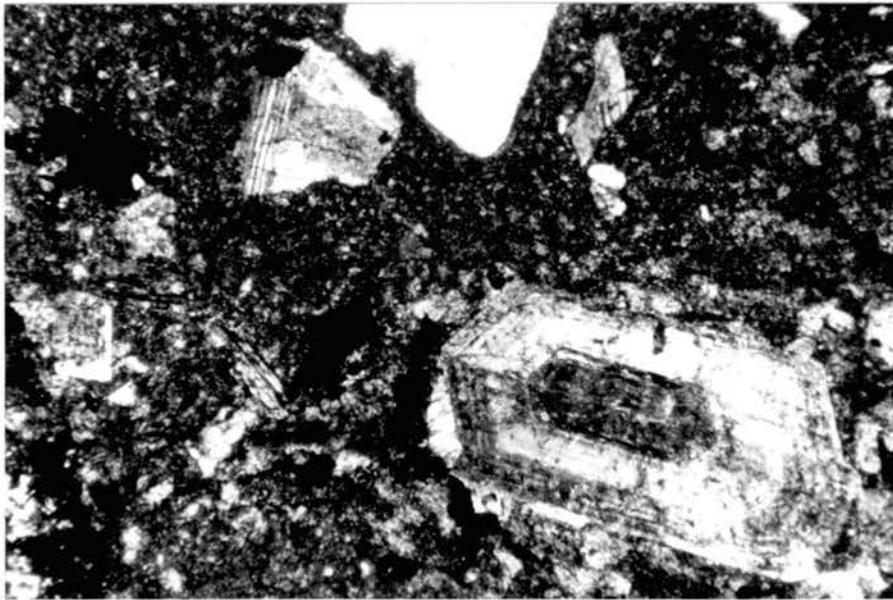
Figure 19. Photomicrograph of quartz latite dike under plain light in which flowing banding is defined by the streaking of glassy groundmass and piling up of smaller crystals behind quartz phenocrysts.

The results of modal analyses of these quartz latite dikes are presented in Table III, page 33. Based upon the mineral content of these dike rocks, obtained by modal analysis, and the aphanitic groundmass, the rocks are classified as quartz latite according to Streckeisen's classification (see Figure 6). It must be noted here that the author, in performing modal analysis on the fine-grained groundmass of the above mentioned quartz latite, attributed half to quartz and half to alkali feldspar.

Quartz Latite Porphyry

The Clara L. Mine was developed along a fault within the Leadville Limestone, southeast of the Star Mine workings. (see Figure 1). Along this fault the Leadville Limestone is well brecciated, and displays intense limonite staining. It was presumed by the author that the Clara L. Mine shaft was started with the idea of finding Zn, Pb, and Ag mineralization at depth. Mine dump samples do show intense pyrite mineralization of the Leadville Limestone. As the shaft was further developed, a quartz latite porphyry dike rock was encountered at depth. It is the author's belief that this quartz latite porphyry is most likely an extension of the quartz latite dike rock exposed within the Star Basin at the southern tip of Italian pond; its well developed porphyritic nature being due to deeper burial whereby it cooled at a slower rate, allowing time for larger crystal growth. A fresh hand sample of this quartz latite porphyry is greenish-gray in color, porphyritic in: plagioclase (0.5 - 2.5 cm in diameter), quartz (0.2 - .5 cm in diameter), and potassium feldspar (0.5 - 2 cm in diameter).

The ferromagnesian minerals biotite and pyroxene are identifiable within a aphanitic groundmass. Microscopically the unaltered quartz latite porphyry is again seen to be porphyritic in quartz, alkali feldspar (sanidine), and plagioclase. The groundmass is finely crystalline, but with a high power objective quartz and alkali feldspar may be discerned. Again the biotite is chloritized and replaced by pyrite, and in places the cleavage planes of biotite are distorted as if subjected to flow after crystallization. The alkali feldspar phenocrysts take the form of subedral to anhedral rectanular shaped crystals, with inclusions of quartz and other alkali feldspar crystals possibly due to unmixing during solidification. Quartz occurs both as euhedral six to eight-sided crystals and as irregular shaped masses. Oscillatory zoning is common amongst the plagioclase crystals, which take the form of laths and rectangles and have oligoclase to andesine composition -An₃₅ (see Figure 20 on next page).



0 1mm

Figure 20. Photomicrograph of sample GS-1 quartz latite porphyry from Clara L. Mine.

Table III, page 33, displays the results of modal analysis performed on this porphyry rock type. Based upon the mineral content obtained by modal analysis, and taking account the porphyry texture, this dike rock was called a quartz latite porphyry according to Streckeisen's classification.

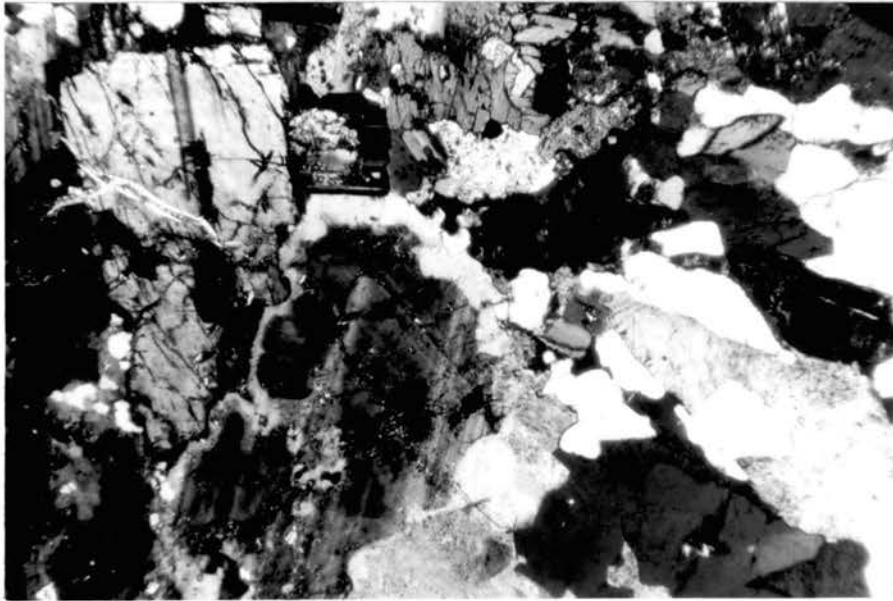
Granophyre and Aplite-Alaskite Dikelets

The last igneous rock forming events, associated with the differentiating parent magma, are represented by the alaskite to aplite dikelets found crosscutting the melanogranodiorite shell of the northernmost intrusive, and by the granophyre found along the

the northeast margin of this northernmost intrusive. The aplite to alaskite dikelets, 3 to 5 inches wide, are found within the granodiorite shell in the extreme northwest map area. Microscopically the alaskite dikelets display: a equigranular aplitic texture, anhedral quartz averaging 2.5 mm in length, euhedral plagioclase crystals of oligoclase composition (An_{19}) less than 1.5 mm in diameter, and perthitic microcline anhedral to subhedral in habit and having an average crystal size of 3 mm in length. No ferromagnesian minerals are present. Microcline also displays some included quartz and myrmekitic texture. Figure 21 below is a photomicrograph of the boundary between the granodiorite and the crosscutting alaskite dikelets, which display a typical aplitic texture and perthitic to myrmekitic microcline.

A primary granophyre, 2 to 3 feet wide, was found along the north-central contact between the Belden shaly limestone member and the granodiorite shell of the northern intrusive of Italian Mountain. In hand sample this granophyre has a granular to equigranular texture. Quartz, alkali, feldspar, amphibole, and a greasy green colored alteration product are identifiable in hand sample. Stringers of quartz also penetrate the whole rock between individual crystals. Microscopically this granophyre can be described as being hypidiomorphic granular to equigranular in quartz and microcline, with hornblende and accessory sphene occurring interstitially. Microcline displays a variety of textures: (1) granophyric--resulting from the exsolution of silica from the microcline and subsequent concentrations as triangular wedges along cleavage planes of microcline, (2) perthitic--resulting from the

exsolution of albite in microcline in the form of stringers along cleavage planes; and, (3) myrmekitic - exsolution of silica from the microcline in the form of worm-like extension from the margins of the microcline crystals into their centers. Figure 21 below illustrates the above mentioned textures.



0 1mm

Figure 21. Photomicrograph of the boundary between granodiorite shell of the northern intrusive and a crosscutting alaskite dikelet which displays an aplitic texture and perthitic to myrmekitic microcline.



0 1mm

Figure 22. Photomicrograph of textures displayed by granophyre from the north-central margin of the northern intrusive: granophyre-gpy, myrmekite-myk, and perthitic microcline (prth).

Amphibolite of East-Central Map Area

A coarse-grained amphibolite was found exposed within the Belden Formation at two locations in the map area: (1) in the east-central map area, only 350 feet from the contact with the southern granodiorite intrusive, and (2) along the high-angle reverse fault at the extreme southeast margin of the same granodiorite intrusive. In hand sample hornblende, biotite, and pyroxene were identified with the help of a hand lens. Microscopically this amphibolite was found to consist of approximately 85 percent hornblende, 12 percent biotite, 2 percent pyroxene, and 1 percent plagioclase. Hornblende displays the typical 4-6 sided cross sections and amphibole cleavage, at 56 and 124 degrees, with crystals averaging 4 mm in length. Euhedral to subhedral biotite and pyroxene occur interstitially to hornblende and display a range in size from less than 1 to 4.5 mm in length. Plagioclase is poikilitically enclosed by biotite and hornblende and is less than 1 mm in diameter.

It is the author's belief that these amphibolite bodies are surface exposures of the Precambrian basement. The Precambrian basement rocks of the general area of Italian Mountain do consist of metamorphosed sediments such as schist and gneiss, which have been intruded by a coarse-grained granite porphyry and by pegmatitic to aplitic dikes and irregular masses. The amphibolite exposure in the east-central map area is found at the crest of a tight anticlinal fold. Subsequent erosion by glaciation was responsible for the exposure of the amphibolite core of this anticlinal fold. Again, along the extreme southeastern margin of the southern granodiorite

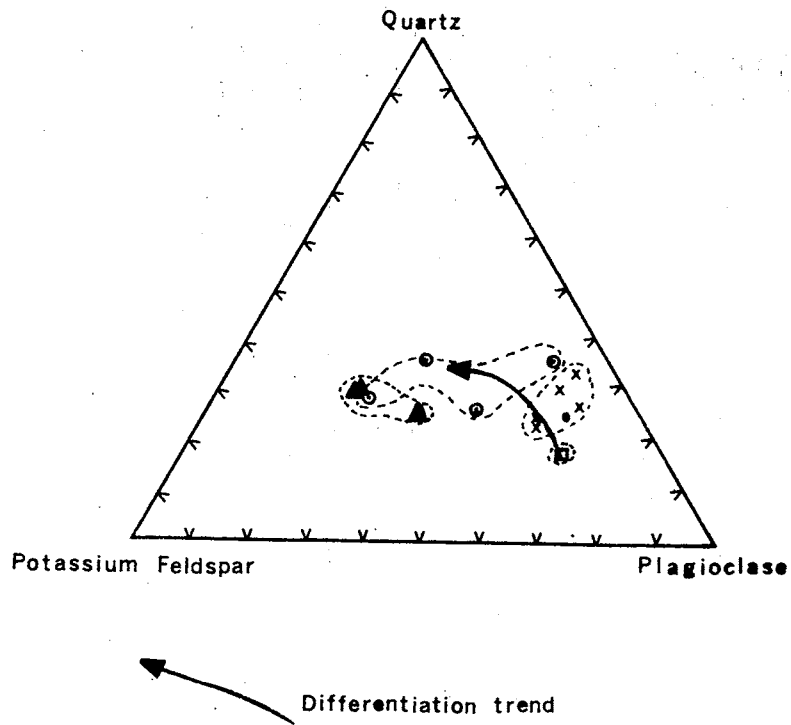
intrusive, the Precambrian basement rock --amphibolite-- has been exposed at the surface along the upthrown side of a high-angle reverse fault within the Belden Formation.

Petrogenesis of Tertiary Igneous Rock Types

The overall granodiorite composition of the Italian Mountain intrusives and the near proximity of the White Rock granodiorite pluton to the northwest suggest that the Italian Mountain igneous complex is an offshoot of a large granodiorite batholith of which the White Rock, Snow Mass, and Sopris intrusives are a part. The emplacement of this proposed batholith was most likely controlled by the northwest-trending Elk Mountain and Castle Creek structure zones. One may then ask how then can you account for the development of the Italian Mountain intrusives, which range in composition from monzodiorite to quartz monzonite, suggesting magmatic differentiation within a magma chamber at depth. To account for the observed compositional changes, from a younger basic member to an older intermediate to acidic member, one might postulate that parts of the magma may have separated from the batholith due to tectonic activity and thus differentiation within separate mini-magma chambers, apart from the batholith, could produce variations from the granodiorite parent melt. These separated portions of parent magma if injected into shallow environments could have undergone differentiation by the subtractive processes of crystal setting during fractionation, and subsequent filter pressing, which could have easily produced the compositional variation prevalent at Italian Mountain - monzodiorite- granodiorite-quartz monzonite.

The variation in the textures observed for the rock types of the Italian Mountain complex, from medium to coarse-grained to porphyritic, suggest intrusion under variable temperature and pressure conditions, which would be expected when a parent magma has been emplaced into varying depth conditions and allowed to differentiate.

Table 3 is a compilation of the mineral percentages obtained by modal analyses for the igneous rock types comprising Italian Mountain, and a subsequent classification based on these mineral percentages. Figures 23 and 24 are ternary plots of the quartz, alkali feldspar, and plagioclase contents of the 4 igneous rock types. These ternary plots demonstrate that, for Italian Mountain, we are indeed dealing with three separate intrusive bodies and a dike rock of distinct composition. The modal variations occur along a single differentiation trend toward alkali enrichment. Weak increases in quartz are also apparent along this differentiation trend.



Oldest □ - Monzodiorite central intrusive.

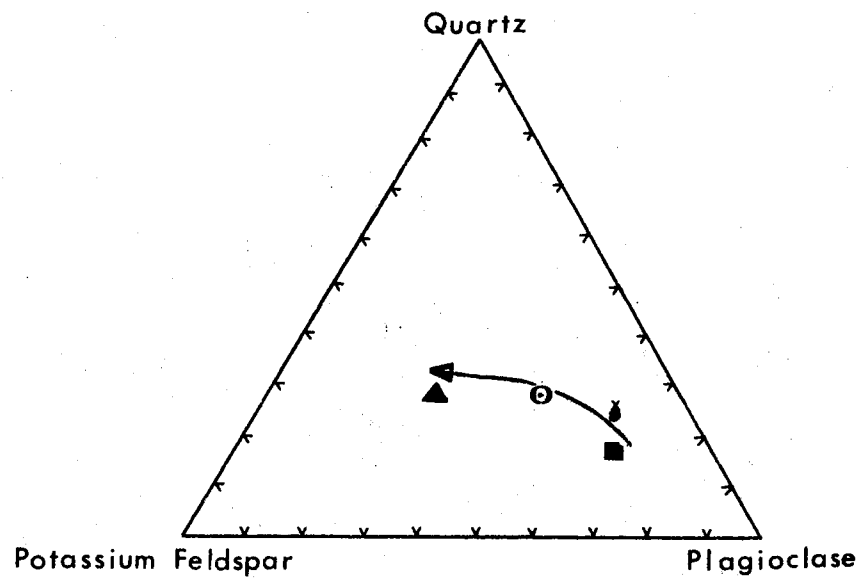
x - Granodiorite southern intrusive

. - Dark colored granodiorite perimeter of northern quartz monzonite stock

⊙ - Quartz monzonite northern monzonite stock

Youngest - Latite to quartz latite prophyry dike rocks

Figure 23. Modal variations of Italian Mountain area igneous rocks.



- Oldest ■ - Monzodiorite central intrusive
- x - Granodiorite of southern intrusive
- . - Dark colored granodiorite from perimeter of northern quartz monzonite intrusive
- ⊙ - Quartz monzonite northern intrusive
- Youngest - Quartz latite to quartz porphyry dike rocks

Differentiation trend

(Percentages of quartz, K-feldspar, and plagioclase based on modal analyses.)

Figure 24. Average modes of Italian Mountain area igneous rocks.

CHAPTER V

ORE DEPOSITS

Because the author did not have access to the actual mine workings of Italian Mountain, the following discussion of the Pb-Ag ore deposits in the study area is based upon previous investigations made by Garrett (1950) and Siebir (1957). The author did collect mine-dump samples of primary sulfides, and within the following pages has presented a paragenetic sequence of deposition of the ore minerals and gangue as revealed by polished section analysis under reflected light.

The three main Pb-Ag mines within the carbonate Paleozoic sediments, which have been intruded by the Italian Mountain intrusives, are: (1) the Star Mine within the Star Basin, located in the southeastern map area, (2) the Stewart Mine found in the east-central map area, and (3) the Ender Mine located in the extreme northwest just out of the map area (see Figure 1).

Garrett (1950) provides a brief history of the discovery and development of the Star Mine. The Pb-Ag mineralization within the Star Basin was first discovered in 1878. The first mining operation was concerned with extracting silver-bearing cerussite ore.

Bulk ore was hauled by mule train over pack trails down to Glacier, Colorado, located approximately five miles south of

Crested Butte, and then by wagon to the smelters in Leadville, Colorado.

Charles Hubbert, in 1880, located further claims of Pb-Ag mineralization within the Star Basin area. A French mining company then took interest in the area and is credited with sinking the Star shaft and incline from which most of the major production was to follow. The French Company, encountering financial difficulties, returned the operation of the Star Mine development to Mr. Hubbert, who developed the first and part of the second levels of the Star Mine. The American Smelting and Refining Company then took a hand in the development of the mine by completing the second level and constructing the incline to the third level, looking for more ore. The ore encountered in the third level was in the form of pods and disseminations of primary galena and sphalerite within massive limestone, and was of lower grade than the secondary cerussite ore of the upper levels. In the early 1920's John Lambertson took a lease on the Star claim, re-worked the upper two levels, and further developed the third level, prospecting for more ore. Scant production figures do exist for the Star Mine and indicate a total value of \$8,224.07 between the years 1927 and 1928 (see Table IV). The price of lead and silver was 5.52¢/lb. and \$1.61 oz. respectively in 1929-1930 as opposed to 16¢/lb. and \$1.77 oz. in 1970.

During the summer of 1971 Dr. Richard Livingston, a retired geology professor from the Colorado School of Mines, and Mr. Michael Pecos of the Beryl Dynamics Company in Gunnison, Colorado, purchased the Star Mine claims from Mr. John Lambertson. An attempt was made

TABLE IV
 PRODUCTION, STAR MINE, 1927-1928
 (FROM GARRETT, 1950)

| Date | Silver Value (Average oz. per ton) | Lead Value (Average percent) | Total Value |
|-----------|--|------------------------------------|---------------|
| 1927 | | | |
| October | 23.15 | 47.4 | \$2,128.45 |
| November | 20.8 | 48.5 | 1,223.23 |
| December | 22.8 | 43.8 | 1,182.57 |
| 1928 | | | |
| January | 30.75 | 38.8 | 1,105.75 |
| August | 30.2 | 39.0 | 1,089.18 |
| September | 32.45 | 37.8 | 1,099.39 |
| October | <u>26.9</u> | <u>31.1</u> | <u>394.50</u> |
| Averages | 26.72 | 40.9 | |
| Total | | | \$8,224.07 |

to reopen the Star shaft and Independent shafts, prospecting for further Pb-Ag replacement deposits. A new adit and shaft were developed in the wedge of Leadville Limestone located to the northwest of the old workings. Mine-dump samples collected from the new workings display primary pyrite, galena, sphalerite, and traces of bornite within a gangue of barite and calcite. Secondary copper mineralization, in the form of malachite and azurite, was also noted in the mine dumps. Owing to a mine accident, where one man was killed by a cave-in, and to the fact that the smelters in Leadville, Colorado, were on strike, Mr. Pecos and Dr. Livingston were forced to close the mine in 1971. During the summer of 1972 when the author was conducting his field work, Dr. Livingston was visiting the Star Mine workings and inspecting the conditions of the main shafts, the Star and Independent shafts. The author was able to talk to Dr. Livingston on various occasions and gleaned some important insights as to the nature of the Pb-Ag replacement deposits in the brecciated Leadville Limestone host rock. Because the main shafts were badly flooded in places and inaccessible due to cave-ins, the author was not able to actually go underground and inspect the Pb-Ag mineralization in situ.

Star Mine

Nature of Ore Deposits

Garrett (1950) describes the Pb-Ag deposits of the Star Mine as being replacement deposits within the Leadville Limestone, and open space-filling as well as replacement deposits within collapse breccias of the Leadville Limestone. The Pb-Ag deposits of the

Star Mine workings consist of both primary sulfides and secondary oxide minerals. The primary mineralization occurs as vugs or pods of sulfide in massive limestone; the chief sulfides being galena, sphalerite, and pyrite in order of decreasing abundance. Barite is the principle gangue mineral and occurs as irregular masses and bladed crystals often arranged in a semiradiating fashion.

The oxide mineralization in the Star Mine is the most important type of mineralization in terms of economic value. This oxide ore is in the form of cerussite which has significant amounts of silver tied up within its crystal lattice. Locally the oxide ore was termed "lead sand" because the cerussite is found mixed with sand within solution cavities and collapse breccias. The cerussite is derived from the oxidation of galena. Cerussite is commonly found replacing galena along its cleavage traces. Only oxidized ore is shipped from the Star Mine because of the lack of appreciable tonnages of primary ore and the higher grade of the oxidized ore. From the production figures cited in Table IV, for the years 1927 and 1928, it is noted that: (1) the ore shipped from Star mine had an average grade of 26.72 ounces of silver per ton; 40.9 percent of lead per ton; and (2) trace amounts of zinc have been recovered in the beneficiation process.

Garrett (1950) reports that during the 1950's the ore shipped to Leadville displayed a grade between 20 and 30 per cent lead per ton, and up to 12 ounces of silver per ton. One hundred and forty-four tons of ore containing 68,430 pounds of lead, 3,648 pounds of zinc, 2,711 pounds of silver, and 2 ounces of gold were shipped from the Star mine in 1950 (Minerals Yearbook).

Controls of Ore Deposition

Garrett (1950) states that the economically important oxidized ores in the Star Mine workings occur in a limestone breccia near the middle section of the Leadville Limestone. This brecciated limestone unit, of the Leadville Limestone, reaches a maximum thickness of 30 feet in the Star Mine area. Cerussite and remnant crystals of galena are found within this breccia throughout the mine area. Both above and below this brecciated member of the Leadville Limestone, are found vugs and pods of primary sulfides parallel to the bedding of the undisturbed limestone.

Within the brecciated limestone, are found curious sand pockets which are very irregular in both shape and size with lengths varying from 2 to 25 feet and from 1 to 20 feet high. Garrett (1950) reports that these sand pockets are "lined with a layer of clay about one inch in thickness, and the sand that fills the pockets is cross-bedded, unconsolidated, and poorly sorted, ranging from a very fine-grained sand to a coarse sand with well-rounded limestone pebbles, ranging from one-fourth inch to four inches in diameter". Garrett states that these "sand pockets" represent solution cavities within a highly soluble and permeable section of the Leadville Limestone. In fact, the limestone breccia most probably owes its origin to the collapsing of the solution cavities, within this highly soluble section of the Leadville Limestone, near a paleowater table interface. Garrett states that heavy mineral separation (bromoform floatation) performed on the sand filling these solution cavities contained abundant biotite fragments, which display foliation, in the heavy

fraction whereas quartz along with orthoclase are found in the light-mineral fraction. The results of the bromoform separation performed on these sands suggests that the solution cavities were filled with sand derived from a biotite gneiss similar to that found on Mount Tilton in the north-central map area. The sand was deposited when the solution cavities were raised above the water table by tectonic activity and subsequent erosion of the biotite gneiss of the Tilton Mountain area produced clastics to be carried away by runoff water.

Garrett (1950) stained a sample of the mineralized limestone breccia with Fairbanks solution and noted that the limestone took on a dark stain, with the lighter nonstained fragments of the breccia representing dolomitized and silicified limestone produced by hydrothermal solutions. Garrett suggests that the relative permeability between the breccia and the undisturbed limestone controlled localization of the mineralization. Mine dump samples indicate that the mineralization of the breccia was more complete in relation to the massive limestone, which displays mineralization in small lenses and pods controlled mainly by the bedding of the Leadville Limestone. The beds dip in towards the nearest contact with the quartz monzonite intrusion of North Italian Mountain at an angle of $35 - 45^{\circ}$ and a strike of $N 15-20^{\circ}E$. Also the fact that the limestone breccia is nearly completely oxidized is a good indication that it was more permeable to surface waters than the bedded limestone containing fresh sulfide.

Thus in summary the brecciated limestone unit of the Leadville Limestone exerted the primary control over ore deposition. Hydrothermal solutions carrying the Pb and Ag flowed through the breccia

with precipitation of sulfides. A stratigraphic control of ore deposition, only of secondary importance, is displayed by the concentration of primary sulfides along the bedding planes of the undisturbed Leadville Limestone.

Genesis of Ore Deposits

Garrett (1950) states that the Pb-Ag deposits of the Star Mine are hydrothermal in origin and that the mineralizing hydrothermal solutions were derived from the differentiating quartz monzonite intrusive of North Italian Mountain. The author agrees that mineralizing solutions responsible for the Pb-Ag deposits in the Star Basin were indeed associated with the differentiating quartz monzonite of North Italian, and will give supporting evidence in the chapter dealing with trace metal analysis.

Based upon the mineralogy and texture: (1) the major hypogene sulfide being galena in a gangue of barite, and (2) the fine to medium crystalline texture of the primary ore, itself, Garrett (1950), classifies the sulfide ores as mesothermal in character.

It is the author's belief that the hydrothermal solutions, emitted with the quartz monzonite intrusive of North Italian Mountain, migrated out into the surrounding Paleozoic sediments along the margins of numerous quartz latite to quartz latite porphyry dikes and major fault zones until the highly permeable limestone breccia units were encountered. The physiochemical nature of the brecciated limestone, being very permeable and soluble, provided an environment well suited for ore deposition. The quartz latite to quartz latite porphyry dikes did suffer argillic alteration and did not present an environment suitable for the concentration of Pb and Ag.

The limestone breccias, because of their high permeability and solubility, also presented the easiest byways for percolating ground water, and thus the sulfides associated with these breccias became highly oxidized.

Stewart Mine

The Stewart Mine, located in the east-central map area, is also found in the highly permeable and soluble upper member of the Leadville Limestone. None of the Stewart Mine workings were accessible and the only hint of the nature of this deposit was obtained from mine dump samples. The Leadville Limestone, exposed at the surface within the vicinity of the Stewart Mine, consists of dark gray to black limestone breccia with secondary calcite veinlets and pyrite mineralization. The extreme permeability and solubility of the section of the Leadville Limestone is well evidenced by the many solution cavities and general sponge-like appearance to the limestone. Only traces of galena in a barite gangue were found on the mine dumps, and in fact most of the primary galena and pyrite seemed to have suffered oxidation to anglesite and jarosite, respectively. It is the author's belief that the mineralization here is similar to that found in the Star Basin where collapse breccias, produced by solution activity, have been mineralized owing to their high degree of permeability and reactive nature.

Ender Mine

The Ender Mine was not investigated by the author because it lies outside the mapped thesis area. Slebir (1957) has described the sulfide deposits of the Ender Mine and the following is a

summary of his findings. The principle hypogene minerals found at the Ender Mine site are galena and sphalerite. The galena was found associated with limonite in a zone four feet wide along a vertical fault within the Leadville Limestone. A typical mineralized zone assays 12 percent lead, 5 percent zinc, and 10 ounces of silver per ton. Closer to the bottom of the mine workings, Slebir (1957) found the mineralization to consist of galena, sphalerite, anglesite, and pyrargyrite. Supergene mineralization is represented by the presence of cerussite, smithsonite, and anglesite. The principle gangue mineral associated with the primary sulfide mineralization in the main mine workings is limonite (jarosite), derived from the oxidation of pyrite. Slebir (1957), also notes that at the surface, where the Manitou Formation displays sulfide mineralization, the main gangue mineral is barite.

Slebir (1957) states that the primary controls over ore deposition are the fractured and minor fault zones associated with the high-angle Ender gravity fault (see Figure 1). The major fault zones served as conduits along which the hydrothermal solutions migrated, whereas the numerous fractures and minor faults intersecting the main faults acted as traps for the hydrothermal solutions, and thus deposition occurred wherever favorable carbonate rock units were intercepted.

The Paleozoic host rocks were made ready for mineralization, during late Cretaceous to early Tertiary times, when the Laramide orogeny contorted and fractured the sedimentary regime. Next followed the magmatic differentiation of the Italian Mountain intrusives, during middle Oligocene to early Miocene time. Again it is the

author's belief that the hydrothermal solutions, which deposited the Pb, Ag and Zn ores of the Ender Mine, were derived from the magmatic differentiation of the northern quartz monzonite stock of Italian Mountain. The mineralizing solutions most likely migrated up through a fractured and faulted zone centered about the Ender Fault, and were deposited in favorable carbonate host rocks.

Spring Creek Mine

The Spring Creek Mine, located in the southwestern map area, was found along a high-angle reverse fault which has moved the Leadville Limestone up over the Belden Formation. Again, access to the mine workings was prohibited by the existence of portal cave-ins. Ore samples, collected from the mine dumps, display pyrite disseminated and in vug-like masses within recrystallized Leadville Limestone. Pyrite is also found disseminated in the Belden Formation. No traces of barite, galena, or sphalerite were found in any of the mine dump samples. The Belden Formation and the Leadville Limestone did display well developed silicification with included pyrite. The pyrite mineralization and silicification of the Paleozoic sediments was produced by hydrothermal solutions expelled from the differentiating granodiorite intrusive of South Italian Mountain. These hydrothermal solutions migrated along the Laramide derived high-angle reverse fault in the Paleozoic sediments until the soluble and chemically reactive Leadville Limestone was encountered, with the underlying Belden Formation forming a stratigraphic trap. As to the exact ore mined in the past, there exist two possibilities: (1) either gold is tied up in the quartz-pyrite veinlets and

.vug-like masses within the Leadville and Belden Formations, or (2) like the Doctor Mine, located 15 miles south along Spring Creek, silver-bearing lead carbonate (cerussite) and zinc carbonate (smithsonite) were produced.

New Star Mine

The New Star Mine workings, located in the northwestern corner of the Star Basin within a wedge of Leadville Limestone, present a variation in the type of mineralization common to the Star Basin. A black dolomitic Limestone member of the Leadville Limestone contains chalcopyrite and trace bornite mineralization in addition to the usual pyrite, sphalerite, and galena. Also, the principal gangue mineral is calcite as opposed to barite in the old Star Mine workings. Figures 25 and 26 show pyrite and galena mineralization of this black dolomitic member of the Leadville Limestone. Figure 27 pictures euhedral pyrite crystals within replaced dolomitic limestone. Clues to the unfolding of the paragenetic sequence of deposition are revealed by the following photomicrographs:

1. Figure 28 shows chalcopyrite replacing pyrite within a gangue of dolomitic limestone.
2. Figure 29 displays sphalerite cutting chalcopyrite.
3. Figure 30 shows sphalerite veinlets crosscutting pyrite but not galena.

Thus, the following paragenetic sequence is suggested: an original black dolomitic limestone replaced by pyrite - chalcopyrite - sphalerite - galena. Supergene alteration of the mineralized black dolomitic limestone breccia has produced an oxidized zone composed

crumbly masses of limonite, malachite, azurite, and galena rimmed with anglesite.

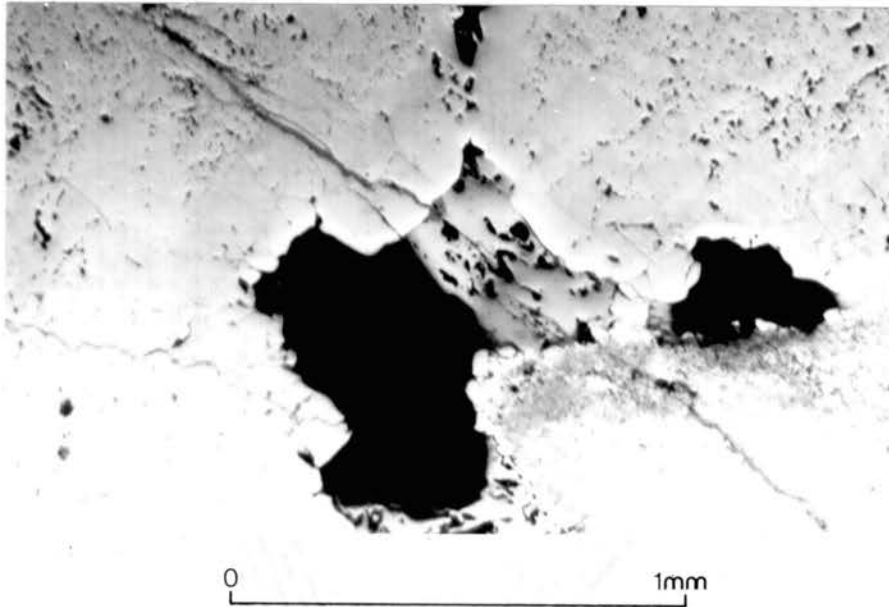


Figure 25. New Star Mine workings -photomicrograph displaying galena encompassing preexisting pyrite .

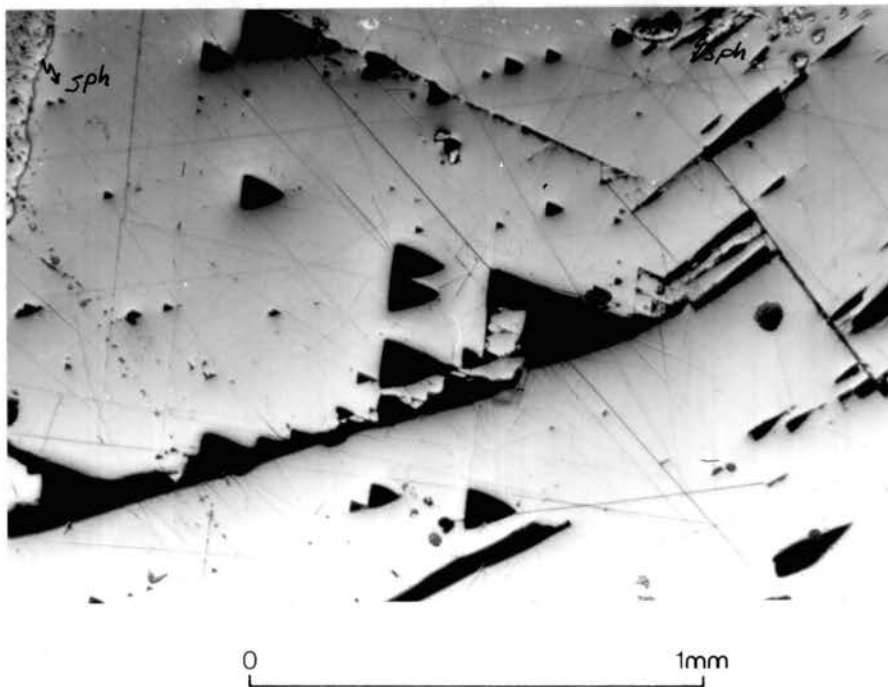
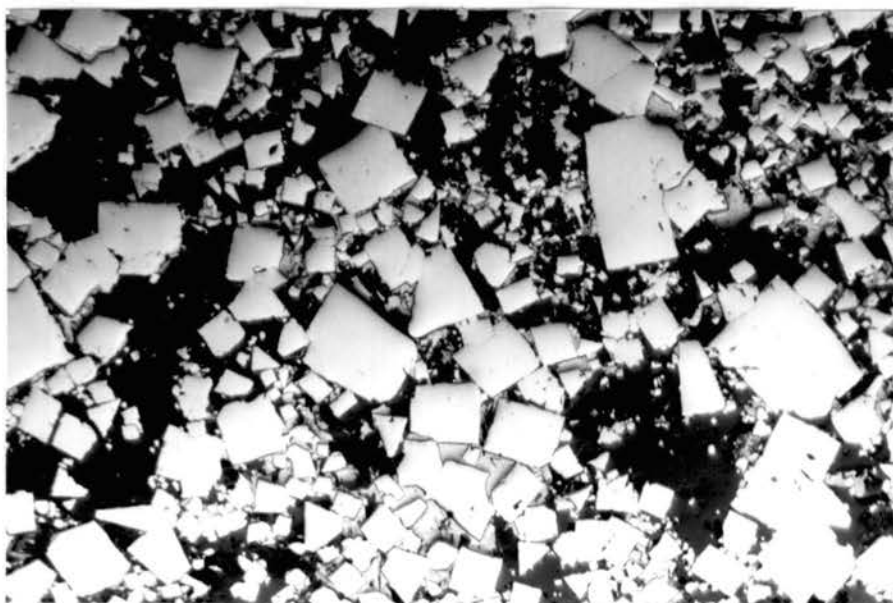
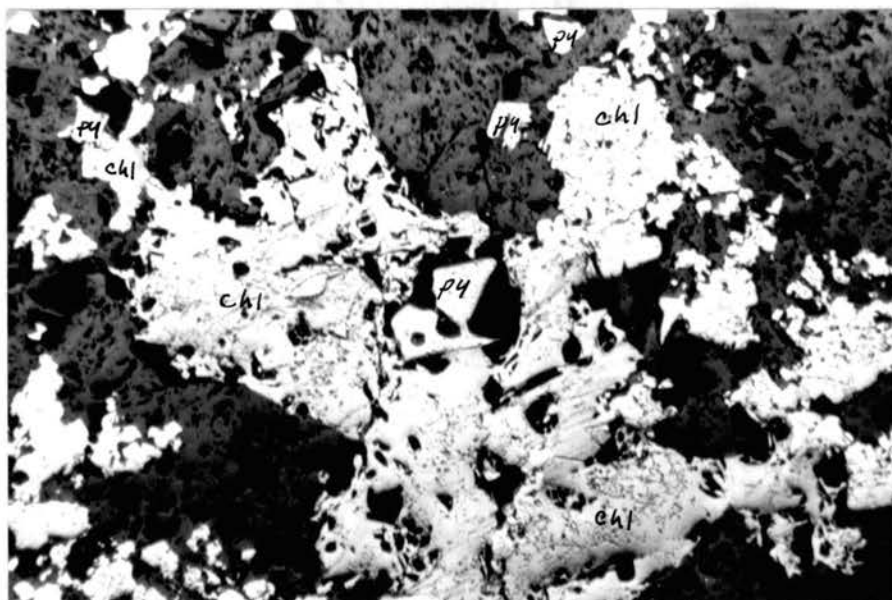


Figure 26. Photomicrograph of triangular pits along cleavage traces in galena, and inclusions of sphalerite (sph) upper right hand corner .



0 1mm

Figure 27. Euhedral pyrite crystals within replaced dolomitic limestone.



0 1mm

Figure 28. Photomicrograph of chalcopyrite (chl) replacing pyrite (py) within a gangue of dolomitic limestone.

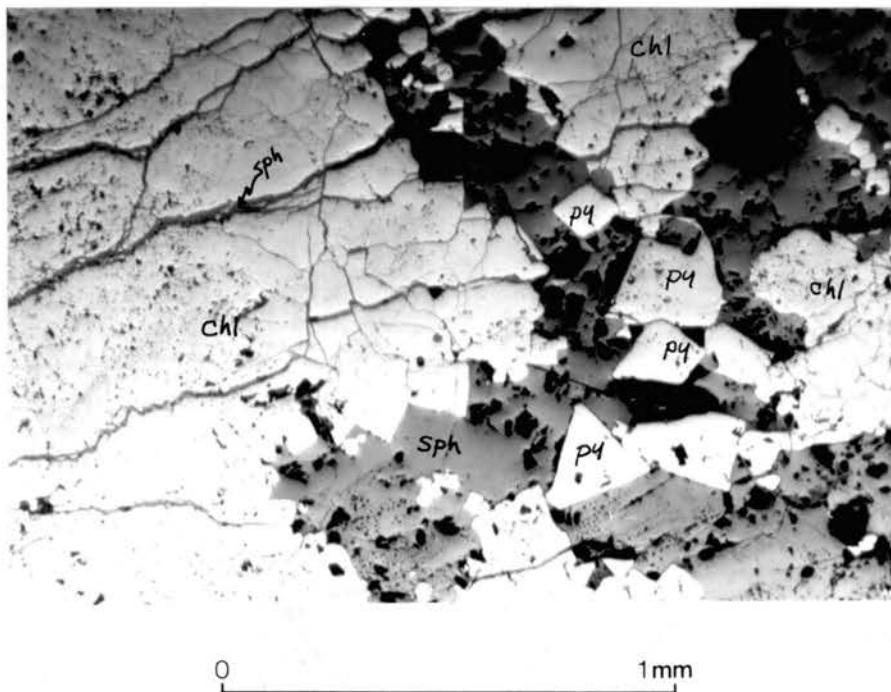


Figure 29. Photomicrograph displaying sphalerite (sph) cutting chalcopyrite (chl).

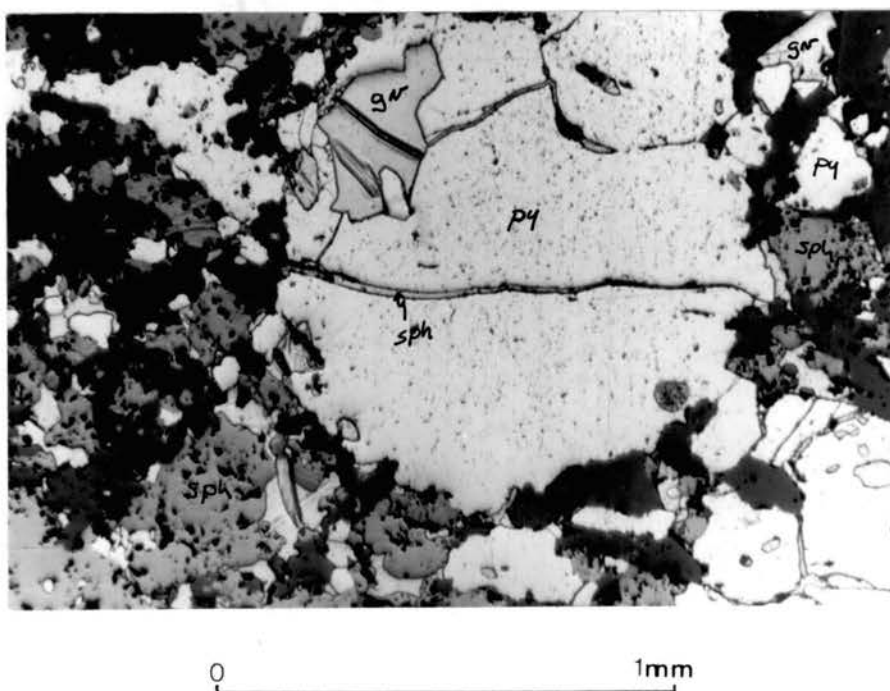


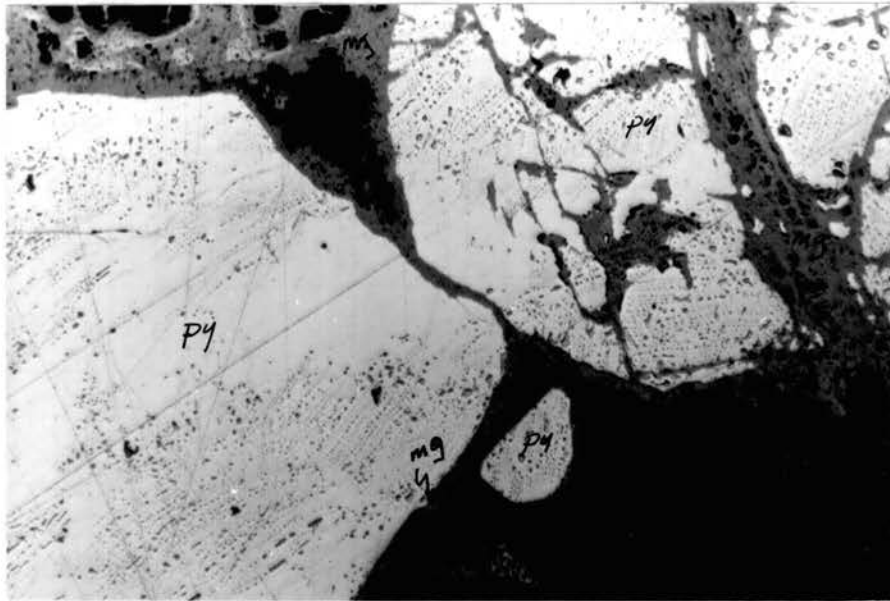
Figure 30. Photomicrograph showing sphalerite (sph) veinlets crosscutting pyrite (py) but not galena (gn).

Minor Oxide Mineralization

A common phenomena observed near the margins of the northern quartz monzonite is the occurrence of magnetite in veins and vug-like masses. Along the north-central map area, magnetite is concentrated within the Leadville Limestone and limey shale member of the Belden Formation as vein-like masses, 5-6 inches in width, consisting of magnetite, and pyrite within a quartz gangue. Figure 31 is a photomicrograph of a magnetite-pyrite mass showing the boundary of a pyrite crystal being rimmed by magnetite. Quartz stringers cut both pyrite and magnetite. Figure 32 again displays magnetite replacing pyrite by the existence of magnetite rims around pyrite crystals. The quartz gangue of these magnetite-pyrite masses contains inclusions of a mineral which displays twinning similar to the Carlsbad-albite twinning common to plagioclase but displays no extinction upon rotation of the stage under crossed nicols. The mineral in question is possibly marcasite. (see Figure 32).

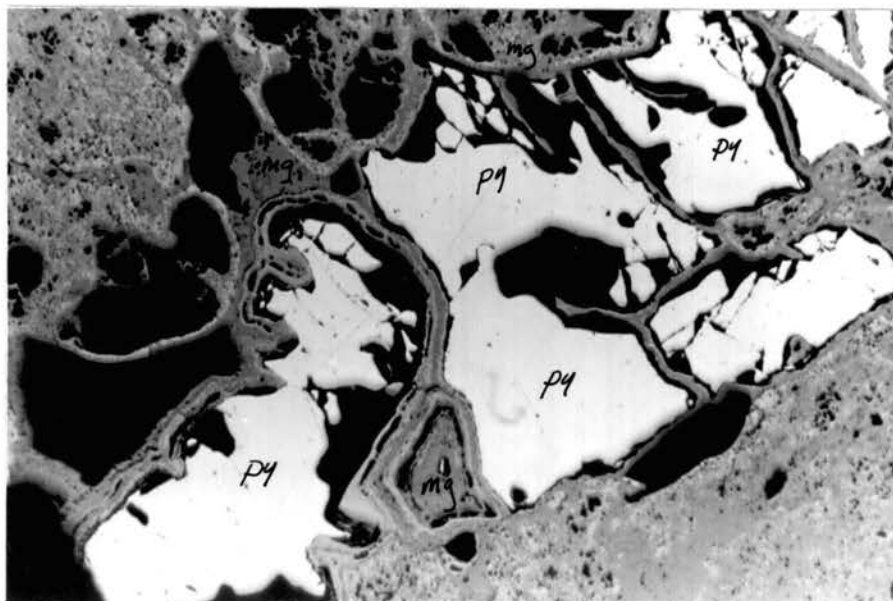
Due to the close proximity to the quartz latite dikes, it is the author's belief that these pyrite-magnetite veins were deposited by hydrothermal solutions which ascended along the dike margins and into the Belden and Leadville Formations along fractures intersecting these quartz latite dikes. The Leadville Limestone and limey shale of the Belden Formation presented favorable chemical and physical environments for the deposition of these pyrite-magnetite veins.

Magnetite, in the form of veins 5-10 feet in width and vug-like masses, was also found along the southwestern margin of the



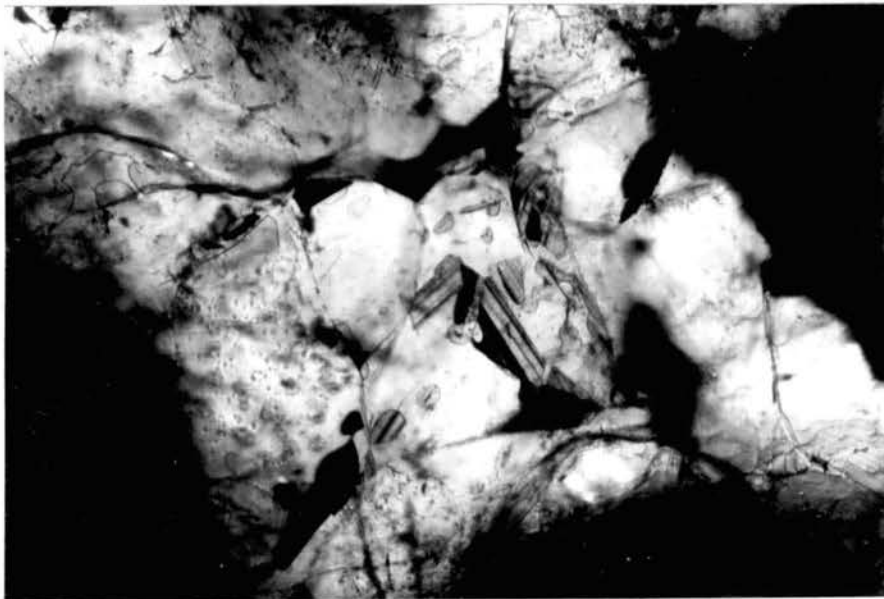
0 1mm

Figure 31. Photomicrograph of Magnetite-Pyrite mass within Leadville Limestone (north-central map area) which displays boundary of pyrite (py) crystals rimmed by magnetite (mg) •



0 1mm

Figure 32. Photomicrograph of Pyrite-magnetite mass with pyrite (py) replaced by magnetite (mg).



0 1mm

Figure 33. Photomicrograph of quartz gangue from the pyrite-magnetite mass displaying inclusions of a mineral with twinning similar to the Carlsbad-albite twinning of plagioclase. (Polished section under crossed nicols).

northern zoned intrusive. The host rock does display chloritization of biotite and alteration of plagioclase to epidote. The development of the magnetite may be attributed to: (1) the rise of iron-rich solutions along the margin of the intrusive during late stage hydrothermal activity, or (2) the flushing of iron from the argillized quartz monzonite interior and subsequent concentration within the marginal propylitic zone. In the interior, where the quartz monzonite has been subjected to argillic alteration, the ferromagnesian minerals have been bleached and oxidized. Outward moving hydrothermal solutions, carrying the bleached ferric iron from the argillic zone, deposited the ferric iron as magnetite in response to the chemical conditions prevalent within the propylitic zone. Also, within the propylitic zone the ferromagnesian minerals present were subjected to alteration whereby: hornblende + biotite \rightleftharpoons chlorite + epidote + magnetite; thus contributing an even higher concentration of magnetite.

It is the author's belief that the quartz latite to quartz latite porphyry dikes of the Italian Mountain area represent late stage emissions from a differentiating parent magma having an original overall granodiorite composition. These dikes later acted as conduits for mineralizing hydrothermal fluids, emitted during the dying stages of the quartz monzonite intrusive phase, and thus suffered argillic alteration and associated pyrite mineralization along their margins.

Mine dump samples collected by the author from the Clara L. Mine displayed dense pyrite crystallization in the form of cubic and hexoctahedral crystals, within the intensely argillized quartz latite porphyry. Intense argillic alteration is represented by the alteration of plagioclase to sericite and/or kaolinite and the complete replacement of biotite by pyrite. Where the Leadville Limestone was crosscut by these dikes it was mineralized with pyrite in irregular masses. These masses possibly represent mineralization along small scale crosscutting fractures or faults intersecting a larger fault occupied by the quartz latite dike.

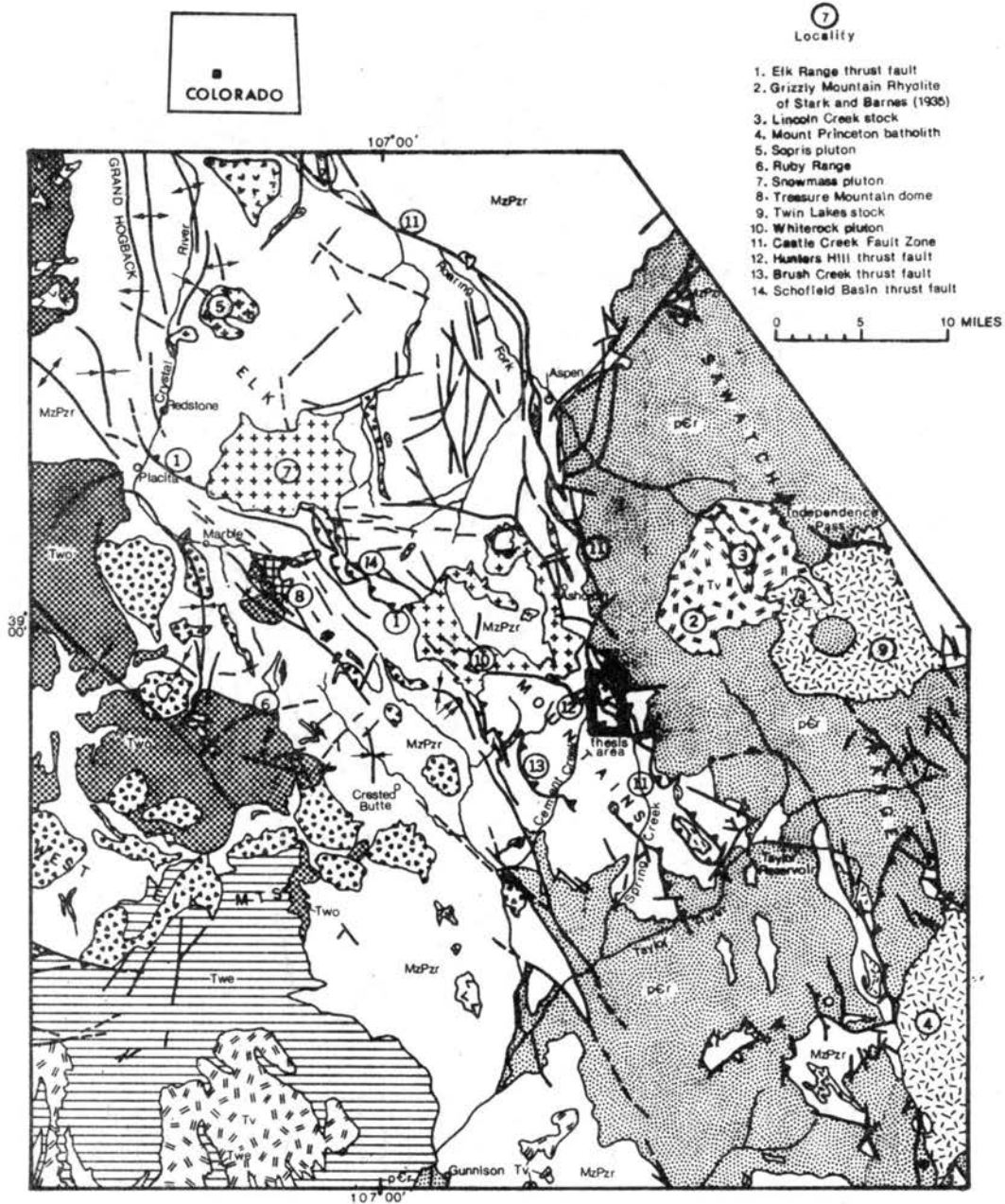
CHAPTER VI

STRUCTURAL GEOLOGY

Two structural trends or lineaments of regional extent within central Colorado have exerted considerable influence upon the local structure of the Italian Mountain area: (1) a northwest-southeast trending lineament represented by the Elk Mountain and Castle Creek fault zones, (Fig. 34) and (2) a northeast-southwest lineament represented by the "transverse" Colorado Mineral Belt. The present position of the Elk Mountain intrusive belt was in fact controlled by the existence of these structural trends.

The Northwest Lineament

As mentioned above, the northwest lineament is represented by two major fault zones, the Castle Creek fault zone in the east and the Elk Mountain fault zone in the west (see Figure 34). The Elk Mountain fault zone extends northwest as a west-dipping monocline called the Grand Hogback monocline. Associated with these northwest trending fault zones are the following characteristic modes of deformation: monoclinial folds, tight folded sedimentary sequences, overturned strata, high-angle reverse faults, and overthrust faults, all believed to have been associated with the Sawatch uplift during Laramide time.



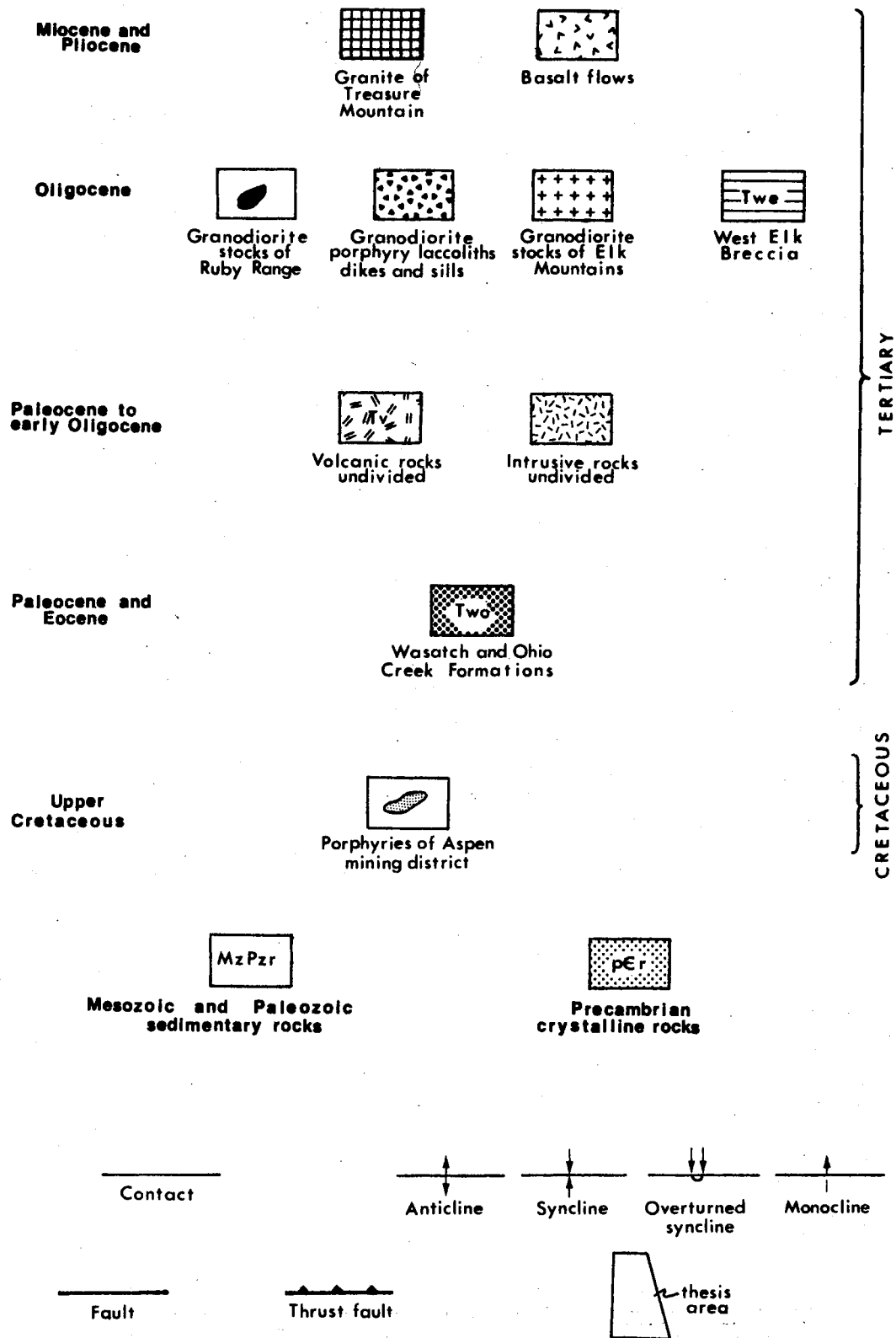


Figure 34b. Explanation for Regional Geologic Map

The Northeast Lineament

The northeast lineament within central Colorado is displayed by the numerous Tertiary intrusive bodies of the Colorado Mineral Belt. Within the Front Range of Colorado this northeast lineament is well defined by a series of parallel shear zones dissecting the exposed Precambrian basement rocks (Tweto and Sims, 1963). It has been postulated that the Tertiary igneous rocks of the Colorado Mineral Belt were intruded along these Precambrian-derived zones of weakness. The intrusive rocks of the Colorado Mineral Belt are best developed where the northeast and northwest lineaments intersect. The Snowmass Mountain stock, the Mount Sopris stock, and the White Rock Mountain pluton parallel the northwest lineament but were intruded along the Precambrian-derived zones of weakness. The Italian Mountain intrusive complex seems to be a mere offshoot of the White Rock pluton and the path of its intrusion was apparently controlled by the northwest-trending Castle Creek fault zone.

Local Structure

The structural fabric of the Italian Mountain area consists of (1) a drape fold along the eastern map area which is transected by east-west trending strike-slip faults, (2) an overthrust fault along the western map area called the Hunter's Hill overthrust, (3) high-angle reverse and normal faults within the Paleozoic sediments as well as the Tertiary intrusives, and (4) tight anticlinal to synclinal folds trending northwest to southeast within the Paleozoic sediments (see Fig. 1).

The local structure of the Italian Mountain area reflects a pattern similar to the regional structure in that two distinct structural lineaments are displayed: (1) a northwest lineament best represented by: a) the Hunter's Hill overthrust, b) the tight synclinal to anticlinal folds within the Paleozoic sediments within the Stewart Basin and the extreme northwest map area, and c) the drape fold along the eastern map area: (2) a less pronounced northeast lineament represented by: a) the northeast trending quartz latite and quartz latite porphyry dikes, and b) the high-angle normal faults within the Paleozoic sediments between the Star and Stewart Basins and along the southwest border of the southern granodiorite intrusive. A third structural lineament is suggested by the east-west trending strike-slip faults which transect the drape fold found along the eastern map area.

The different stress fields which are thought to be responsible for the observed structural features of the Italian Mountain area are: (1) steeply inclined maximum vertical stress, associated with the vertical uplift of the Sawatch Mountains, which is responsible for high-angle reverse faults in the basement and drape folds in overlying sedimentary rocks, (2) local compressional stress, or maximum horizontal stress, generated by vertical uplift and resulting in gravity gliding (overthrust faulting of the Hunter's Hill fault zone) of the Upper Paleozoic sediments off of the Sawatch uplift, and (3) extensional stress, or maximum vertical stress, exerted by Tertiary activity resulting in the formation of high-angle normal faults. The author tentatively suggests that the stress field responsible for the generation of the east-west

trending strike-slip faults was compressional stress generated by gravity gliding of the Paleozoic sediments off the Sawatch uplift, because these faults are confined to the drape folds within the eastern map area.

Deformation observed within the Italian Mountain area has involved the Precambrian basement complex with the overlying Paleozoic sediments representing but a thin veneer draping the basement rocks. Thus, the structural fabric of the sediments may reflect the heterogeneity of the basement rocks. These basement rocks were subjected to deformation for a vast amount of time, and many well-developed zones of weakness have undoubtedly resulted. The deformation due both to the Laramide orogeny and the Tertiary intrusives is thought to have been greatly influenced by these pre-existing zones of weakness, a relationship which would have contributed further to the structural complexity of the area.

Local Structural Relationships

The strike-slip faults, associated with the folds along the eastern map area, are characterized by the following features: (1) transverse orientation to the general northwesterly strike of the folds, (2) considerable dip separation, and (3) a somewhat sinuous trace on the geologic map (see Fig. 1).

The surficial Hunter's Hill overthrust, mapped by Prather (1964), is genetically related to the Castle Creek structure zone, and within the Italian Mountain area the Gothic Formation is displaced over the top of Maroon Formation along this overthrust. The following features are displayed along the Hunter's Hill overthrust

within the Italian Mountain area: (1) erratic variation in strike of the Permo-Pennsylvanian beds on either side of the fault plane, and (2) moderate amounts of brecciation along the fault plane.

An examination of cross section A-A' shows that at the surface this fault dips gently to the east. It is thought not only to flatten at depth, but also show a reversal of dip from east to west in the subsurface. This interpretation follows the one set forth by Walstrom and Hornback (1962) for the Williams Range thrust fault located on the west flanks of the Colorado Front Range, where extensive subsurface data support gravity gliding as the fault mechanism.

To the east of the granodiorite intrusive, the Hunter's Hill fault zone converges with a high-angle reverse fault which dips to the east (see cross section B-B', and Fig. 1).

In cross section B-B' (Fig. 35) the high-angle reverse fault is shown to steepen with depth, as Badgley (1965) and others have determined for high-angle reverse faults on the flanks of foreland uplifts.

In the Star Basin the author mapped a normal fault trending N 35°W and dipping to the east. It is the author's belief that this normal fault was produced by extensional stress generated by the intrusion of the northern melangrondiorite to quartz monzonite igneous body. This normal fault extends across the entire Star Basin and is terminated against the overturned Paleozoic sediments in the area between the Stewart and Star Basins.

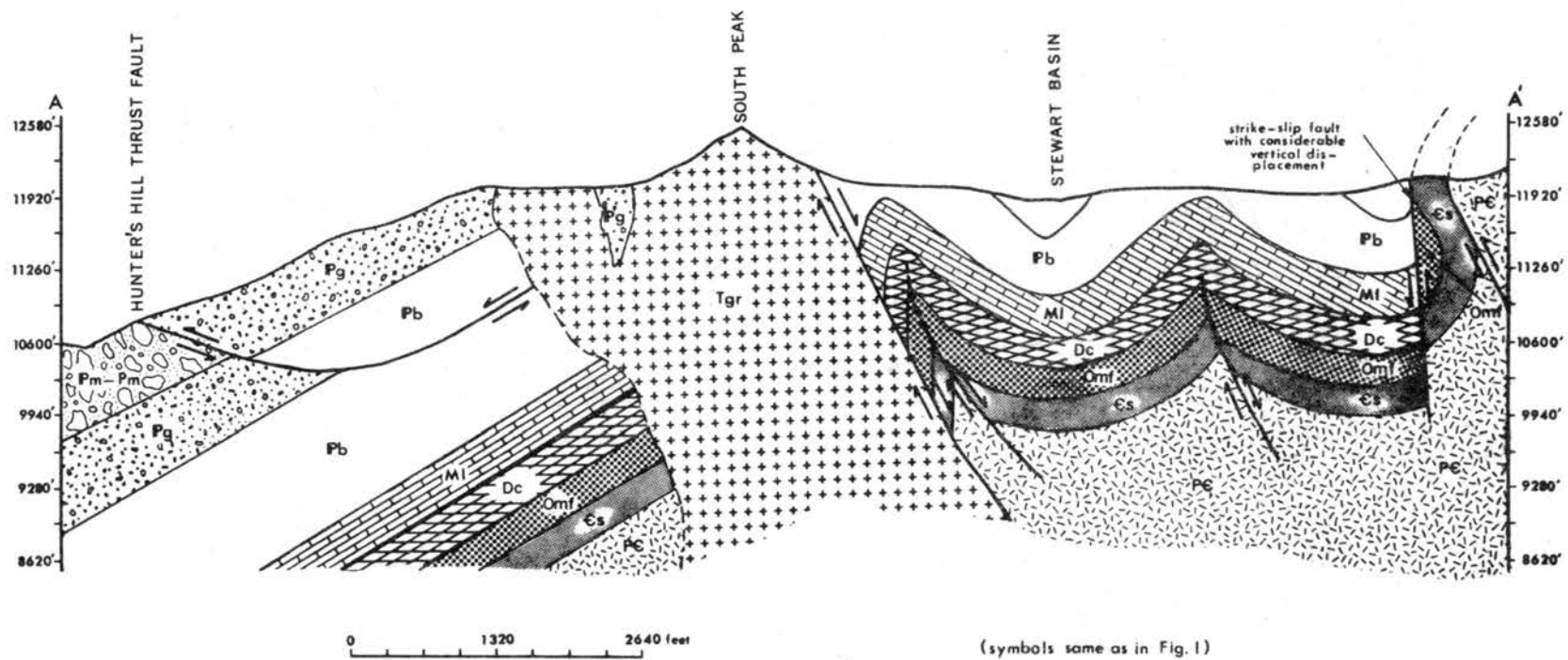
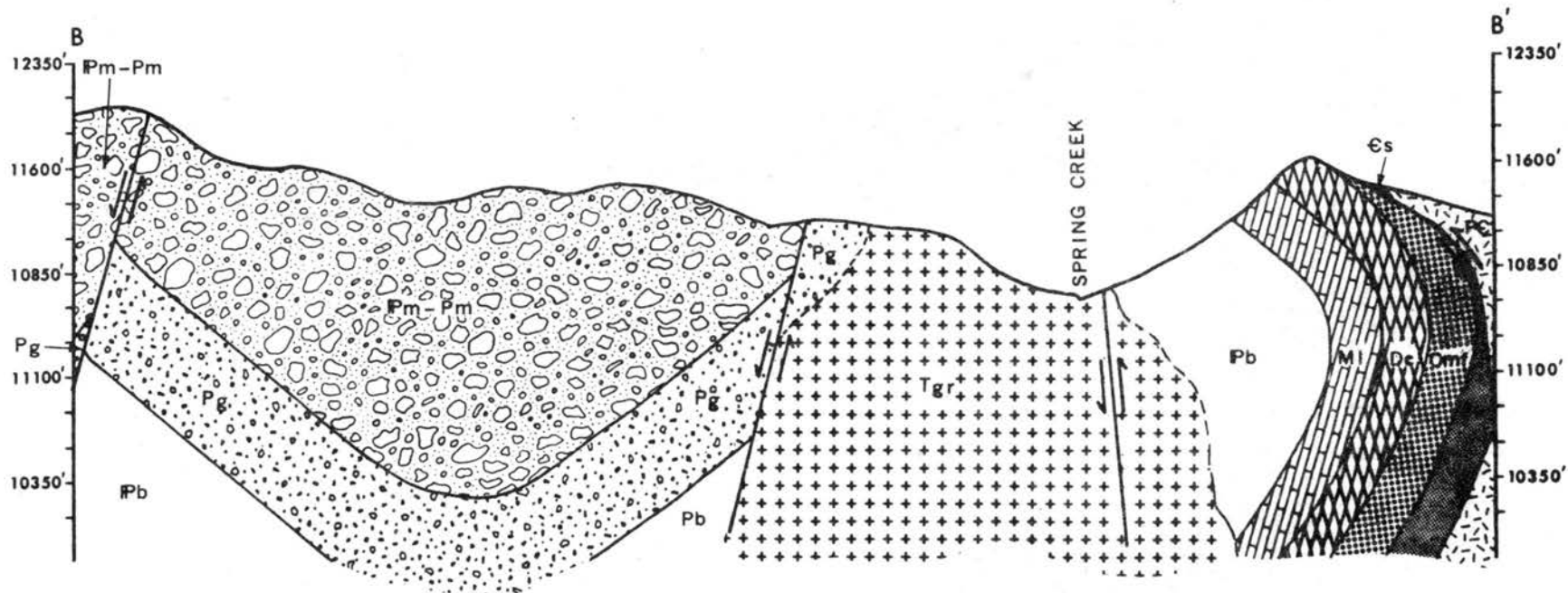


Figure 35. Cross-section A-A', South Italian Mountain



Vertical Scale: 1" = 1,250 feet

Horizontal Scale: 1" = 1,320 feet

(symbols same as in Fig. 1)

Figure 36. Southernmost Cross-section, B-B'.

A series of tight folds, with axes trending northwest-southeast, are found within the Paleozoic sediments of the Stewart Basin (see cross section A-A' and Fig. 1). These folds are thought to be related primarily to the reduced space condition caused by the high-angle reverse faults and Tertiary intrusive uplift (see cross-section A-A').

CHAPTER VII

CONTACT METAMORPHISM

Within the Italian Mountain area contact metamorphic effects are best expressed within the Leadville Limestone and the shaly limestone member of the Belden Formation, which are in contact with the northern monzonite and the central monzodiorite intrusives. The contact zone between the southern granodiorite intrusive and the Paleozoic sediments displays only mere traces of contact metamorphism due to: (1) poor exposure of the actual contact itself because of talus cover, and (2) unfavorable Paleozoic host rocks for the expression of contact metamorphic mineral assemblages. The entire western margin of this southern granodiorite stock is in contact with the Gothic and Maroon Formations (non-marine conglomerates and arkose sandstones for the most part). The author will therefore restrict his discussion to the contact metamorphic effects expressed by the contact zones between the Paleozoic sediments and the northern quartz monzonite and the central monzodiorite intrusive bodies.

Description of Contact Metamorphic Assemblages

To define the extent of the contact mineral assemblages, developed within the Paleozoic sediments intruded by the northern quartz monzonite and the central monzodiorite, traverses were made

along the contacts. In conducting these traverses characteristic mineral assemblages were noted along with the approximate width of each mineral zone. Some contact metamorphic minerals were not readily identifiable so hand samples were taken in the field and positive identification of the unknown minerals was accomplished through the use of index oils in the laboratory. The variety of garnets developed within the skarn or tactite zones presented a problem in that their refractive indices exceeded the highest index oils available to the author. Thus to ascertain the different species of garnets the author employed spectrographic analysis for the determination of major cations, and simple specific gravity tests. Cross and Shannon (1927) were also consulted to confirm the author's findings.

The only decent exposure of the contact between the northern quartz monzonite intrusive and the Leadville Limestone is found in the northern map area (see transverse G-G' on contact metamorphic facies map, Fig. 41, p. 121). Here the contact aureole is only five feet wide and consists of the following mineral assemblages moving out from the immediate contact with the quartz monzonite: a diopside-grossularite-vesuvianite zone to a wollastonite-diopside assemblage, and finally to minute diopside crystals embedded in recrystallized Leadville Limestone. This last mineral association represents initial thermal metamorphism of impure Leadville Limestone whereby traces of silica were added to the Leadville along with heat and water vapor from the intruding magma. The Leadville Limestone does display extreme recrystallization with

some calcite rhombohedrons up to 3 inches in length. The recrystallization effects of thermal metamorphism within the Leadville Limestone extend from 500 to 600 feet from the quartz monzonite contact. The melanogranodiorite shell along the contact zone has suffered some metamorphic effects itself. Phenocrysts of metasomatic hornblende 1-2 cm in length have been formed and the plagioclase does display some alteration to diopside, in thin section.

To the south of the above traverse the quartz monzonite intrusive is in contact with the Belden Formation which is represented by a limey shale to shaly limestone sequence. The traverse was started along the contact between the recrystallized Leadville Limestone in the east and proceeded west to the intrusive contact. Along this traverse (H-H' on the facies map) a variation in the mineral assemblage reflects the nature of the strata encountered.

The limey shale displays the metamorphic mineral assemblage tremolite-anorthite-diopside, whereas the shaly limestone displays diopside-grossularite-calcite with minor amounts of wollastonite. This particular aureole measured about 1330 feet along the traverse taken. The expanded thickness of this zone reflects the extension of the quartz monzonite intrusive at a shallow depth.

Traverse I-I' (Fig. 41) was taken along the wedge of Belden Formation between the quartz monzonite and monzodiorite intrusives within the west-central map area. The quartz monzonite along the contact with the Belden limey shale to shaly limestone displays from 2 to 5 feet of alteration in which the rock is enriched in metasomatic anorthite, which along with the original magmatic plagioclase (of andesine to oligoclase composition) has suffered hydro-

thermal alteration to diopside. Due to orthomagmatic conditions the quartz monzonite also displays an enrichment in hornblende which along with biotite has been replaced by pyrite due to later hydrothermal activity. The entire Belden sequence, here represented by a shaly limestone, has been metamorphosed and displays the following mineral assemblages proceeding toward the monzodiorite; diopside-tremolite-plagioclase, diopside-grossularite to andradite-calcite, and diopside-andradite-radiating prisms of vesuvianite-calcite (minor wollastonite). The absence of tremolite and the appearance of vesuvianite and wollastonite with calcite reflect the higher temperature generated by the central monzodiorite intrusive. This monzodiorite intrusive displays considerable albitization and epidote development, and also quartz stringers and vugs along its contact with the Belden Formation.

Traverse J-J' (Fig. 41), located within the north-central map area along the contact between the quartz monzonite intrusive and the shaly limestone unit of the Belden Formation, displays a contact metamorphic aureole 10-15 feet wide consisting throughout of the anorthite-diopside-tremolite mineral assemblage. Near the quartz latite dikes the shaly limestone of the Belden Formation is impregnated with magnetite along fractures, in addition to displaying diopside-tremolite development. This assemblage possibly could represent a tactite zone formed by the escape of solutions rich in Mg, Fe, and Si from the cooling magma during the metamorphic cycle or may be due to later hydrothermal emissions whose alteration effects have been superimposed upon the metamorphic mineral assemblage.

Traverse K-K' (Figure 41) was made across the duck-bill-shaped roof pendant of Belden Formation found within the north-central portion of the quartz monzonite intrusive. The Belden Formation here consists of a black fissile shale interbedded with the typical shaly limestone. Along the contact between the Belden Formation and the quartz monzonite to the north, the quartz monzonite has been transformed to a rock composed of quartz, anorthite and alkali feldspar with essentially all the ferromagnesian minerals removed. This metamorphic zone extends three feet into the igneous proper itself. Two basic mineral assemblages and a skarn zone distinguish this metamorphic aureole: (1) diopside-garnet (grossularite to andradite)-calcite, (2) diopside-garnet (grossularite to andradite)-vesuvianite, and a skarn composed of either magnetite-chalcopyrite-diopside-garnet (andradite) or hematite-diopside (minute crystals)-clinochlore-garnet (andradite-red-black)-vesuvianite. A quartz latite dike cuts through the approximate center of this metamorphosed pendant of Belden Formation, and the black fissile shale unit along its perimeter has been converted to graphite with minute black garnet crystals most likely of almandine composition. The quartz monzonite of the southern contact contains hematite vugs, is enriched in diopside, and is depleted in biotite.

The contact metamorphic mineral assemblage present within the paw-shaped embayment of Belden Formation projecting into the quartz monzonite in the northwestern map area (traverse L-L', Figure 41) is grossularite-wollastonite-quartz, with traces of diopside. This contact mineral assemblage mentioned above occurs as patches within a silicified marly limestone, very light gray to off

white in color. Grossularite is the dominant mineral present. Wollastonite occurs as encrustations upon the dodecahedrons of garnet and diopside fills the interstices between garnet crystals. The garnet dodecahedrons range in size from 2-30 mm in diameter and display a transparent pale green to amber or ginger color. Along this contact the quartz monzonite is enriched in quartz, potassium feldspar, diopside and minor hornblende.

Traverse M-M', taken across the northwest end of the toe-shaped extension of Belden Formation between the quartz monzonite intrusive to the north and the monzonite intrusive to the south, displays some interesting phenomena. Dikelets 2-3 inches wide consisting of diopside, anorthite, tremolite, and hornblende were found within the monzonite intrusive near its contact. The segment of Belden Formation between these two intrusives displays a new type of contact metamorphic mineral assemblage: tremolite, hornblende, biotite and interstitial anorthite. A green micaceous mineral believed to be a chloritoid is also associated with the hornblende and tremolite.

The southern margin of the monzodiorite stock does display diopside, tremolite, plagioclase, and quartz mineralization along fractures.

The actual contact of the monzodiorite with the Belden Formation is obliterated by a pyrite zone 250-300 feet wide along the perimeter of the monzodiorite and extending into the Belden Formation. This pyrite mineralization represents a hydrothermal event

which occurred subsequent to the metamorphic episode.

Near the contact with the southern granodiorite intrusive, traces of hornblende mineralization were found within the talus. The granodiorite in fact displays calcite vugs, diopside and tremolite mineralization along fractures and slight potassium feldspar enrichment, and quartz veins, 1/4 - 1/2 inch in width, near the contact zone.

The most pronounced development of calc-silicate-hornfels and tactite was found within the roof pendant of Belden Formation on top of Central Italian Mountain. The typical calc-silicate mineral assemblage consists of vesuvianite-diopside-garnet-wollastonite. Vesuvianite $[Ca_{10}(Mg,Fe)_2Al_4SiO_4)_5(Si_2O_7)_2(OH_4)]$, occurs as transparent yellowish-green to olive-green crystals displaying a bipyramidal to short prismatic (tetragonal) habit and striated to columnar masses 3-8 cm in length. Its mode of occurrence is rather peculiar in that it is found within cavities or vugs developed in a fine grained matrix of diopside, garnet, interstitial wollastonite and a white fibrous zeolite (scolecite). Diopside besides occurring in massive fine-grained form, also displays light gray-green or olive gray-green crystals of prismatic to pyramidal habit (monoclinic), as large as 8 -10 mm in length. Within this roof pendant garnet displays a wide variety of colors: pale brown to buff, and reddish-brown to dark brown reflecting a variable composition. The pale brown to buff colored garnet was found to be the lime-alumina garnet grossularite $[Ca_3Al_2Si_3O_{12}]$, while the reddish-brown to dark brown variety represents the lime-ferric iron garnet andradite. In all cases

garnet displays crystals, 1-5 mm in diameter, of dodecahedron habit which are modified by the more narrow faces of the hexoctahedron. Its mode of occurrence is as linings along open spaces in a dense-garnet-diopside hornfels or as clusters of loosely intergrown dodecahedrons.

Stages of Contact Metamorphism

It is the author's belief that the Paleozoic sediments in contact with the Italian Mountain intrusives have undergone two distinct stages of igneous metamorphism: (1) thermal metamorphism at the time of the intrusion of the central monzodiorite and northern quartz monzonite igneous bodies, and (2) subsequent contact metasomatism. Initially the intruding magma supplied heat and water vapor to the Paleozoic host rocks bringing about recrystallization and rearrangement of the original constituents, within an essentially closed system, to form minor amounts of calc-silicate hornfels. The heat generated by the cooling magma may have also stimulated the circulation of meteoric water and connate water within the sediments themselves, thus providing a means of transporting impurities toward the alteration front. During this state of thermal metamorphism the Leadville Limestone cut away from the immediate contact zone was marbelized, bleached white, and recrystallized into a coarse network of calcite rhombohedrons with minute crystals of interstitial diopside. Thermal metamorphism of the Paleozoic host rocks continued to operate during the solidification of an outer shell or crust consisting of melanogranodiorite for the northern intrusive and monzodiorite for the central intrusive.

Upon further cooling great pressure built up within the incased liquid magma and fractures developed within the solidified crust

allowing for magmatic emanations into the Paleozoic sediments which had been made ready by previous thermal metamorphism. The magma chamber contributed vast amounts of such elements as silica, alumina, iron, fluorine, and sulfur, transported in hot solutions or gases which reacted with the host rocks, through the process of metasomatism, to form calc-silicate hornfels.

Evidence supporting the theory that development of the major calc-silicate hornfels occurred after solidification of the outer margin of the intruding magma, is obtained by noting that: (1) the most intense tactite and calc-silicate mineralization is found near quartz latite dikes (representing previous fault zones) and other fracture zones; (2) quartz veins and vug-like masses consisting of quartz, hornblende, orthoclase, and diopside were found within the outer margins of the central monzodiorite intrusive, and (3) one to three inch wide dikelets composed of diopside, wollastonite and anorthite were found penetrating the monzodiorite along its contact with the wedge-shaped extension of Belden Formation and the northern monzonite intrusive in the north-central map area.

The mechanism of metasomatism involves the alteration of a rock whereby its minerals are replaced with others in less than equal amounts as demonstrated by vuggy products and by euhedral crystals. This replacement usually is accomplished by pore solutions dissolving some minerals and immediately depositing others, so that the rock preserves its solid state in the course of the replacement. During wall rock metasomatism aqueous solutions, emitted by the magma, percolate along fissure zones by the process of infiltration, whereas the interaction of the percolating solutions with the wall rock takes place by diffusion

of components through stationary pore solutions. Circulation of pore solutions by the process of infiltration not only effects the delivery of components to the replacement front but also the removal of mobile components. Thus metasomatism takes place within an open system where a compensating reaction takes place between the host rock and the source rock emanating the enriching solutions.

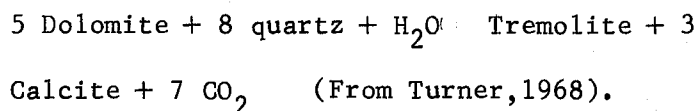
Types of Metasomatism

The formation of garnet from the Leadville Limestone implies a great addition of silica, alumina, and ferric iron with an associated loss of calcium oxide and elimination of CO_2 from the system. The type of garnet which results is a function of the Fe/Al ratio inherent to the metasomatizing solutions. Diopside formed where magnesium was concentrated within the Leadville Limestone by thermal metamorphism. Infiltrating solutions supplied silica, alumina, and ferrous iron. Silica substituted for CO_2 which was removed from the system, and CaO was extracted from the host rock and carried away by infiltrating solutions. The formation of wollastonite required a large addition of silica to the limestone with little addition of Mg, Fe, or Al. Silica substitutes for carbon dioxide is represented by the following univariant equilibrium equation: $\text{CaCO}_3 + \text{SiO}_2 \rightleftharpoons \text{CaSiO}_3 + \text{CO}_2(\text{g})$.

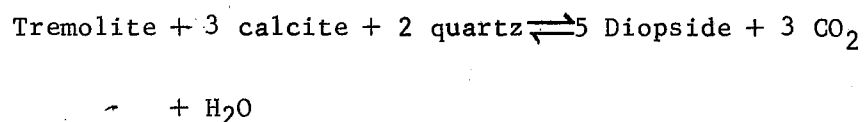
The contact between the Leadville Limestone and the quartz monzonite intrusion CaO is added to the intrusive body as a consequence of the reactions between the limestone and the solutions emitted from the magma. The addition of large amounts of CaO to the quartz monzonite at the contact has brought about endometamorphism of the intrusive itself. This endometamorphism of the intrusive contact is represented by the

occurrence of anorthite, hornblende, diopside and minor amounts of andradite along fractures within the intrusive mass. The alteration of the plagioclase and hornblende (whether by metasomatic solutions or by subsequent hydrothermal solutions) of the intrusive rock by the addition of CaO tends to liberate soda which subsequently forms albite rims around the calcic plagioclase crystals (see Figure 8, page 36). As with the Leadville Limestone, the introduction of Si, Mg, and Fe from the quartz monzonite and monzodiorite magma has produced the metasomatic mineral assemblage garnet-diopside-wollastonite within the Belden Formation. Due to the presence of more iron and aluminum impurities within the shaly intervals of the Belden Formation, garnet mineralization is well developed and displays a wide range in composition from buff to brown colored grossularite to reddish-brown to dark brown andradite. Tremolite-actinolite, hornblende, anorthite, and minor chloritoid were most probably added to the contact mineral assemblage by simple recrystallization and reorganization of elements to form new minerals.

Tremolite-actinolite and massive diopside could also have been formed by Bowen's decarbonation process whereby, with increasing temperature at some constant value of P_{CO_2} (assume $P_{CO_2} = P_{H_2O}$), a series of reactions occurs involving the progressive elimination of CO_2 from the solid phase assemblages. Assuming that the limestone beds within the Belden Formation have been altered to a dolomite composition as a result of the addition of Mg from the shale during the process of thermal metamorphism, the reaction of quartz with dolomite at $P_{H_2O} = P_{CO_2} = 1$ bar, and 180° C, would produce tremolite or tremolite by:



Turner (1969) shows that further decarbonation results in the disappearance of the hydrous silicate tremolite from the metamorphic assemblage by the reaction:



at $P_{\text{H}_2\text{O}} = P_{\text{CO}_2} = 1 \text{ bar}$ and 230° C .

The additional occurrence of vesuvianite $[\text{Ca}_{10}(\text{Mg,Fe})_2 \text{Al}_4 (\text{SiO}_4)_5 \cdot (\text{Si}_2\text{O}_7)_2 (\text{OH})_4]$, scapolite, and epidote with a high fluorine content (these last two minerals were found at Italian Mountain by Shannon and Cross, 1927) within the metamorphosed Belden Formation, suggest a high partial pressure of fluorine and chlorine during contact metasomatism. Turner and Verhoogen (1960) have pointed out the importance of the activity of chlorine and fluorine as "carriers" of iron. Iron metasomatism, important to the development of the andradite as well as magnetite enrichment along contact zones, has been facilitated by the iron transporting activity of these two halides.

ACF and A¹KF Diagrams

It is important to be acquainted with the chemical compositions of magmatic and sedimentary rocks because the metamorphic mineral assemblage derived from these rocks is a consequence of their compositions. Figure 37 from Winkler (1965), is a schematic presentation of the chemical compositions for the common magmatic and sedimentary rocks comprising the earth's crust, plotted on ACF and

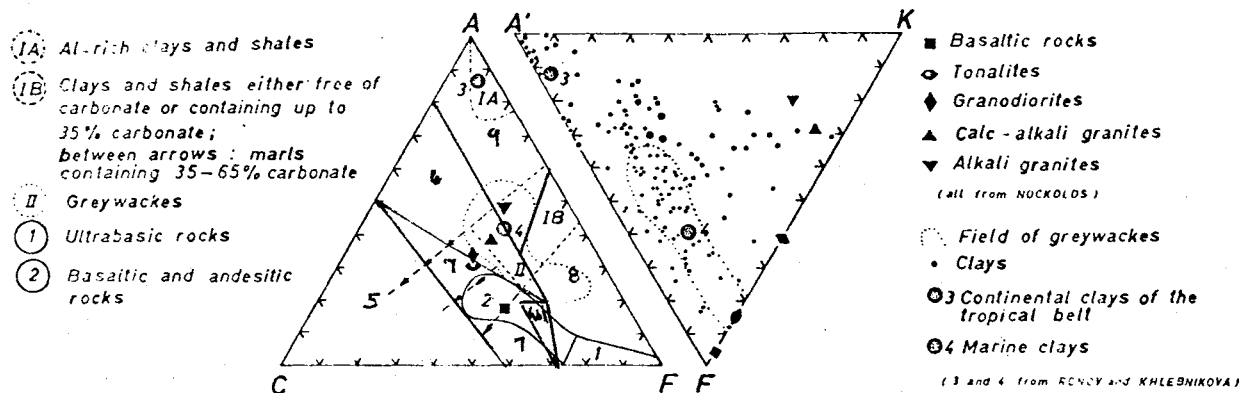


Figure 37. The chemical composition of various magmatic and sedimentary rocks plotted on an ACF and A'FK diagram. Note the considerable variation of the K values of clays and shales in the A'FK diagram (Winkler, 1965).

A'FK diagrams according to the stipulations originally set forth by Eskola (1915). For the ACF diagrams: $A = Al_2O_3 + Fe_2O_3 - (Na_2O + K_2O)$, $C = CaO$ and $F = MgO + FeO + MnO$; and for A'KF diagrams: $A' = [Al_2O_3] + [Fe_2O_3] - [Na_2O] + [K_2O] + [CaO]$, $K = [K_2O]$ and $F = [FeO] + [MgO]$. Knowing the position of a rock of a particular composition on this diagram one can predict what assemblages will be generated within any hornfels facies, by simply locating the same position on the ACF and A'KF diagrams for the selected facies. Figure 38 (a,b,c) displays the three hornfels facies of contact metamorphism with their most common assemblages on ACF and A'KF diagrams according to Winkler (1965). A multitude of ACF and A'KF diagrams have been constructed on the basis of petrographic and chemical analyses of metamorphic mineral assemblage developed within a particular facies or subfacies. Because the author was not able to run chemical analysis on the contact metamorphic mineral assemblages of Italian Mountain, ACF and A'KF diagrams had to be borrowed from the literature to fit the contact mineral assemblages present on Italian Mountain. By matching the mineral assemblages found within the contact zones of Italian Mountain with the characteristic ACF diagram, which best accounts for the observed mineral assemblages, the author was able to establish what facies of contact metamorphism are present within the contact zones of Italian Mountain.

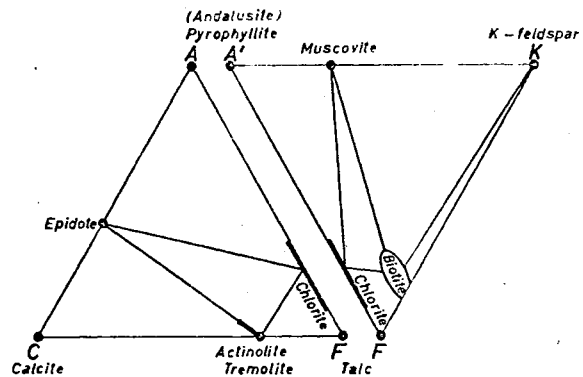


Fig. 38 a-Albite-epidote-hornfels facies (andalusite may occur in the highest-temperature part of this facies)

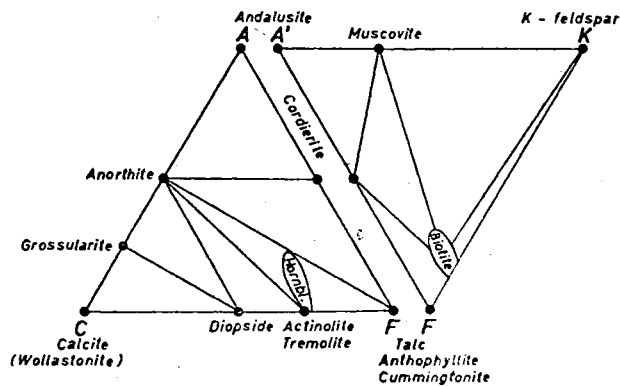


Fig. 38 b- Hornblende-hornfels facies (wollastonite may occur in the highest-temperature part of this facies)

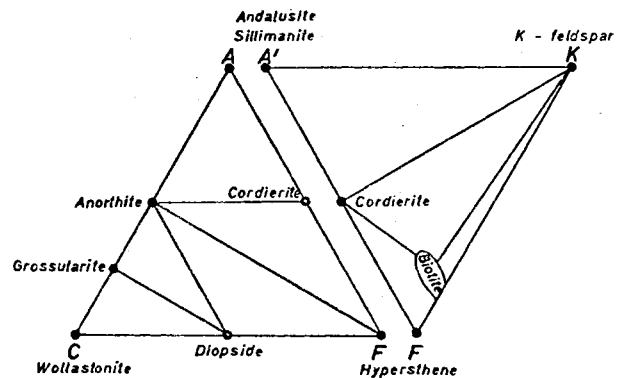


Fig. 38 c- Pyroxene-hornfels facies (sillimanite, instead of andalusite occurs in the highest-temperature part of this facies)

Figure 38. Three hornfels facies and their common mineral assemblages (Winkler, 1965).

Contact Metamorphic Facies

Referring to Figure 37 the Leadville Limestone occupies the distal apex of the C side of the ACF diagram within the area of triangle 5 (representing rocks of calcareous composition). Within triangle 5 moving towards area 7 the limestones give way to dolomites and finally marls (shaly limestones). The Belden Formation of Italian Mountain is composed of marine clays and shales with varying amounts of limestone and thus may be found anywhere within the section designated as IB, and located between the lined arrows on the ACF diagram. The average composition of the Belden Formation is most nearly approximated by the composition of granodiorite and tonalite (quartz-mica diorite) located at A = 50%, C = 50% and F = 50%. However, there are some fairly pure limestone beds within the Belden Formation. Knowing the compositions of the two formations one can then predict what assemblages will most likely be generated for each of the three hornfels-facies using Figure 38 (a,b,c). Thus for the Leadville Limestone metamorphosis at the albite-epidote hornfels facies level should produce the following assemblage: calcite, epidote, and actinolite-tremolite; whereas the Belden Formation which has more SiO_2 and K_2O than the Leadville Limestone can display albite and microcline in addition to epidote, actinolite-tremolite, biotite and minor muscovite, as well as the mineral assemblage characteristic of a fairly pure limestone. The Leadville Limestone when subjected to the temperature and pressure conditions of the hornblende-hornfels facies of contact metamorphism can be expected to display the following assemblages: diopside-

anorthite-grossularite and calcite where it is fairly pure, and diopside-anorthite-grossularite if a dolomite to marl composition is approached. Wollastonite may also be present in the higher temperature phase of this facies. The Belden Formation when subjected to the same hornblende-hornfels facies will display the following mineral assemblages: either anorthite-diopside-actinolite-tremolite or anorthite-hornblende-actinolite-tremolite, both accompanied by an additional albite-muscovite-biotite assemblage, which is characteristic of a rock rich in K_2O and SiO_2 . Again the fairly impure limestone beds interbedded with the marly beds will express a mineral similar to that of the hornblende-hornfels facies except for: (1) the disappearance of the hydrous silicates actinolite and tremolite, (2) the disappearance of hornblende, (3) the replacement of calcite by wollastonite (calcite minor and interstitial to wollastonite), and (4) the disappearance of muscovite and an increase in the cordierite content to a degree such that it is recognizable in hand sample. This last mineral assemblage is characteristic of only the marly member of the Belden Formation which is rich in K_2O and SiO_2 .

Based upon the above predictions, as to the characteristic mineral assemblages expected to be associated with the Leadville Limestone and the Belden Formation when subjected to the three facies of contact metamorphism, two distinct metamorphic facies are displayed along the contact zones of Italian Mountain: the pyroxene hornfels and the hornblende-hornfels facies. A less distinct albite-epidote hornfels facies distinguished by the presence of chlorite, epidote, albite and tremolite was noted within the Belden

Formation at the outside perimeter of the hornblende-hornfels facies. Thermal metamorphic effects are expressed within the Leadville limestone and the limestone-rich layers of the Belden Formation by the recrystallization of the limestone to an aggregate of coarse calcite rhombohedrons. This recrystallization zone extends outside the albite-epidote zone away from the intrusive contact.

The hornblende-hornfels facies is displayed within the Leadville Limestone in contact with the quartz monzonite along traverse G-G' in the north-central map area and within the marly limestone beds of the Belden Formation. The characteristic mineral assemblage is diopside-grossularite-vesuvianite-wollastonite. The disappearance of tremolite and the predominance of wollastonite over calcite seem to contradict Winkler's (1965) proposed metamorphic assemblages for the hornblende-hornfels facies. This observed discrepancy may be resolved by observing another example of contact metamorphic assemblages developed within calcareous sediments subjected to the hornblende-hornfels facies of contact metamorphism. Winkler (1965), relates that within the Sierra Nevada batholith near Visalia, California, the pelitic to calcareous host rocks have been metamorphosed to the hornblende-hornfels facies characterized by the assemblage displayed in Figure 39. The absence of tremolite and the predominance of wollastonite over calcite merely suggests that we are dealing with a relatively high metamorphic grade of the hornblende-hornfels facies and are about to enter the pyroxene-hornfels facies. The fact that the quartz monzonite is enriched in hornblende at the contact zone assures us that we are still dealing with the hornblende-hornfels facies. The presence of vesuvianite,

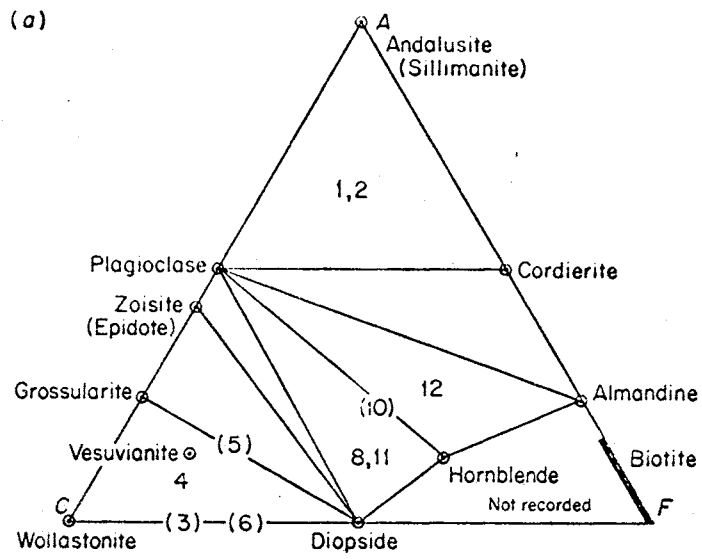


Figure 39. Hornblende-hornfels facies, near Visalia, Sierra Nevada, California. (a) ACF diagram. Quartz and plagioclase are possible additional phases. K-feldspar may occur (sometimes with muscovite) in assemblages of triangle 1, 2 (Winkler-1965).

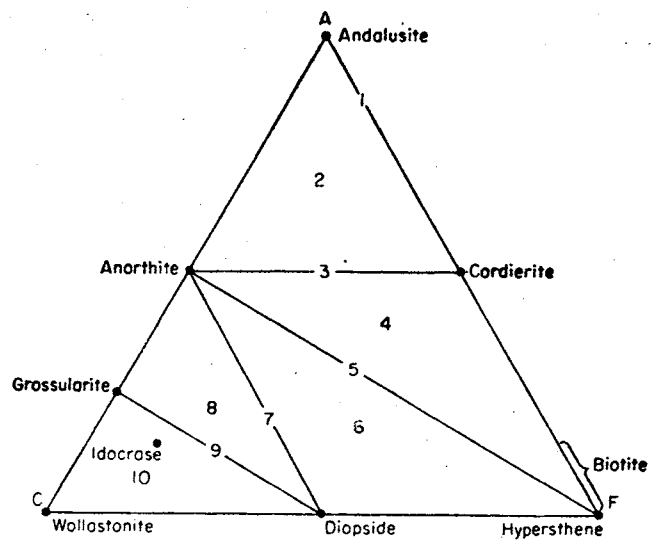


Figure 40. Pyroxene-hornfels facies: ACF diagram for rocks with excess SiO₂. Quartz and orthoclase are possible members of each assemblage.

within the hornblende-hornfels facies assemblage, indicates that there existed an appreciable partial pressure of fluorine during metamorphism.

The mineral assemblages described, along the traverse H-H', I-I', J-J', L-L', M-M' and along the contact between the Belden Formation and the southern margin of the central monzodiorite intrusive, for the marly shale and marly beds of the Belden Formation fit quite well into Winkler's (1965) hornblende-hornfels facies of contact metamorphism.

The pyroxene-hornfels facies is displayed within the two roof pendants of Belden Formation associated with the northern quartz monzonite intrusive, one within the north-central quartz monzonite intrusive (traverse K-K', Figure 41) and the other on top of Central Italian Mountain. The mineral assemblage is characterized by diopside-grossularite to andradite-wollastonite-vesuvianite, which is in direct agreement with the assemblage predicted by Winkler (1965) using the ACF and A'KF diagrams. In fact, the contact metamorphic assemblages displayed by these two roof pendants of Italian Mountain are very similar to those described by Goldschmidt for the Oslo region of Norway, depicted in Figure 40. The roof pendant along traverse K-K' displays some interesting variations. A true skarn zone has developed here due to extreme iron metasomatism whereby magnetite, clinocllore and an interstitial garnet are concentrated as irregular shaped pods and weins within the calc-silicates. Copper in the form of malachite was also observed in the magnetite masses. Due to iron metasomatism the particular species of garnet displays a variable composition from grossularite to andradite.

in a direction moving toward the contact. Calcite is predominant over wollastonite suggesting a lower grade facies than the Central Italian Mountain roof pendant. Shale beds have been metamorphosed into graphite containing black crystals of almandite garnet, along the quartz latite dike crosscutting this roof pendant. The presence of hypersthene enrichment within the melanogranodiorite along the contact provides further evidence that we are dealing with the pyroxene-hornfels facies.

Figure 41 is an idealized contact metamorphic facies map depicting the zonation of the three hornfels-facies about the Italian Mountain intrusives. As the label implies, this map is idealized in that: (1) the thicknesses of these zones are not true thicknesses; (2) the positions of individual zones were based upon the traverses made; thus extensions of particular zones from one traverse to another are purely interpretive; and (3) the albite-epidote facies is poorly defined in places.

At pressures less than 1 kb the mineral assemblages present in the Italian Mountain area require certain limits of temperature for contact metamorphism. The pyroxene-hornfels rocks of the roof pendants formed at maximum temperatures of 650-700°C. Hornblende-hornfels assemblages because of the presence of wollastonite formed between 475 and 650°C.

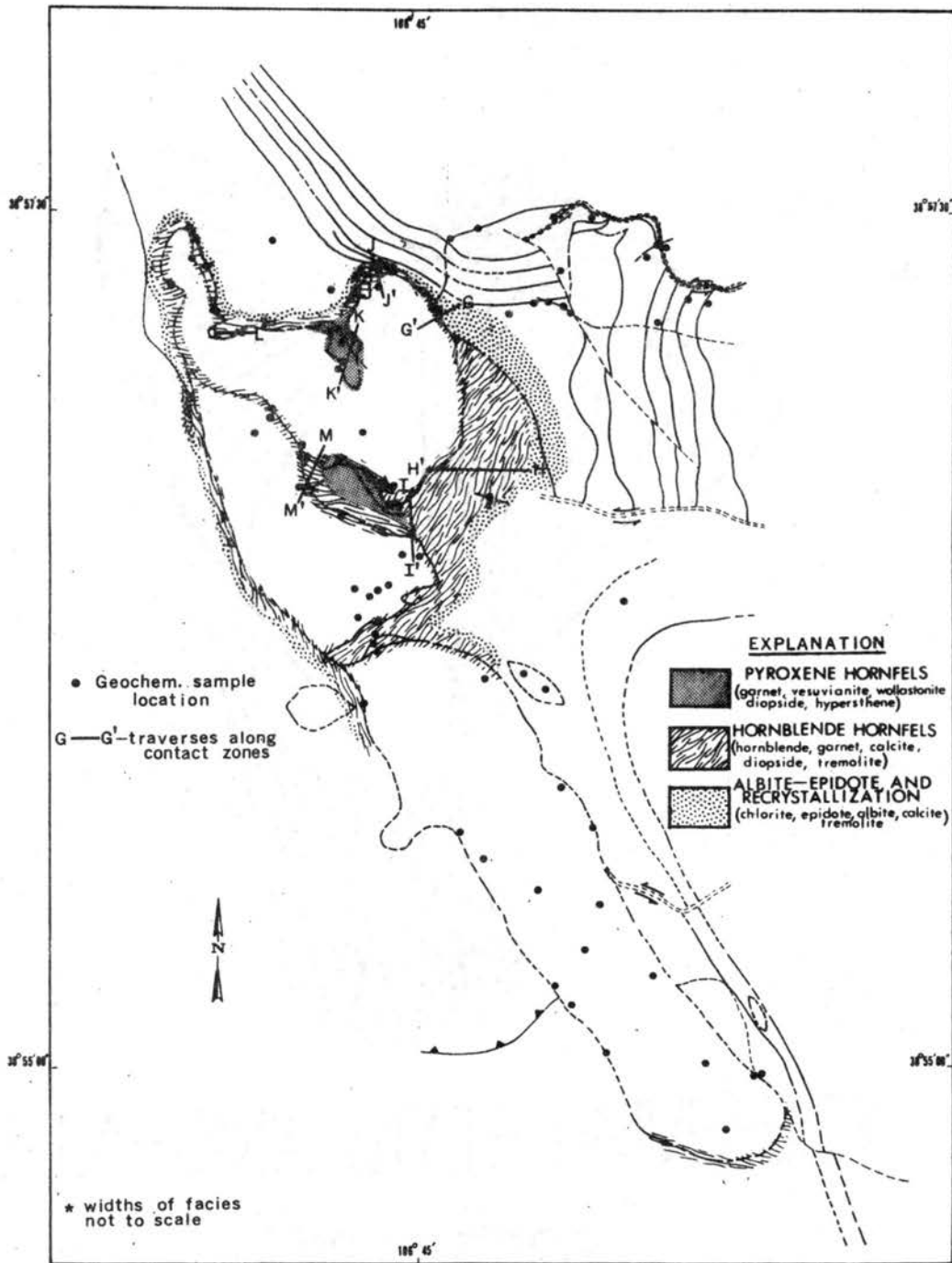


Figure 41. Contact metamorphic facies map, idealized.*

CHAPTER VIII

TRACE METAL ANALYSIS

The concept of trace metal analysis, as a guide to ore mineralization, is based upon the geologic principle that most ore deposits are surrounded by halos or aureoles of metal concentrations above the average background values for the particular rocks involved. For the Italian Mountain area noted Pb-Ag mineralization occurs within the Paleozoic sediments (especially the Leadville Limestone and Belden Formation) surrounding the intrusive complex. No precise source for this Pb-Ag mineralization has been proven but it has been suggested that the mineralizing episode was associated with the differentiating quartz monzonite intrusive of North Italian Mountain, based upon the fact the most intense sulfide (Star Mine) mineralization lies within close proximity to this intrusive. Therefore, the author collected rock chip samples over: (1) the three intrusive bodies of Italian Mountain, (2) the associated quartz latite dikes, and (3) the Paleozoic host rocks surrounding the intrusive complex (see sample location map, Fig. 42). Through trace metal analyses of these rock chip samples the author hoped to demonstrate either a definite trend or gradient (defined by contouring trace metal values) in metal concentration from one of the intrusives to the Pb-Ag mineralization or high concentrations (above the normal background values for the particular rock

types) of Pb, Zn, Cu or Mo within one of the intrusives.

Sampling Procedure

The steep slopes coupled with the existence of many extensive talus slopes, prohibited the use of a grid system for sample collection in the field. Rock chip samples were collected: (a) along fault zones, (b) along dike rocks, c) along gouge zones, d) within the fresh to slightly altered margins and interiors of the three intrusives, and (e) within the surrounding Paleozoic sediments both along the contact zones and far removed from the igneous intrusives themselves (see Fig. 42 for sample locations). At each location 2-4 rock chip samples were taken randomly at sites 5-10 feet apart.

Trace Metal Values

The 88 rock chip samples collected over the igneous and sedimentary rocks of Italian Mountain were prepared for atomic absorption analysis by first digesting them by the standard HF-HNO₃-HClO₄ (hydrofluoric-nitric-perchloric acid) treatment and then bringing the residue into solution with concentrated HCl (see Appendix C for the exact procedure). These unknown solutions were then analysed on a Perkin-Elmer (403) atomic absorption spectrophotometer from which trace metal concentrations (Cu, Mo, Pb, Zn-multiplied by a dilution factor of 50) were determined for each sample location. Appendix B is a tabulation of the results of trace metal analyses for the 88 rock chip sample locations displayed in Figure 42. Contour maps were constructed for each metal analyzed using a 10 ppm contour interval. Where the concentrations became

exceedingly high a 50 to 100 ppm contour interval had to be used (see Figures 43-46).

In order to engender meaningful interpretations of these contour maps of trace metal values the statistical parameters of: population mean, standard deviation, and threshold value were employed. The mean (m) is the arithmetic average calculated by:

$$m = \frac{\sum x(n)}{n}$$

where: x = metal content in parts per million

n = number of samples

Standard deviation (D) is calculated by the following formula:

$$D = \pm \sqrt{\frac{\sum(nX^2) - \sum X^2}{n(n-1)}}$$

where: x = metal content in part per million

n = number of samples

Using the mean and standard deviation a threshold value (T) can then be calculated by:

$$T = m + 2[D].$$

This threshold value was initially defined, by Hawkes and Webb (1962), as the upper limit of normal background values. Thus, any trace metal concentration above the threshold value is considered as being anomalous.

Mean values, standard deviation, and thresholds were calculated for each trace metal (Zn, Cu, Pb, Mo) associated with a particular rock type and for the combined rock type population (see Tables V-X1). To prevent distortion of calculated threshold values ranges had to be set up for each trace element analyzed. Any value above the range value is not used in calculating the threshold.

TABLE V

STATISTICAL PARAMETERS FOR ALL
ROCK TYPES COMBINED

| | Mean | SDEV | THRS (M+2 SDEV) |
|------|-------|-------|-------------------|
| 1-Zn | 63.15 | 44.52 | 152.18 |
| 2-Cu | 15.54 | 22.13 | 59.80 |
| 3-Pb | 27.24 | 14.67 | 56.58 |
| 4-Mo | 2.59 | 5.44 | 13.46 |

(ppm)

TABLE VII

STATISTICAL PARAMETERS FOR CENTRAL MON-
ZODIORITE TO GRANODIORITE INTRUSIVE

| | Mean | SDEV | THRS (M+2 SDEV) |
|------|-------|-------|-------------------|
| 1-Zn | 36.67 | 15.61 | 67.89 |
| 2-Cu | 8.12 | 3.72 | 15.57 |
| 3-Pb | 15.56 | 6.82 | 29.20 |
| 4-Mo | 2.78 | 5.65 | 14.08 |

(ppm)

TABLE VI

STATISTICAL PARAMETERS FOR
QUARTZ MONZONITE

| | Mean | SDEV | THRS (M+2 SDEV) |
|------|-------|-------|-------------------|
| 1-Zn | 56.67 | 25.40 | 107.47 |
| 2-Cu | 11.88 | 7.27 | 26.42 |
| 3-Pb | 33.67 | 15.17 | 64.01 |
| 4-Mo | 1.33 | 2.29 | 5.91 |

(ppm)

TABLE VIII

STATISTICAL PARAMETERS FOR
SOUTHERN GRANODIORITE

| | Mean | SDEV | THRS (M+2 SDEV) |
|------|-------|-------|-------------------|
| 1-Zn | 59.71 | 33.89 | 127.48 |
| 2-Cu | 6.76 | 3.93 | 14.62 |
| 3-Pb | 16.47 | 5.80 | 28.07 |
| 4-Mo | 2.06 | 6.14 | 14.34 |

(ppm)

TABLE IX

STATISTICAL PARAMETERS FOR
THE QUARTZ LATITE DIKES

| | Mean | SDEV | THRS (M+2 SDEV) |
|------|-------|-------|----------------------|
| 1-Zn | 60.00 | 54.54 | 169.10 |
| 2-Cu | 9.00 | 5.07 | 19.14 |
| 3-Pb | 34.67 | 17.67 | 70.02 |
| 4-Mo | 5.00 | 6.81 | 18.63 |

(ppm)

TABLE X

STATISTICAL PARAMETERS FOR
THE BELDEN FORMATION

| | Mean | SDEV | THRS (M+2 SDEV) |
|------|-------|-------|----------------------|
| 1-Zn | 88.08 | 47.02 | 108.11 |
| 2-Cu | 40.00 | 29.94 | 99.87 |
| 3-Pb | 33.85 | 11.02 | 55.89 |
| 4-Mo | 6.56 | 9.08 | 24.72 |

(ppm)

TABLE XI

STATISTICAL PARAMETERS FOR
THE LEADVILLE LIMESTONE

| | Mean | SDEV | THRS (M+2 SDEV) |
|------|-------|-------|----------------------|
| 1-Zn | 98.91 | 55.94 | 210.79 |
| 2-Cu | 30.00 | 45.53 | 121.05 |
| 3-Pb | 36.56 | 9.90 | 56.36 |
| 4-Mo | 1.92 | 4.35 | 10.62 |

(ppm)

The range values were determined by: (1) plotting actual ppm concentrations versus the frequency of occurrence of the particular ppm concentration, and (2) noting the bell-shaped log-normal distribution curve the limiting range value was chosen where the curve was noted to flatten out and become parallel to the x-axis. The frequency plot for Zn displayed a bimodal distribution reflecting a contrast in concentration between the igneous rocks, with a relatively low concentration, and the surrounding sedimentary rocks with higher concentrations. For the Mo trace metal concentrations the frequency plot was not log normal in nature and thus could not be used to set a range value. Molybdenum displays a range in distribution from 0 to 60 ppm thus the author chose the arithmetic average (30) as the limiting range value. The following range values were finally used in calculating the threshold values: Zn-300 ppm, Pb - 75 ppm, Cu - 200 ppm, and Mo - 30 ppm.

Observations and Interpretations

In order to facilitate interpretations of the trace metal values the mean values and threshold values for the six rock types (Tables V -X1) were plotted for each trace element in Figures 47 and 48. Observations made from these figures are as follows: (1) the similar mean and threshold values for Cu and Mo within the three intrusive rock types reflect a common magmatic source; (2) quartz latite dikes display the highest threshold values of the igneous rocks for Mo, Pb, and Zn thus reflecting a higher concentration due to the migration of mineralizing solutions along these dikes or because they represent the last stages of magmatic differentiation; (3) the

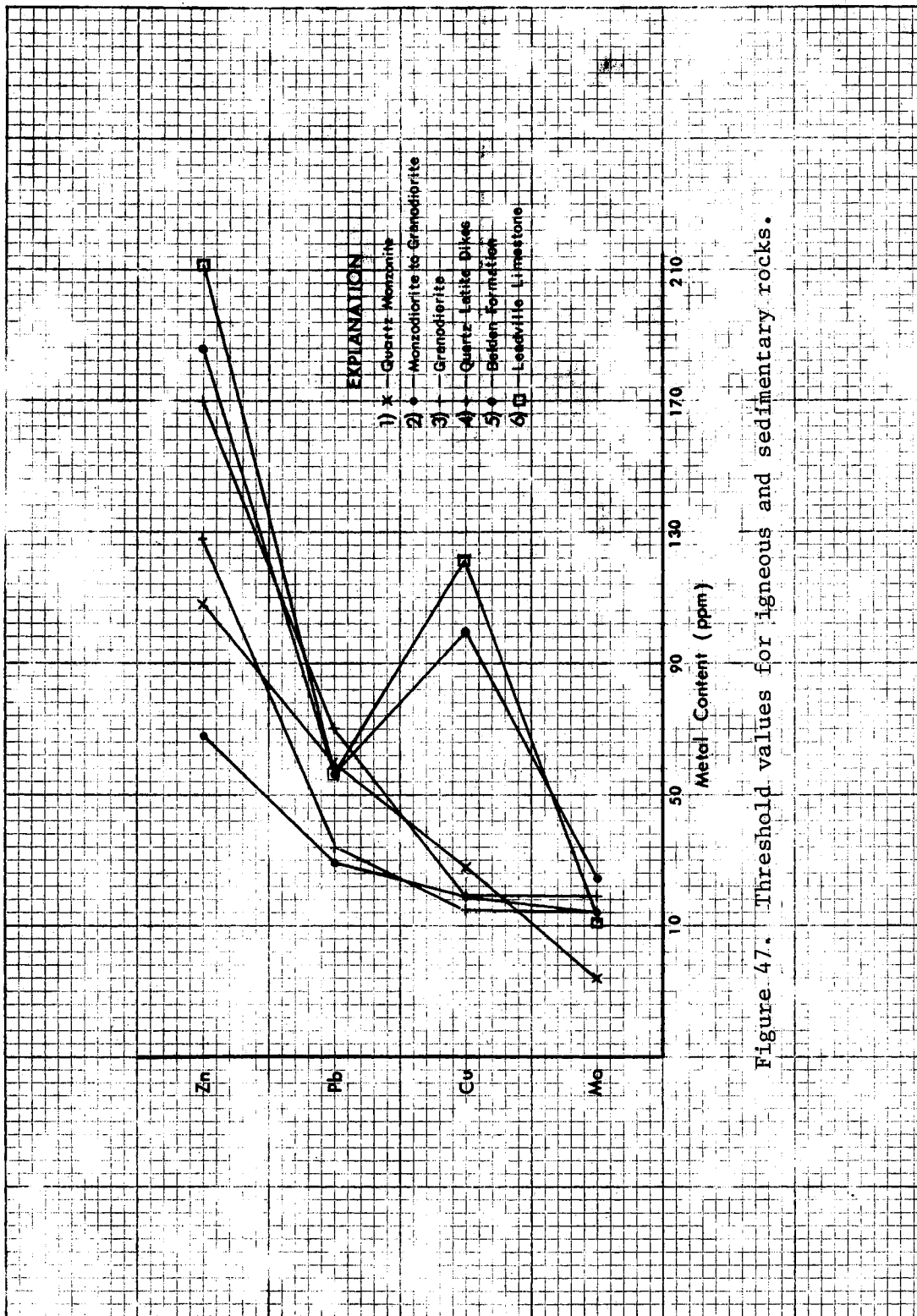


Figure 47. Threshold values for igneous and sedimentary rocks.

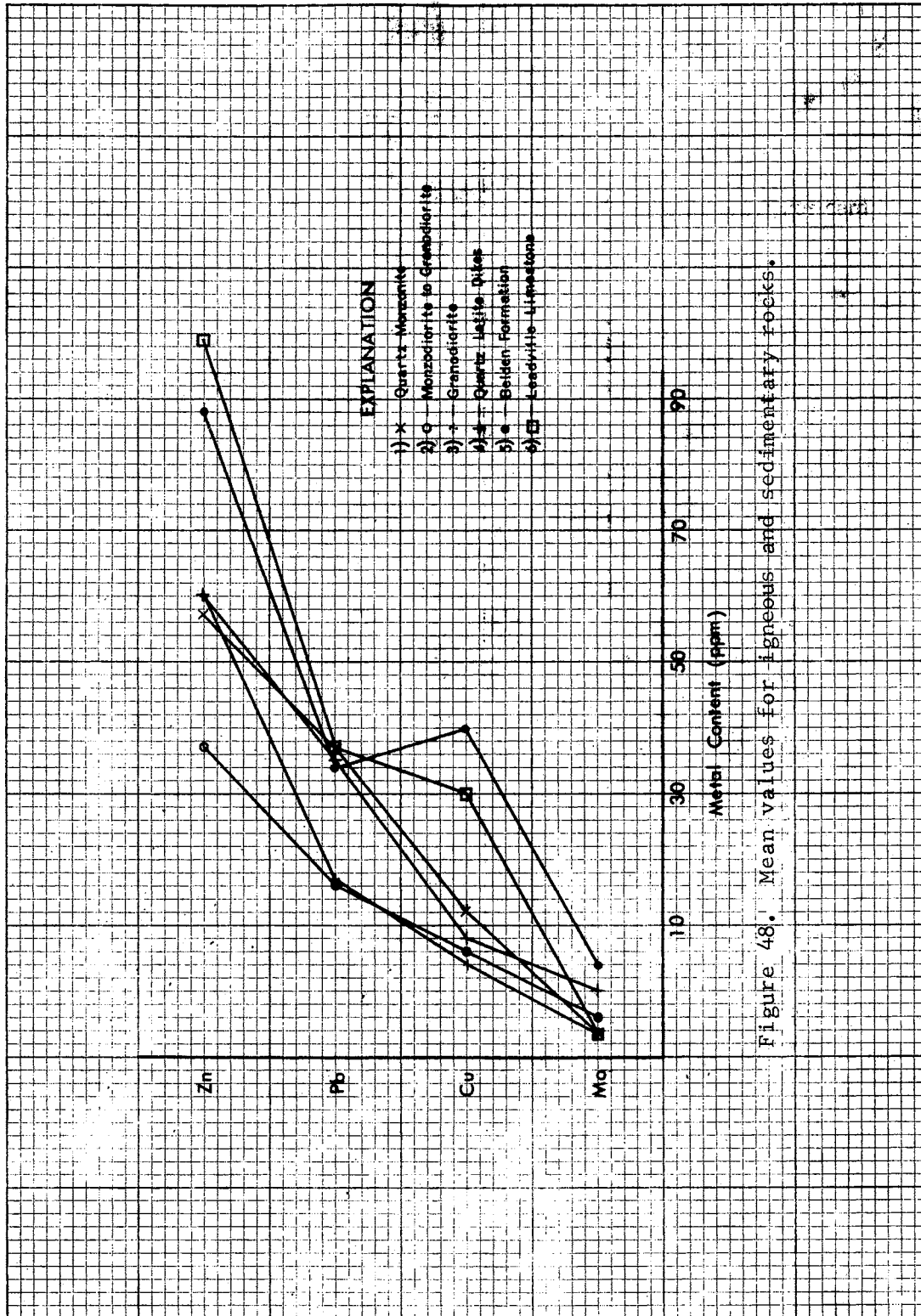


Figure 48. Mean values for igneous and sedimentary rocks.

higher copper content of the Belden Formation and Leadville Limestone reflect enrichment within skarn zones and limestone along quartz latite dikes (see Fig. 44); (4) of the three intrusive rock types quartz monzonite displays the highest mean and threshold for Pb; (5) the high concentration of Zn in surrounding sedimentary rocks is due to the high mobility of Zn, and (6) the wide spread in threshold values for Zn in the three intrusives is possibly due to two periods of Pb-Zn mineralization, one associated with the granodiorite differentiation in the south and the other associated with the differentiatian quartz monzonite intrusive in the north. However, inspection of the mean values for the southern granodiorite intrusive and the northern quartz monzonite reveals a similarity in Zn concentration, thus suggesting a common parent magma.

Knowing the threshold values for the six rock types of Italian Mountain and for all rocks combined the following observations and interpretations were made concerning the trace metal distribution maps (Fig. 43-46). The Cu, Pb, and Zn trace metal distribution maps display two linear trends: (a) a distinct northwest to southeast trend conforming to the trend of the intrusive complex itself, and (b) a less distinct east-northeast to west-southwest trend running parallel to the quartz latite dikes (see Figures 44, 45, 46). Molybdenum displays a negative anomaly over all three intrusive types. Positive anomalies for molybdenum occur: (a) as nodes associated with the quartz latite dikes, (b) in skarn zones (within the Belden Formation) associated with the northern and central intrusives, and (c) along fault zones bisecting the southern granodiorite intrusive. The largest molybdenum anomalies are associated with the

northern quartz monzonite intrusive (see Fig. 43). Copper, like molybdenum, displays a negative anomaly over the southern granodiorite intrusive, the central monzodiorite intrusive, and over most of the northern quartz monzonite intrusive. Positive anomalies for Cu are displayed: (a) over the skarn zone developed within the roof pendant of Belden Formation and the quartz latite dike swarm east-northeast of the quartz monzonite intrusive, (b) over the contact zone between the thumb-shaped wedge of Belden Formation and the northern perimeter of the monzodiorite intrusive, and (c) within the wedge of Leadville Limestone in the extreme northeast map area. The quartz latite dikes seem to have acted as channel-ways for the copper-bearing solutions. A positive copper anomaly, within the wedge of Leadville Limestone, occurs over the New Star Mine workings. This is the only place significant amounts of copper in the form of bornite, chalcopyrite, and malachite were found within the Leadville Limestone. The pronounced northwest-southeast trend of Pb distribution suggest structural control of mineralization along the Castle Creek structure zone. Lead displays a negative anomaly over the southern granodiorite intrusive and the central monzodiorite to granodiorite intrusive, whereas a well defined positive anomaly exists over the northern quartz monzonite intrusive. Another positive Pb anomaly is displayed in the north-central map area along a quartz latite dike and the wedge of Leadville Limestone bounded by a fault to the west. No surface expression of Pb mineralization within the Star Mine area is evident from the Pb distribution map (see Figure 45). Zinc, like Pb, shows a negative anomaly over the southern and central intrusives whereas a strong positive anomaly is found over the northern quartz

monzonite intrusive. Both the Star Mine and Stewart Mines are represented by strong positive anomalies. Other positive anomalies for Zn are found: (a) along the contact zones between the Belden Formation and the central monzodiorite intrusive as well as the northwest perimeter of the southern granodiorite intrusive. The trace Zn distribution about this southern granodiorite intrusive displays low concentrations within its interior with the zinc content increasing to anomalous proportions towards its perimeter and outward into the surrounding Paleozoic sediments (see Figure 46). This distribution of zinc is possibly due to its extreme mobility and susceptibility to leaching, by either hydrothermal solutions or meteoric water.

The above observations reveal that the Cu-Pb-Zn mineralization of Italian Mountain was indeed closely associated with the differentiating quartz monzonite intrusive of North Italian Mountain. The quartz latite dikes, radiating out from the northern quartz monzonite intrusive, and numerous Laramide or Tertiary-derived faults served as conduits along which mineralizing solutions passed until chemically and physically receptive host rocks were encountered.

Correlation Coefficients

Koch, G. S. (1970) defines the correlation coefficient as the measure of adequacy of fit to a straight line, or the degree of linear relationships between observations. Correlation coefficients were calculated for the four trace metals. Table XII displays the results. It must be noted that new threshold values were calculated.

culated, for the six rock types, in which no restrictive ranges were established, in order to enhance the significance of the correlation coefficients. According to Neville and Kennedy (1964), meaningful correlation coefficients, at the 5% significance level with 4 variables considered, for the six rock types are as follows: (1) quartz monzonite with 16 samples, 0.615, (2) monzodiorite to granodiorite with 9 samples, 0.75, (3) granodiorite with 17 samples, 0.601, (4) quartz latite dikes with 15 samples, 0.630, (5) Belden Formation with 13 samples, 0.664, and (6) Leadville Limestone with 13 samples, 0.664.

Thus, for the northern monzonite intrusive there are no real meaningful correlations, however, there is a suggestion of a direct correlation between Pb and Zn and an inverse correlation between Pb and Mo, which further supports the belief that this intrusive was the source of the Pb-Zn mineralization in the surrounding sedimentary rocks. A significant correlation exists between Cu and Zn for both the monzodiorite and the quartz latite dikes which suggests a common parent magma for these two igneous rock types. The granodiorite intrusive displays a meaningful correlation between Mo and Zn as opposed to Cu and Zn for the quartz latite dikes and central monzodiorite, thus, demonstrating that we are indeed dealing with a composite intrusive complex for Italian Mountain. There are no meaningful correlations for the Belden Formation but the correlation coefficient between Mo and Cu is near to being significant, thus reflecting their common association in skarn zones.

TABLE XII

MATRICES OF CORRELATIONS COEFFICIENTS

| | Zn | Cu | Pb | Mo |
|----|----|------|------|-------|
| Zn | | 0.07 | 0.46 | -0.08 |
| Cu | | | 0.00 | -0.16 |
| Pb | | | | -0.49 |
| Mo | | | | |

Quartz Monzonite Intrusive
n=16, at 5% ~ 0.615

| | Zn | Cu | Pb | Mo |
|----|----|------|-------|-------|
| Zn | | 0.80 | 0.37 | 0.22 |
| Cu | | | -0.03 | -0.17 |
| Pb | | | | 0.28 |
| Mo | | | | |

Monzonite to Granodiorite
n=9, at 5% ~ 0.75

| | Zn | Cu | Pb | Mo |
|----|----|------|------|------|
| Zn | | 0.48 | 0.44 | 0.75 |
| Cu | | | 0.15 | 0.23 |
| Pb | | | | 0.30 |
| Mo | | | | |

Granodiorite Intrusive
n=17, at 5% ~ 0.601

| | Zn | Cu | Pb | Mo |
|----|----|------|-------|-------|
| Zn | | 0.75 | -0.05 | -0.08 |
| Cu | | | 0.04 | -0.26 |
| Pb | | | | 0.19 |
| Mo | | | | |

Quartz Latite Dikes
n=15, at 5% ~ 0.630

| | Zn | Cu | Pb | Mo |
|----|----|------|-------|------|
| Zn | | 0.06 | -0.12 | 0.05 |
| Cu | | | -0.12 | 0.48 |
| Pb | | | | 0.18 |
| Mo | | | | |

Belden Formation
n=13, at 5% ~ 0.664

| | Zn | Cu | Pb | Mo |
|----|----|-------|-------|-------|
| Zn | | -0.18 | 0.62 | -0.22 |
| Cu | | | -0.21 | 0.94 |
| Pb | | | | -0.13 |
| Mo | | | | |

Leadville Limestone
n=13, at 5% ~ 0.664

For the Leadville Limestone a meaningful correlation exists between Pb and Zn reflecting their simultaneous deposition and close association. Copper and Mo display a fairly close correlation for the Leadville Limestone thus reflecting their common association and deposition at a time either before or after Pb-Zn mineralization.

CHAPTER IX

SUMMARY AND CONCLUSIONS

The sedimentary regime of Italian Mountain can be divided into two basic units: (1) a lower-most Paleozoic marine shelf-type sedimentary section represented by the Sawatch Quartzite, Cambrian in age; Manitou Dolomite, Ordovician in age; Fremont Limestone, Ordovician in age; Chaffee Formation, Devonian in age; and the Leadville Limestone, Mississippian in age; (2) a thick section of Permo-Pennsylvanian clastic sediments deposited in the Central Colorado basin in the form of coalescing alluvial fans off the Sawatch and Uncompahgre Ranges. These coarse grained sediments consist of the Belden Formation of Pennsylvanian age, the Gothic formation of Permian age, and the Maroon Formation of Permian-Pennsylvanian age.

The Tertiary igneous complex of Italian Mountain consists of three main igneous rock types: (1) quartz monzonite in the North Italian Mountain region, (2) monzonite to granodiorite in the central region, and (3) a granodiorite in the South Italian Mountain map area (see Figure 1). It is therefore a composite intrusive complex.

Assuming a common parent magma for the three intrusive bodies of Italian Mountain, and based upon crosscutting relationships and the process of magmatic differentiation, the author proposes the

following age sequence from oldest to youngest. (1) The central intrusive consisting of monzodiorite to granodiorite, represents the initial magma composition. (2) A granodiorite body was forcefully intruded in the southern sector of Italian Mountain upon further differentiation and accumulation of volatiles. (3) The quartz monzonite of North Italian Mountain represents the final intrusive phase. This intrusive body displays a definite zonation from a ferromagnesian-rich granodiorite around its perimeter to a coarse-grained quartz monzonite, with a well developed quartz monzonite porphyry at the interior, which displays phenocrysts of zoned plagioclase up to 4 cm in length and quartz phenocrysts up to 4 mm in length. (4) Next the quartz latite to quartz latite porphyry dikes, found radiating from the perimeter of the northern intrusive body, were injected into the surrounding Paleozoic sediments along fractures developed by the intrusion of the quartz monzonite and previous intrusive activity. These quartz latite dikes were produced through continuing differentiation of a parent igneous melt common to both the quartz monzonite intrusive and the dike rocks. (5) The last stages of magmatic melt emission before hydrothermal fluid expulsion from the parent magma chamber are represented by the series of aplite to alaskite dikelets, 3-6 inches wide, found impregnating the quartz monzonite at its extreme northwest perimeter, and a granophyre zone, 1-2 feet wide, along the northern contact with the Belden Formation.

A sample of light-gray granodiorite rock from the Whiterock pluton of the Hayden Peak quadrangle, Pitkin County, gave a radiometric K-Ar age date of 33.9 ± 10 million years or early Oligocene

(Obradovich, Mutschler, and Bryant, 1969). Thus, if the Italian Mountain intrusives are considered as part of the Whiterock granodiorite pluton at depth a early Oligocene age can be assigned to them. On the other hand if these intrusives represent later stage stocks emplaced after the large granodiorite pluton (Whiterock) had crystallized, a late Oligocene to early Miocene age is quite conceivable.

Two orogenic episodes are responsible for the structural geology of the Italian Mountain area: (1) Sawatch uplift of Laramide time, and (2) intrusion of the Italian Mountain igneous bodies themselves during the Tertiary. Lateral compression generated by gravity gliding and vertical uplift, both associated with the two orogenic episodes, have produced thrust faults, strike-slip faults, high-angle reverse and normal faults, drape folds, as well as overturned beds and tight fold structures. These structural features are aligned along two lineaments or trends: (1) a northwest lineament which is part of the regional Castle Creek structure zone, and (2) a northeast lineament parallel to the regional shear zones found within the Precambrian rocks of the Sawatch Range.

The Pb-Zn (minor Cu at the new Star Mine) deposits, which are found far removed from the contact between the Paleozoic sediments and the Tertiary igneous rocks, are mesothermal in character and occur as replacement deposits along bedding planes and within collapse breccias in the Leadville Limestone. The typical bedding-replacement deposits consist of pyrite, sphalerite, and silver-rich galena in a gangue of barite. Due to the extreme permeability of the collapse breccia deposits the primary sulfides have been

oxidized to limonite (goethite), smithonite, and carrusite (silver-tied up in its crystal lattice) respectively. These supergene ores are of higher grade than the primary sulfides and thus were the only ones mined.

The Paleozoic sediments in contact with the Italian Mountain intrusives have undergone two stages of igneous metamorphism; (1) thermal metamorphism at the time of the intrusion of the central monzodiorite and northern quartz monzonite igneous bodies, and (2) subsequent contact metasomatism. Initially the intruding magma supplied heat and water vapor to the Paleozoic host rocks bringing about recrystallization and rearrangement of the original constituents, within an essentially closed system, to form minor amounts of calc-silicate hornfels. Heat generated by the cooling magma stimulated the circulation of meteoric and connate water within the sediments themselves thus providing a means of transporting impurities towards the alteration front.

Upon further cooling, great pressure built up within the incased liquid magma and fractures were generated within the solidified crust allowing for magmatic emanations into the Paleozoic sediments. The magma chamber contributed vast amounts of such elements as silica, alumina, iron, fluorine, and sulfur transported in hot solutions or gases which reacted with the host rocks, through the process of metasomatism, to form calc-silicate hornfels. The mechanism of metasomatism involves the alteration of the rock whereby its minerals are replaced with others in less than equal amounts as demonstrated by vuggy products and by euhedral crystals.

This metasomatism took place within an open system where a compensating reaction proceeded between the host rock and the solidifying magma emanating the enriching solutions.

Two distinct metamorphic facies are displayed by the contact zones of Italian Mountain: (1) the pyroxene-hornfels represented by the mineral assemblage: diopside-grossularite to andradite-wollastonite-vesuvianite (similar to that described by Goldschmidt for the Oslo region of Norway); (2) hornblende-hornfels facies represented by the mineral assemblages: (a) diopside-grossularite-vesuvianite-calcite (minor wollastonite), for the fairly pure Leadville Limestone, (b) diopside-anorthite-grossularite where a dolomite to marl composition is approached, (c) anorthite-diopside-actinolite-tremolite or anorthite-hornblende-actinolite-tremolite and possible albite-muscovite-botite (rocks rich in K_2O and SiO_2), for the Belden Formation. A less distinct albite-epidote-hornfels facies, distinguished by the presence of chlorite, epidote, and tremolite was noted at the outside perimeter of the hornblende-hornfels facies. Thermal metamorphic effects are expressed within the Leadville Limestone and the limestone-rich layers of the Belden Formation by the recrystallization of the limestone to an aggregate of coarse calcite rhombohedrons. This recrystallization zone extends outside of the albite-epidote zone away from the intrusive contact.

The following observations provided by trace metal analysis reveal that the Mo-Cu-Pb-Zn mineralization of Italian Mountain was directly associated with the differentiating quartz monzonite intrusive of North Italian Mountain and that the quartz latite dikes

and numerous Laramide and Tertiary-derived faults served as conduits along which mineralizing solutions passed: (1) quartz latite dikes display highest threshold values for Mo, Pb, and Zn; (2) of the three igneous rock types the quartz monzonite displays the highest mean and threshold for Pb; (3) the largest Mo anomalies are associated with the quartz monzonite intrusive; (4) Pb-Zn display negative anomalies over the southern granodiorite intrusive and the central monzodiorite to granodiorite intrusive, whereas well defined positive anomalies exists over the northern quartz monzonite; (5) zinc displays a positive anomaly along the quartz latite dike swarm in the north-central map area; (6) there exists a slight suggestion of a direct correlation between Pb and Zn for the quartz monzonite rock type; (7) a meaningful correlation exists between Pb and Zn for the Leadville Limestone along the contact with the northern quartz monzonite intrusive, reflecting their simultaneous deposition and close association.

REFERENCES CITED

- Badgley, P. C., 1965, *Structural and Tectonic Principles*: New York, N.Y., Harper and Row Publishers, pp. 157-272.
- Bryand, B., 1971, *Disseminated Sulfide Deposits in the Eastern Elk Mountains, Colorado*: U. S. Geol. Survey Prof. Paper 750-D, pages D13-D25.
- Cross, Whitman and Shannon, E. V., 1927, *The Geology, Petrography, and Mineralogy of the Vicinity of Italian Mountain, Gunnison County, Colorado*: *Proceedings of the National Museum*, v. 71, article 18, 42 pp.
- Cunningham, C. G., Jr., 1973. *Multiple Intrusion and Venting of the Italian Mountain Intrusive Complex, Gunnison County, Colorado [abs.]*, *Geological Society of Amer. Rocky Mountain Section 26th Annual Meeting*, Vol. 5, no. 6, p. 474.
- Fife, W. S., Turner, F. S., and Verhoogen, S., 1958, *Metamorphic Reactions and Metamorphic Facies*: *The Geol. Soc. of Amer. Memoir 73*, pp. 199-215.
- Garrett, H. L., 1950, *The Geology of Star Basin and Star Mine*: unpub- M.S. thesis, Colorado School of Mines, no. 670, 45 pp.
- Gaskill, D. L., 1956, *Geology of White Rock Mountain Area. Gunnison County Colorado*: unpublished M.S. thesis, University of New Mexico, 175 pp.
- Hake, B. F., Willis, R., and Addison, C. C., 1942, *Folded Thrust Faults in the Foothills of Alberta*: *Geol. Soc. of American Bull.*, v. 53.
- Hawkes, H. E., and Webb, J. S., 1962, *Geochemistry in Mineral Explor- ation*: New York, N.Y. and Evanston, Ill., Harper and Row, 415pp.
- Hubbert, M. K., and Rubey, W. W., 1959, *Role of Fluid Pressure in Mechanics of Overthrust Faulting*: *Geol. Soc. of Amer. Bull.*, v. 70, pp. 115-166.
- _____, 1960, *A Reply*: *Geol. Soc. of Amer. Bull.*, v. 71, pp. 617-628.
- Johnson, J. H., 1944, *Paleozoic Stratigraphy of the Sawatch Range*: *Geol. Soc. Amer. Bull.*, v. 55, pp. 303-378.


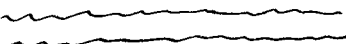
- Kerr, P.F., 1959, Optical Mineralogy, Third edition: New York, N.Y., McGraw-Hill Book Company, pp. 260-262.
- Koch, G. S., St., 1970, Statistical Analysis of Geological Data. Vol. One: New York, N. Y., John Wiley and Sons, Inc., 375 p.
- _____, 1971, Statistical Analysis of Geological Data, Volume Two: New York, N. Y., John Wiley and Sons, Inc., pp. 350-355.
- Langenheim, R. L., 1952, Pennsylvanian and Permian Stratigraphy in the Crested Butte Quadrangle, Gunnison County, Colorado: Amer. Assoc. Petrol. Geologists Bull., v. 36, pp. 543-574.
- Martin, A. J., 1950, U. S. Bureau of Mines: Minerals Yearbook, U.S. Department of the Interior, Gov. Printing Office, Washington, p. 1454.
- Moorhouse, W. W., 1959, The Study of Rocks in Thin Section: New York, N. Y., Harper and Row, Publishers, pp. 152-156.
- Murphy, J. H., 1951, Geology of the Upper Cement Creek Area, Gunnison County, Colorado: unpublished M.S. thesis, University of Kentucky, 57 pp.
- Neville, A. M., and Kennedy, S. B., 1964, Basic Statistical Methods for Engineers and Scientists: Scranton, Penn., Intern. Text-book Company, 325 pp.
- Obradovich, S. D., Mutschler, F. E., and Bryant, Bruce, 1969, Potassium-argon Ages Bearing on the Igneous and Tectonic History of the Elk Mountains and Vicinity, Colorado --A Preliminary Report: Geol. Soc. Amer. Bull., v. 80 no. 9, p. 1749-1756.
- _____, 1964, Stratigraphy and Structural Geology of the Elk Mountains, Colorado: unpublished Ph. D. thesis, Department of Geology, University of Colorado, 115 pp.
- Slebir, E. J., 1957, The Geology of the North Cement Creek Area, Gunnison County, Colorado, School of Mines, No. 846, 93 pp.
- Streckeisen, A. L., 1967, Classification and Nomenclature of Igneous Rocks: Neues Jahr 6, Mineral., Abh., v. 107, no. 3, 00. 215-240.
- Tweto, O., and Sims, P.K., 1963, Precambrian Ancestry of the Colorado Mineral Belt Geol. Soc. of Amer. Bull., v. 74, pp. 991-1014.
- Turner, F. J., 1968, Metamorphic Petrology: New York, N. Y., McGraw-Hill Book Co., Inc., pp. 172-259.

- Turner, F. S., and Verhoogen, J., 1960, *Igneous and Metamorphic Petrology*, 2nd edition: New York, N. Y., McGraw-Hill Book Co., Inc., pp. 450-508.
- Troger, W. E., 1938, Eruptivgesteinsnamen.-Fortschr. Miner; v. 23, pp. 41-53.
- Wahlstrom, E. E., and Hornback, V. Q., 1962, Geology of the Harold D. Roberts Tunnel, Colorado: West Portal to Station 468-49, Bull. Geol. Soc. Amer., v. 73, pp. 1477-1498.
- Winkler, H. F., 1965, *Petrogenesis of Metamorphic Rocks*: New York, N. Y., Springer-Verlag Publishing Co., pp. 1-60.
- Vanderwilt, S. W., 1935, Stratigraphy of the Hermosa Formation in the Elk Mountains, Gunnison County, Colorado: Amer. Assoc. Petroleum Geologists, v. 19, pp. 1668-1667.
- Eskola, P., 1915, The Mineral Facies of Rocks, *Norst geol. tidsskr.*, v. 6, pp. 143-194.

APPENDIX A

STRATIGRAPHIC SECTION OF PALEOZOIC SEDIMENTS

AMERICAN FLAG MOUNTAIN

| Unit | Description | Thickness |
|-------------------------------------|---|-----------|
| LEADVILLE FORMATION - Mississippian | | 327' |
| 42 | Black to dark blue gray massive limestone weathers to a light blue gray, highly permeable with many solution cavities and collapse breccias, calcite veins (up to 1½' wide) run parallel and transverse to bedding, solution cavities contain siderite and galena, upper portion of Leadville contains dolomite stringers coated with hematite, and bedding changes from massive to medium and even small scale - Leadville is an excellent cliff former. | 210' |
| 41 | Gray to light gray limestone, massive bed over 3' veined with calcite along fracture zones, horn corals found in. | 65' |
| 40 | Grayish brown limestone beds, very finely crystalline, solution cavities and calcite veinlets present. | 8' |
| 39 | Light gray limestone, slabs like shale, a valley former subject to erosion, displays criss-cross pattern of calcite veinlets. | 10' |
| 38 | Single massive bed of dark gray to black very finely xlline, limestone with calcite veinlets. | 8' |
| |  erosion surface | |
| 37 | Brown to grayish brown limestone with a considerable variation in thickness of bedding, 4" to 3', some interbedded black limestone, very fine grained. | 18' |
| 36 | Alternating and interfingering beds of dark gray and grayish-brown dolomitic limestone, separates the Chaffee Fm. below from Leadville above. | 6' |
| |  distinct erosion surface | |
| CHAFFEE FORMATION | | 175.5" |
| DYRER DOLOMITE MEMBER | | |
| 35 | Gray to dark gray dolomitic limestone finely crystalline, lower portion contains small calcite vugs (2"), middle section displays prominent calcite veins, in the upper section calcite vugs increase in size (4") bedding of medium scale for entire unit (2-6'). | 85' |

| Unit | Description | Thickness |
|---------------------------------|--|-----------|
| PARTING MEMBER | | |
| 34 | Reddish-gray sandstone, medium to coarsely crystalline, coarse towards the top, very angular quartz grains, silica cement evident in that rock fractures across quartz grains. | 4" |
| 33 | Reddish-brown sandy dolomite, thin bedded, 5-6"; coarse grained, angular quartz fragments. | 10' |
| 32 | Yellowish-green mudstone, with beds varying from 1-2" thick, contains calcite vugs and green shale partings, up to 2" thick. | 20' |
| 31 | Maroon and yellowish-brown shale, easily eroded into chips, very fissile thin-bedded, forms gaps in slope. | 5' |
| 30 | Series of various colored mudstones with interbeds of sandstone; color varies from yellow-brown at the base to maroon in the middle and white at top; lower and middle sections are thin-bedded; upper pure white mudstone is massive and displays concoidal fracturing and a criss-cross network of calcite veinlets. | 33' |
| 29 | Alternating sequence of greenish-gray fissile shale and fine to medium-grained sandstone with dolomite inclusions, bedding varies from less than 2" at bottom to 8" of sandstone at the top, bedding surfaces display flexure. | 10' |
| 28 | Gray-brown dolomite beds, finely xlline, dendrites found along fracture and parting surfaces. | 2' |
| 27 | Light brown to tan shale and sandy shale more blocky than fissile, dendrites along bedding planes. | 4' |
| 26 | Alternating and intertonguing beds of light gray finely crystalline dolomite and medium to coarse-grained calcareous sandstone, beds vary from 2-6" quartz grains well rounded and sorted. | 2.5' |
| FREEMONT LIMESTONE - ORDOVICIAN | | 80.5' |
| 25 | Dolomitic limestone ranging from light gray in its lower section to dark gray towards the top, scale of bedding increases from medium to large scale at the top, whole unit is finely crystalline, displays calcite veinlets and coatings along fractures, crinoid fragments and corals more abundant towards top. | 65' |

| Unit | Description | Thickness |
|------|--|-----------|
| 24 | Dark gray dolomitic limestone beds 2-5' thick finely xline, ceinoid fragments along bedding planes. | 15' |
| 23 | Reddish-brown shale, very fissile grading into light gray sandy dolomite at base, these two units are marked beds for the bottom of the Fremont limestone. | ½' |
| | MANITOU DOLOMITE ORDOVICIAN | 260' |
| 22 | Dark gray dolomite, very finely xline, large scale bedding 5-6 ft. top surface is irregular with expression of possible flute casts. | 25' |
| 21 | Gray to black dolomite medium-bedded with very few stringers and nodules of chert. | 12' |
| 20 | Dolomite, black in color, medium scale bedding 2-3'. abundant stringers of black chert found parallel to bedding planes, finely crystalline. | 25' |
| 19 | Black massive dolomite, weathers brown, with a few small nodules of gray chert. | 20' |
| 18 | Dark gray, fine to medium xlinity, dolomite with no chert, beds 1-3' thick, calcite along fractures. | 12' |
| | Light gray dolomite, weathers buff in color, beds vary from 1.5-3 feet, finely xline, stringers and nodules of chert found parallel to bedding, change in color of chert from cream white at bottom to black at top, stands out on weathered surfaces. | 35' |
| 16 | Dark gray dolomite, light tan on weathered surface, thick beds (6"), finely xline, with absence of chert. | 6' |
| 15 | Light gray dolomite with beds 1-3' thick, medium crystallinity, milky gray to dark gray chert nodules and stringers along bedding planes, some 2" in diameter. | 60' |
| 14 | Gray dolomite weathers yellow-gray, medium crystallinity, few or no chert stringers along bedding planes, and beds vary from 1-3, 5' thick. | 50' |
| 13 | Gray dolomite, beds 6"-2' thick, bedding planes uneven, fine-medium crystallinity, streaked throughout with tiny veinlets of chert. | 15' |

| Unit | Description | Thickness |
|------|--|-----------|
| | SAWATCH QUARTZITE CAMBRIAN | 274.5' |
| | PEERLESS SHALE MEMBER | |
| 12 | Brown calcareous sandstone beds with graded bedding. | |
| | UPPER QUARTZITE MEMBER | 20' |
| 11 | Massive beds of light brown fine grained quartzite, bedding attitude N 55 E, 26 NW. | |
| | GLAUCONITIC SANDSTONE MEMBER | 102' |
| 10 | Alternating beds of sandstone (medium grained) and fine grained quartzite, both units brown to greenish in color, glauconite stringers along bedding planes. | 33' |
| 9 | Grayish-brown very fine grained sandstone with angular fragments, dense black sand along bedding planes is more resistant and thus stands out in relief. | 30' |
| 8 | Sandstone, fine to medium grained, light green in color due to glauconite content, slabby beds, calcareous cement. | 4' |
| | Greenish gray fine grained quartzite | 8' |
| 7 | Greenish-brown sandstone fine-grained, display fine to medium grained, highly fractured, fractures stained with black hematite, also hematite stringers | |
| 6 | along bedding planes which stand out in relief on weathered surface. | 24' |
| | LOWER MEMBER OF SAWATCH QUARTZITE | 149.42' |
| 5 | Section of thin bedded (1-2') fine grained white quartzite. | 60' |
| 4 | Conglomeratic quartzite with quartz pebbles $\frac{1}{2}$ " in diameter. | 1' |

| Unit | Description | Thickness |
|------|--|-----------|
| 3 | Light brown to light gray very fine grained quartzite in beds from .5-2' thick, shale partings found along bedding planes. | 32' |
| 2 | White quartzite beds 2-3.5' thick, fine to coarse grained, display cross-bedding and graded bedding, beds 6-8" thick, weathers brown in color, interbedded with quartzite are brown medium-grained sandstone beds 1-3" thick, and brown to green shale drapes. | 36' |
| 1 | Lower quartzite member, white with iron staining, conglomeratic quartzite displaying small scale cross-bedding 6-10" between top set and bottom set, graded-bedding evident, pebble-sized quartz grains rounded with silica or feldspathic cement. | 20.42' |
| | Uniformity <i>~</i> conglomerate rich in feldspar. | |
| | Precambrian Basement Rock-Silver Plume or Pikes Peak Granite. | |

APPENDIX B

TRACE METAL ANALYSIS

NEAHOMA STATE UNIVERSITY
TULSA, OKLAHOMA
74106-3098

| Number | Sample Number | ppm Zn | ppm Cu | ppm Pb | ppm Mo |
|--------|---------------|--------|--------|--------|--------|
| 1 | Bgs-2 | 20 | 30 | 30 | 0 |
| 2 | Brpw-1 | 130 | 10 | 45 | 0 |
| 3 | Bci-1,2 | 60 | 5 | 40 | 0 |
| 4 | Aes-2 | 155 | 70 | 20 | 0 |
| 5 | BTsc-1,2 | 35 | 35 | 35 | 0 |
| 6 | BTsc-3 | 45 | 20 | 270 | 0 |
| 7 | Bma-2 | 150 | 5 | 25 | 0 |
| 8 | Bql-7 | 30 | 5 | 5 | 0 |
| 9 | Bto-1 | 2500 | 265 | 100 | 0 |
| 10 | Bto-2 | 1110 | 45 | 205 | 10 |
| 11 | BTo-4 | 130 | 80 | 40 | 20 |
| 12 | Bro-6 | 2700 | 8300 | 55 | 0 |
| 13 | BNW-1 | 285 | 20 | 30 | 0 |
| * 14 | BSe-1,2 | 90 | 50 | 15 | 0 |
| 15 | Brp-2 | 50 | 5 | 30 | 0 |
| 16 | Es-1 | 10 | 5 | 25 | 0 |
| * 17 | Gs-2 | 30 | 5 | 45 | 0 |
| 18 | Gs-3 | 30 | 5 | 45 | 0 |
| 19 | Gs-5 | 15 | 5 | 40 | 10 |
| 20 | LNe-5 | 15 | 10 | 45 | 0 |
| 21 | LNe-2 | 1592 | 10 | 547 | 0 |
| 22 | LNe-3 | 200 | 5 | 90 | 0 |
| 23 | Le-2 | 30 | 25 | 25 | 0 |
| * 24 | Mbsci-1,2 | 35 | 10 | 20 | 0 |
| 25 | Mc-1 | 45 | 15 | 25 | 15 |
| 26 | MLST-2 | 1801 | 5 | 375 | 0 |
| * 27 | Mqb-4 | 25 | 5 | 15 | 0 |
| 28 | MSc-1 | 40 | 5 | 10 | 10 |
| * 29 | Msc-2 | 40 | 5 | 25 | 0 |
| 30 | Msc-4 | 25 | 10 | 5 | 0 |
| * 31 | Msc-5,6 | 35 | 5 | 15 | 0 |
| 32 | Mwc-2 | 15 | 10 | 10 | 0 |
| 33 | Mcw-2 | 70 | 500 | 15 | 0 |
| 34 | NIYL-9 | 100 | 599 | 35 | 15 |
| 35 | NITL-14 | 80 | 25 | 20 | 0 |
| 36 | NITL-15 | 123 | 15 | 44 | 0 |
| 37 | NITL-12 | 125 | 64 | 40 | 5 |
| 38 | NITL-13 | 170 | 15 | 105 | 5 |
| 39 | NITL-21 | 65 | 5 | 35 | 0 |
| 40 | PEe-IR | 20 | 35 | 20 | 0 |
| * 41 | PENW-1 | 50 | 10 | 25 | 10 |
| 42 | PEnw-3 | 50 | 5 | 10 | 0 |
| 43 | PEs-1 | 25 | 5 | 15 | 0 |
| 44 | QDc-1 | 35 | 10 | 30 | 10 |
| 45 | QDc-2 | 40 | 5 | 40 | 0 |
| 46 | Qdc-5,6 | 105 | 20 | 75 | 0 |
| 47 | Qdc-5,6 | 35 | 10 | 20 | 0 |
| * 48 | Qdc-5 | 70 | 10 | 20 | 5 |
| 49 | Qdc-7 | 20 | 10 | 15 | 5 |

| Code Number | Sample Number | ppm Zn | ppm Cu | ppm Pb | ppm Mo |
|-------------|---------------|--------|--------|--------|--------|
| 50 | Qc-A | 235 | 20 | 15 | 0 |
| 51 | Qc-B | 85 | 5 | 55 | 25 |
| 52 | Qms-1 | 35 | 5 | 15 | 0 |
| 53 | Qms-5 | 70 | 5 | 15 | 0 |
| 54 | Qms-6 | 70 | 5 | 15 | 5 |
| 55 | Qms-7 | 70 | 5 | 15 | 0 |
| * 56 | Qms-8 | 75 | 20 | 15 | 0 |
| 57 | Qms-9 | 35 | 5 | 10 | 0 |
| 58 | Qms-10 | 100 | 10 | 10 | 5 |
| 59 | Qms-11 | 25 | 5 | 10 | 0 |
| 60 | Qms-12 | 20 | 5 | 10 | 0 |
| 61 | Qms-13 | 40 | 5 | 15 | 0 |
| 62 | Qms-14 | 30 | 5 | 15 | 0 |
| * 63 | Qms-15a,b | 25 | 5 | 25 | 0 |
| * 64 | Qm-1 | 75 | 20 | 25 | 5 |
| 65 | Qm-2 | 340 | 25 | 95 | 0 |
| 66 | Qm-3 | 70 | 5 | 40 | 5 |
| 67 | Qm-4 | 45 | 5 | 35 | 0 |
| 68 | Qms-2,3 | 5 | 5 | 20 | 5 |
| 69 | QLN-I | 70 | 10 | 45 | 5 |
| * 70 | Qmbd-1 | 65 | 5 | 25 | 5 |
| 71 | Qmd-1 | 30 | 5 | 40 | 5 |
| 72 | Qmc-1 | 25 | 15 | 15 | 0 |
| * 73 | Qmi-1 | 70 | 5 | 65 | 0 |
| 74 | Qmwc-1 | 20 | 10 | 30 | 0 |
| 75 | Qmwc-2 | 20 | 10 | 10 | 5 |
| * 76 | Qmw-1,2 | 55 | 10 | 35 | 0 |
| 77 | Qmci-1,a | 40 | 20 | 20 | 60 |
| * 78 | Qmtn-1 | 40 | 15 | 20 | 0 |
| * 79 | Qmsi-4 | 150 | 10 | 25 | 25 |
| * 80 | Qmsc-2 | 45 | 5 | 15 | 0 |
| 81 | Qmro-1 | 95 | 25 | 65 | 0 |
| 82 | Qmrw-2 | 105 | 10 | 25 | 0 |
| * 83 | Qmgs-1 | 80 | 5 | 20 | 0 |
| 84 | Smw-2 | 70 | 165 | 30 | 0 |
| 85 | Sm-1,2 | 115 | 10 | 50 | 0 |
| 86 | Sm-4 | 60 | 10 | 40 | 0 |
| 87 | Pys-1 | 35 | 35 | 25 | 15 |
| 88 | Pgc-1 | 90 | 10 | 30 | 0 |

*Indicates thin sections were made from bulk samples (see Figure 42 for location).

| Code Number | Sample Number | Polished Sections | Thin Sections Not Included in Above Table) |
|-------------|---------------|-------------------|--|
| 89 | Lne-10 | Yes | _____ |
| 90 | Sm-6 | Yes | _____ |
| 91 | Smw-3 | Yes | _____ |
| 92 | Smw-7 | Yes | _____ |
| 93 | Smw-8 | Yes | _____ |
| 94 | Qmpe-1 | _____ | Yes |
| 95 | AES-1 | _____ | Yes |
| 96 | MQmd-0 | _____ | Yes |

APPENDIX C

SAMPLE PREPARATION FOR ATOMIC ABSORPTION

Procedure

1. Rock chip samples were first crushed to a $\frac{1}{2}$ inch diameter population in a jaw crusher.
2. This half inch diameter population was then pulverized to a fine powder in a ball mill.
3. Powdered samples were dried in an oven for three hours at a temperature of 90°C .
4. One gram (weighed to closest 0.1 mg on Metler balance) samples of the dried powder were placed in Teflon beakers and dissolved in 25 ml HF and 10 ml HNO_3 . Digestion was allowed to proceed for 12 hours.
5. One to two ml of HClO_4 were added to the above Teflon beakers which were then heated on a hot plate until fuming stopped and the residue assumed a burnt crust appearance. It is critical at the beginning of this stage to keep the temperature below boiling (93.99°C) until the reagents have been evaporated, otherwise one takes the risk of contamination between beakers.
6. Two drops of distilled water were added to the residue in the Teflon beaker to form a slurry.
7. Slurry was taken into solution with 5 ml concentrated HCl and heated to boiling while stirring. If residue remains after heating add distilled water (do not exceed 10 ml.) and heat again, then bring solution up to a 10 ml. volume.
8. All beaker contents were transferred to a 50 ml volumetric flask. Beaker walls were washed with distilled water and the contents were added to the volumetric flask.
9. The fluid level in the flask was then increased to 50 ml. in

increments, fluid was swirled between increments to dissipate heat.

10. The 50 ml. solutions were then transferred from the flasks to labelled wide-mouthed polyethylene bottles (4 oz.) capped, and stored in a cool place until analyzed by atomic absorption-spectrophotometry.

APPENDIX D

PREPARATION OF STANDARD SOLUTIONS

I. Equipment

- 1) Six 100 ml. volumetric flasks.
- 2) 10 and 15 ml. size polyethylene graduated cylinders.
- 3) glass pipets, 10, 5, 2 and 1 ml. sizes.
- 4) four 50 ml. pyrex beakers.
- 5) ten 4 oz. wide mouth polyethylene bottles.

II. Reagents

- 1) Distilled water.
- 2) HNO_3 (conc.) HCl (conc.).
- 3) 1000 ppm stock solutions
 - a) 1000 ppm Pb, in salt of $\text{Pb}(\text{NO}_3)_2$ and matrix dilute nitric acid.
 - b) 1000 ppm Mo, in salt of $(\text{NH}_4)_6\text{Mo}_7\text{O}_{24}$, matrix distilled water.
 - c) 1000 ppm Zn, in salt of $\text{Zn}(\text{NO}_3)_2$ matrix of dilute HNO_3 .
 - d) 1000 ppm Cu, in salt of CuSO_4 , aqueous matrix.

III. Procedure

- 1) Add approximately 20 ml. of each 1000 ppm stock solutions (Cu, Pb, Zn, Mo) to separate 50 ml pyrex beakers.
- 2) Rinse pipettes in stock solution before preparing standard solution.
- 3) Pipette, 10 ml. of each 1000 ug/ml stock solution (Cu, Pb, Zn, Mo) into a 100 ml. volumetric flask.
- 4) Add 5 ml. of HNO_3 (conc.) to the 100 ml. volumetric flask and bring solution to 100 ml. with distilled H_2O . This gives a standard solution of 100 ug/ml (Cu, Pb, Zn, and Mo).
- 5) This 100 ug/ml standard solution was then further diluted according to the following schedule:

| Pipette (x) ml of 100 ug/ml standard | Add 5 ml HCl | Make to 100 ml with distilled H ₂ O | Gives (x) ug/ml solution |
|---|--------------|---|-----------------------------|
| 1 ml (100 ppm sol.) | " | " | 1 ppm |
| 3 ml (100 ppm sol.) | " | " | 3 ppm. |
| 5 ml (100 ppm sol.) | " | " | 5 ppm. |
| 7 ml (100 ppm. sol.) | " | " | 7 ppm. |
| 10 ml (100 ppm sol.) | " | " | 10 ppm. |
| 15 ml. (100 ppm sol.) | " | " | 15 ppm. |

*Note: 1 ug/ml = 1 ppm

(6) Dilution below 1 ppm was accomplished by pipetting 10 ml of 100 ug/ml standard solution into a separate 100 ml volumetric flask and making the volume to 100 ml by adding distilled H₂O. This gives a standard solution of 10 ug/ml concentration. Further dilution was accomplished by:

| Pipette (x) of 10 ug/ml standard | Add 5 ml HCl | Make to 100 ml with distilled H ₂ O | Gives (x) ug/ml solution |
|-------------------------------------|--------------|---|-----------------------------|
| 1 ml (10 ppm sol.) | " | " | 0.1 ppm |
| 3 ml (10 ppm sol.) | " | " | 0.3 ppm |
| 5 ml (10 ppm sol.) | " | " | 0.5 ppm |
| 7 ml (10 ppm sol.) | " | " | 0.7 ppm |

The particular range in standard solutions needed was determined by noting the optimum working range and detection limit of the Perkin-Elmer 403 atomic absorption unit for the metals analyzed for (Cu, Mo, Pb, Zn). The optimum working range and detection limits for trace metals analyzed for are as follows:

| Metal | Optimum Working Range | Detection Limit |
|-------|-----------------------|-----------------|
| Cu | 2 to 20 ug/m1 | 0.005 ug/m1 |
| Mo | 10 to 100 ug/m1 | 0.12 ug/m1 |
| Pb | 4 to 40 ug/m1 | 0.07 ug/m1 |
| Zn | 0.2 to 3 ug/m1 | 0.002 ug/m1 |

VITA

Emery Bernard Roy

Candidate for the Degree of

Master of Science

Thesis: GEOLOGY OF THE ITALIAN MOUNTAIN INTRUSIVES AND ASSOCIATED
Pb-Ag REPLACEMENT DEPOSITS CRESTED BUTTE AND TAYLOR PARK
QUADRANGLES, GUNNISON COUNTY, COLORADO

Major Field: Geology

Biographical:

Personal Data: Born in San Diego, California, February 9, 1948,
the son of Mr. and Mrs. Mrs. Clinton J. Roy.

Education: Graduated from Duluth Cathedral High School, Duluth,
Minnesota, in June of 1966; received Bachelor of Arts
degree from the University of Minnesota, Duluth, in Decem-
ber, 1970, with a major in Geology; enrolled in Masters of
Science program in Geology at Oklahoma State University,
Stillwater, Oklahoma, in August, 1971; completed require-
ments for Masters of Science degree at Oklahoma State
University in July, 1973.

Professional Experience: Undergraduate teaching assistant,
Department of Geology, Oklahoma State University,
1972-1973.

FIGURE 1

GEOLOGIC MAP OF THE ITALIAN MOUNTAIN AREA

Emery B. Roy, 1973

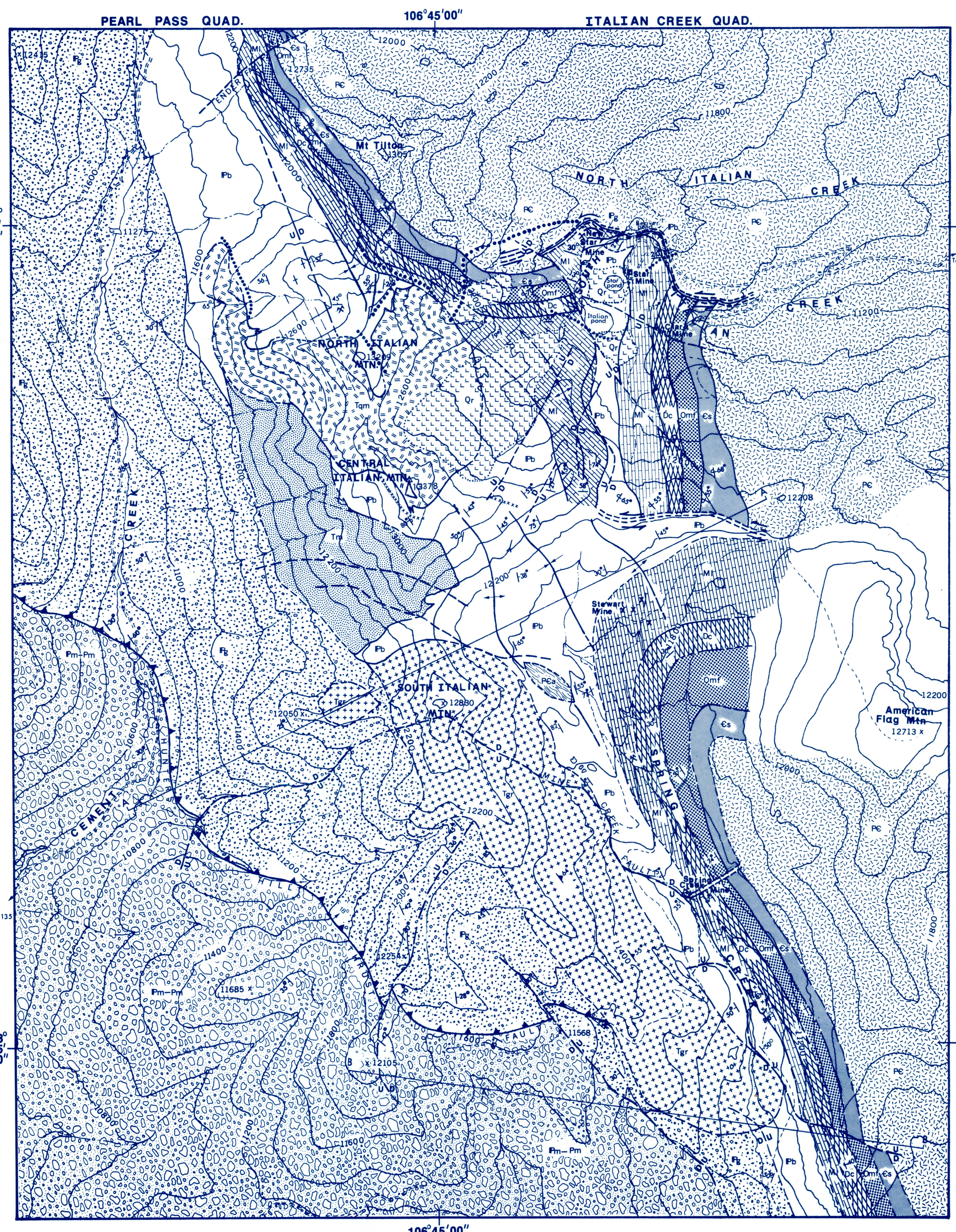
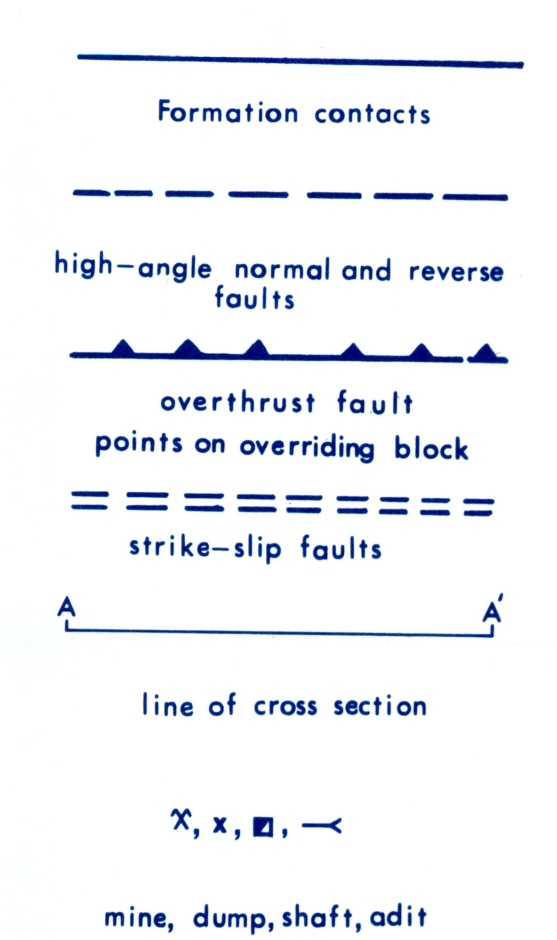
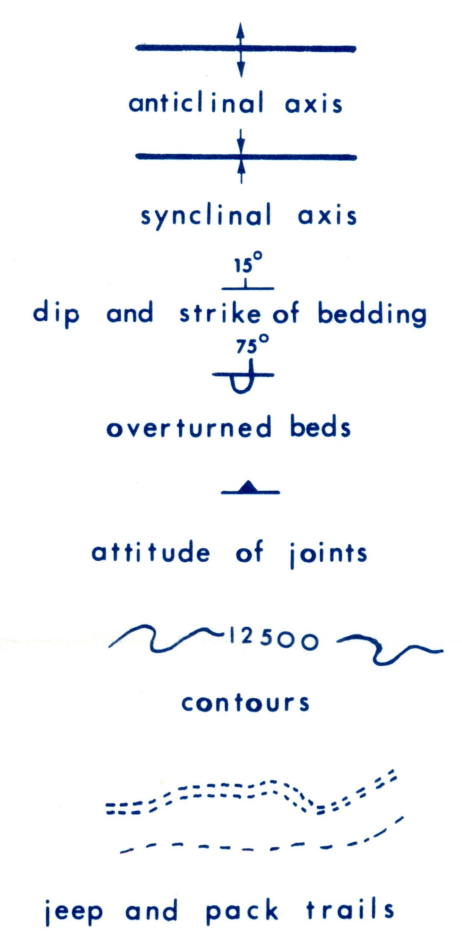
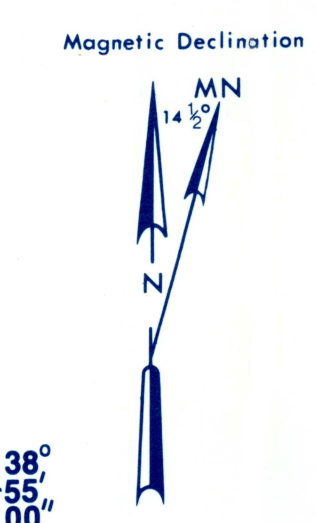
EXPLANATION

SEDIMENTARY ROCKS

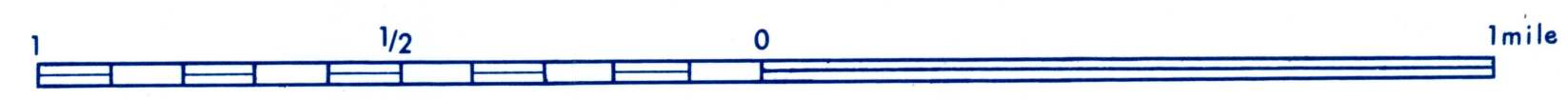
- Quaternary
 - Rock glaciers
- Permo-Pennsylvanian
 - Maroon Formation
- Pennsylvanian
 - Gothic Formation
 - Belden Formation
- Mississippian
 - Leadville Limestone
- Devonian
 - Chaffee Formation
- Ordovician
 - Manitou Dolomite and Fremont Limestone
- Cambrian
 - Sawatch Quartzite

IGNEOUS ROCKS

- Tertiary
 - Quartz Latite to Quartz Latite porphyry Dikes
 - Quartz Monzonite offshoots
- Early Oligocene to Early Miocene
 - Quartz Monzonite with a Melanogranodiorite shell
- Granodiorite
- Monzodiorite
- Precambrian
 - Amphibolite
 - Granite (metamorphic rocks in north-central map area)



Scale 1:15840



CONTOUR INTERVAL 200 FEET

FIGURE 42. Sample Location Map

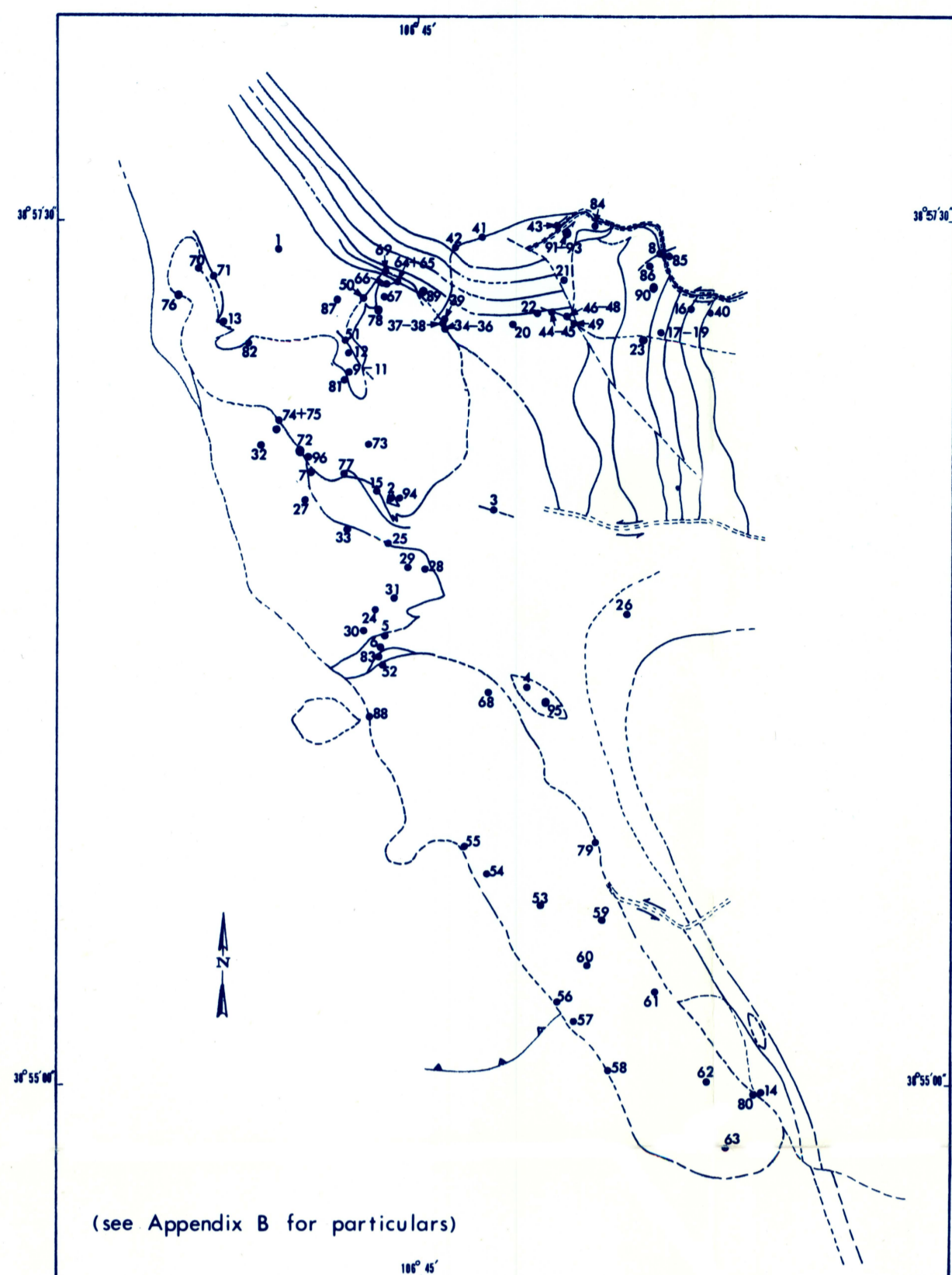
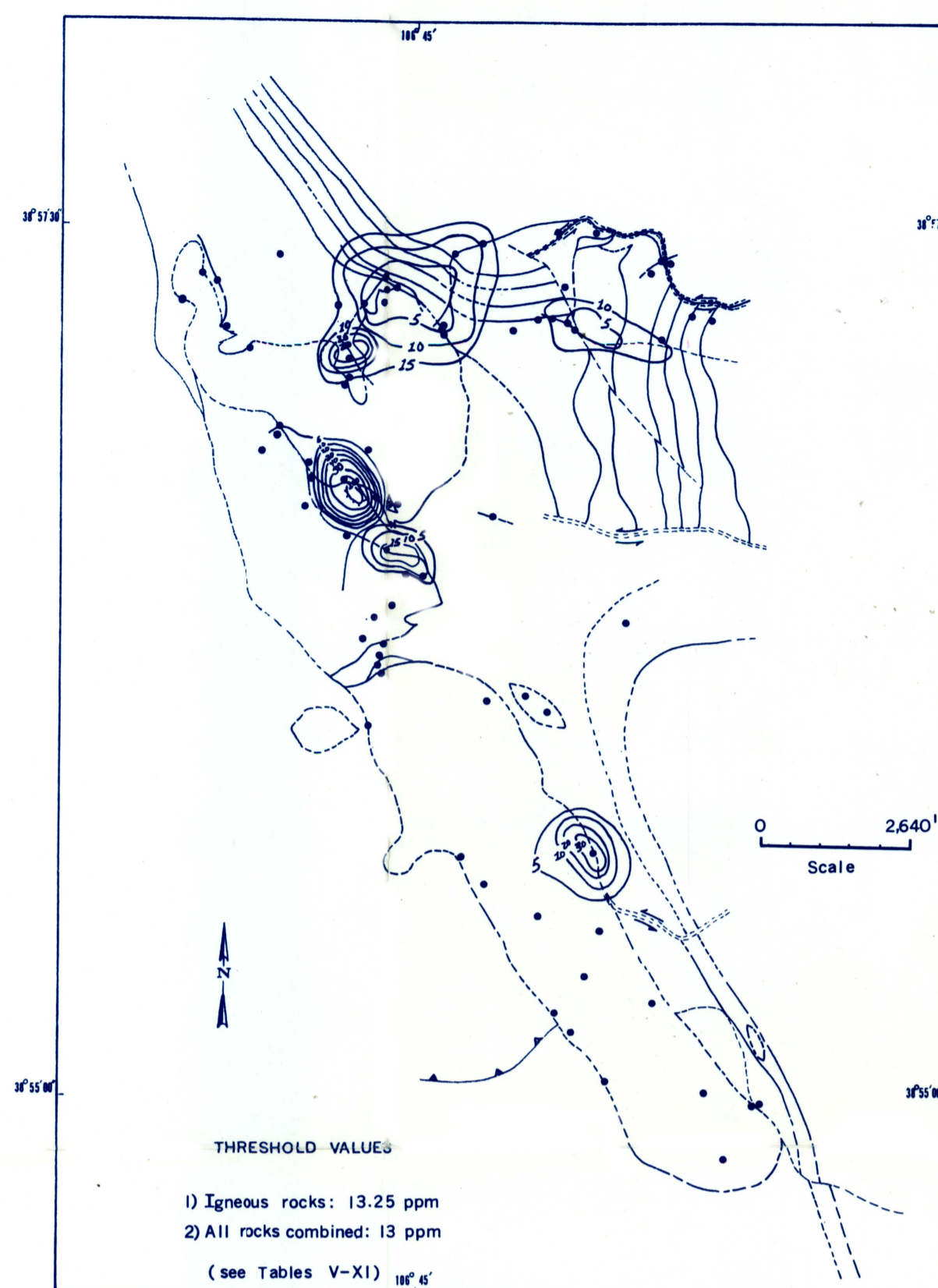


FIGURE 43. Trace metal Distribution of Mo (ppm)



FIGURES 42-46

TRACE METAL DISTRIBUTION

MAPS FOR:

LEAD, ZINC,

MOLYBDENUM,

AND COPPER

Emery B. Roy, 1973

FIGURE 44. Trace metal Distribution of Cu (ppm)

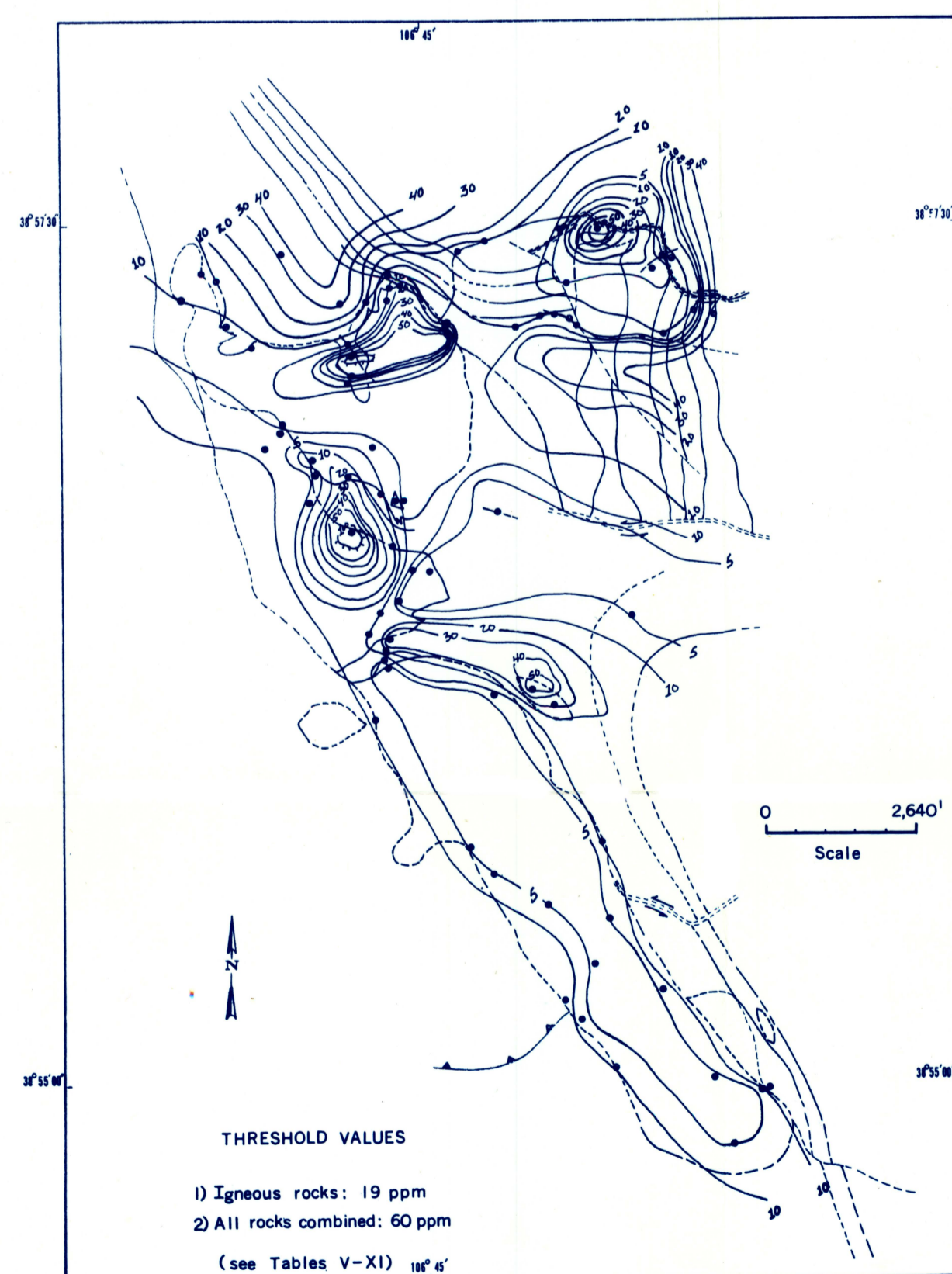


FIGURE 45. Trace metal Distribution of Pb (ppm)

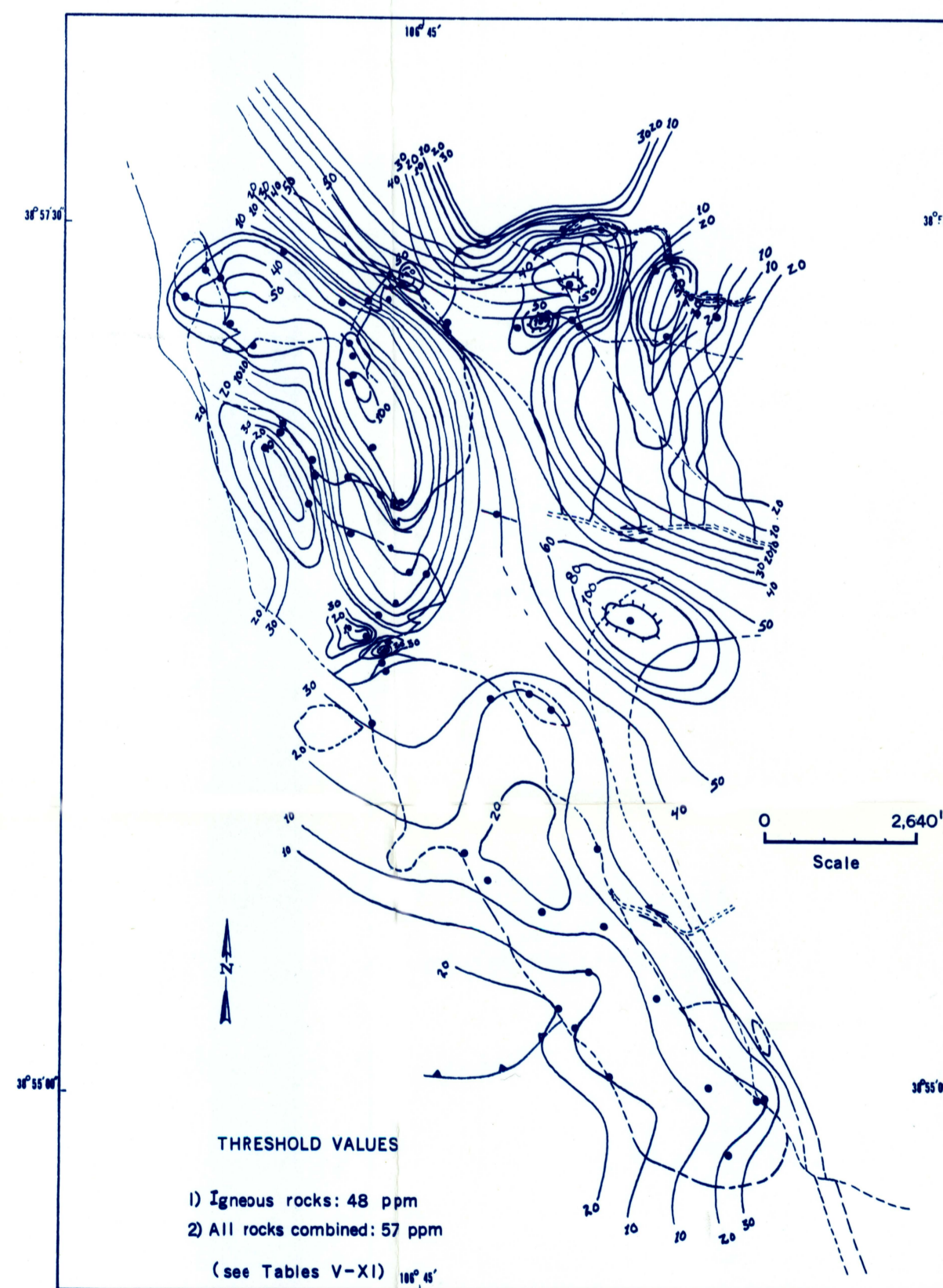


FIGURE 46. Trace metal Distribution of Zn (ppm)

